1968

Magnetic and spectral characterization of some Group VB and VIB transition metal halide complexes

Jimmy George Converse
Iowa State University

MAGNETIC AND SPECTRAL CHARACTERIZATION OF SOME GROUP VB AND VIB TRANSITION METAL HALIDE COMPLEXES

by

Jimmy George Converse

A Dissertation Submitted to the
Graduate Faculty in Partial Fulfillment of
The Requirements for the Degree of
DOCTOR OF PHILOSOPHY

Major Subject: Inorganic Chemistry

Approved:

Signature was redacted for privacy.

In Charge of Major Work

Signature was redacted for privacy.

Head of Major Department

Signature was redacted for privacy.

Dean of Graduate College

Iowa State University
Ames, Iowa

1968

TABLE OF CONTENTS

	Page
INTRODUCTION	1
Review of Previous Work	1
EXPERIMENTAL	12
Materials	12
Synthesis	17
Analytical Procedures	23
Physical Measurements	25
Magnetic Susceptibility	26
Data Processing	40
RESULTS AND DISCUSSION	45
Diamagnetic Core Corrections	45
Paramagnetic Cluster Compounds	51
Temperature Independent Paramagnetism	66
Characterization of the Phases $TaCl_{2.83}$ and $TaBr_{2.83}$	79
Non-Equilibrium Tribromide Phase	100
Mononuclear Tungsten(IV) Complexes	105
SUMMARY	128
SUGGESTIONS FOR FUTURE WORK	131
ACKNOWLEDGEMENTS	133
BIBLIOGRAPHY	135
APPENDIX	140

INTRODUCTION

A significant lack of information about the magnetic properties of the Group V B and VI B heavy transition metal halides has prompted this investigation. The magnetic susceptibility of some tantalum, niobium, and tungsten lower halides has been studied and interpreted. Vibrational and electronic spectra have been employed along with the chemical behavior of these compounds to aid in the characterization of their molecular and electronic structure. This dissertation has been divided into two parts. The first part is concerned with the polynuclear or cluster compounds containing metal-metal bonds within an array of six metal atoms. The second part is devoted to monomeric heavy metal complexes. It is hoped that the results of this investigation will lead to a better understanding of the chemistry of these elements.

Review of Previous Work

Metal cluster compounds

The tantalum-tantalum chloride, bromide and iodide systems have been investigated by Schäfer, et al. (1,2,3) and the phases $TaCl_4$, $TaCl_3$, $(Ta_6Cl_{12})Cl_3$, $TaBr_4$, $TaBr_3$, $(Ta_6Br_{12})Br_3$, TaI_4, and $(Ta_6I_{12})I_2$ have been reported. Kuhn and McCarley (4) have reported preparative methods for the lower tantalum

halides by reduction of the pentahalide with aluminum metal. The tantalum-tantalum bromide and iodide equilibrium phase diagrams have been determined by Boatman and McCarley (5) and a review of tantalum halide chemistry is reported therein. The phases reported by Boatman were $TaBr_5$, $TaBr_4$, $TaBr_{2.83}$, $(Ta_6Br_{12})Br_3$, $(Ta_6Br_{12})Br_2$, TaI_5, TaI_4, and $(Ta_6I_{12})I_2$ while $TaBr_3$ was proposed to be a non-equilibrium phase. Schäfer reported the trihalide phase had a range of homogeneity with the X/Ta molar ratio varying from 3.1 to 2.9. The x-ray powder patterns of the chloride and bromide were analogous to the $NbCl_3$ phase (6) which had a homogeneity range with the Cl/Nb ratio varying from 3.13 to 2.67. A crystal structure determination (7) of $NbCl_{2.67}(Nb_3Cl_8)$ showed trimeric units of metal atoms imbedded in a close packed chloride lattice such that the cluster of three metal atoms was bound to 13 chlorine atoms. Schäfer (8) has proposed a mixed crystal model of M_3X_8 and $M_2X_8(MX_4)$ units to explain the homogeneity range in the niobium and tantalum trihalide phases. The x-ray pattern of $TaBr_3$ reported by Boatman does not correspond to the tribromide reported by Schäfer. The $TaBr_{2.83}$ phase found by Boatman (5) was suggested to be $Ta_6Br_{12}Br_5$; this phase was not observed by Schäfer (2). The $TaCl_{2.83}$

phase identified by Hamilton[1] has not been previously reported or characterized.

Structural characterization of compounds of the type $(M_6X_{12})X_3$ and $(M_6X_{12})X_2$ was reviewed recently by Schäfer (8). Discrete M_6X_{12} units occur in the crystal lattice with bridging between these clusters via the outer halogens. The compound Nb_6F_{15} (9) was observed to be cubic with three dimensional bridging of the external fluorides such that the six coordination sites extending radially from the metal atoms were occupied. The M_6X_{12} moiety in Nb_6Cl_{14} (10) and Ta_6I_{14} (11) was observed to be distorted from the idealized cubic arrangement by compression along one of the 4-fold axes and a model utilizing bridging of some of the internal halogens was proposed. The structure of $Ta_6Cl_{14}\cdot 7H_2O$ was reported by Burbank (12) to have layers of $Ta_6Cl_{14}\cdot 4H_2O$ units alternating with layers of three H_2O units. The M_6X_{12} cluster was elongated to form a tetragonal bipyramid with two chlorides at the apical positions and four waters at the equatorial positions. Schäfer and Bauer (13) had previously claimed proof that the composition of the hydrate was $Ta_6Cl_{14}\cdot 8H_2O$.

---

[1]Hamilton, J. B., Ames, Iowa. On the tantalum-tantalum chloride equilibrium phase diagram. Private communication. 1966.

McCarley, Hughes, Cotton, and Zimmerman (14) have reported on the two electron oxidation of the $M_6X_{12}^{2+}$ ion for niobium and tantalum. The sulphate derivatives of the chloride and bromide $Ta_6X_{12}^{4+}$ ion were isolated. Espenson and McCarley (15) have reported on the kinetics and mechanisms of the oxidation of $Ta_6Cl_{12}^{2+}$ by iron(III) in acidic solution. They proposed two one-electron oxidations with $Ta_6Cl_{12}^{3+}$ as a stable species which could be oxidized to $Ta_6X_{12}^{4+}$ in the presence of excess iron(III).

Bonding in M_6X_{12} and M_6X_8 cluster units has been proposed by Sheldon (16) in terms of hybridized atomic orbitals for simple covalent metal-metal and metal-halogen bonds. Gillespie (17) elaborated on this valence bond approach by suggesting a square antiprismatic bonding arrangement. Such an arrangement would require the metal-halogen bonds to be severely bent. A molecular orbital treatment was presented by Duffey, Crossman, and Olsen (18) and parametric expressions for the energy levels were obtained.

Interpretation of the electronic spectrum of $Ta_6X_{12}^{2+}$ and $Nb_6X_{12}^{2+}$ ions has been presented by Allen and Sheldon (19) in terms of a molecular orbital diagram by Cotton and Haas (20). This scheme was based on the formation of metal-

metal bonds within the M_6 moiety using the LCAO-MO method. The assumption was made that no interaction occurred between the bridging halogens and the metal orbitals. Calculations were carried out to determine the ordering of the molecular energy levels. The bonding orbitals of the M_6X_{12} unit were A_{1g}, A_{2u}, T_{1u}, and T_{2g}. The relative energy of the orbitals was determined as a function of α, the Slater orbital exponent, and R, the internuclear distance. Similar treatment of the M_6X_8 unit gave A_{1g}, T_{1u}, T_{2g}, E_g, and T_{2u} as bonding orbitals. Robin and Kuebler (21) have interpreted the electronic spectrum of the niobium and tantalum clusters using a molecular orbital scheme involving both metal-metal and metal-halogen interactions. A set of independent subsystems was proposed consisting of a combination of atomic orbitals of the proper symmetry. Consideration of the metal-halogen interaction yielded a different ordering of the levels within the dz^2 and d_{xy} orbital subsystems than obtained from metal-metal interactions only. Distortion of the metal octahedron in the tantalum cluster was proposed to explain splitting of the absorption maxima in the spectrum. The niobium cluster appeared to be undistorted. Kettle (22) has pointed out the similarity of the bonding between the M_6X_{12} and M_6X_8 units.

The far infra-red vibrational spectrum of some niobium and tantalum cluster compounds was reported by Boorman and Straughan (23). The preparation and infra-red spectrum of several polynuclear tantalum halide compounds has recently been reported by Meyer (24).

McCarley, Fleming, and Mueller (25) have reported preparative methods of some lower niobium halides and McCarley, Dougherty, and Fleming (26) have made note of their spectral and magnetic properties. Schneider and Mackay (27) have investigated the spectral and magnetic properties of several derivatives of the niobium cluster and have presented a bonding scheme which considered the entire $M_6X_{12}X_6^{n-}$ system. They propose that distortion of the tantalum cluster is not necessary to explain the electronic spectrum as a 1:1 correspondence was observed between niobium and tantalum. The compound $[(C_2H_5)_4N]_2[(Nb_6Cl_{12})Cl_6]$ was diamagnetic while $[(C_2H_5)_4N]_3[(Nb_6Cl_{12})Cl_6]$ was observed to be paramagnetic. Both compounds exhibited a temperature independent paramagnetism of ca. 500×10^{-6} emu/mole.

The magnetic susceptibilities of $Ta_6Cl_{14}\cdot 7H_2O$ and $Nb_6Cl_{14}\cdot 7H_2O$ were measured by Krylov (28). Both compounds were reported as being paramagnetic with temperature dependent

moments. Hughes (29) reported that $Ta_6Cl_{12}(SO_4)_2 \cdot 7H_2O$, $Ta_6Br_{12}(SO_4)_2 \cdot 7H_2O$, $Ta_6Cl_{14} \cdot 10H_2O$, and $Ta_6Br_{14} \cdot 8H_2O$ were paramagnetic obeying the Curie law with moments of ca. 0.5 B.M. Robin and Kuebler (21) reported $Nb_6Cl_{14} \cdot 7H_2O$ to have a temperature independent paramagnetic susceptibility of 850×10^{-6} emu/mole. They proposed that the diamagnetism was approximately equal in magnitude to the temperature independent (Van Vleck) paramagnetism for all of the other hydrated niobium and tantalum chloride and bromide cluster compounds in order to explain the essentially zero susceptibility. Schäfer (10,1) reported the anhydrous Nb_6Cl_{14} to be diamagnetic and Ta_6Cl_{15} to be paramagnetic with a moment corresponding to one unpaired electron per cluster unit. Schäfer (2) also reported the bromide $TaBr_{3.16}$ to be diamagnetic while the bromide $TaBr_{2.9}$ and $(Ta_6Br_{12})Br_3$ were paramagnetic.

The lack of information and the disagreement among reported data pointed out the need for a systematic study of the magnetic properties of the cluster compounds. A Faraday balance was constructed for this purpose using the nature of the information desired to set the design specifications. The Faraday method requires only small quantities of sample and sets no constraints on the sample geometry. It lends

itself readily to studies of temperature and field dependence of the magnetic susceptibility. The choice of an electronic microbalance allowed detection of susceptibilities of the order of ca. 10^{-9} emu/g. An extensive investigation of the variables affecting the reliability of magnetic susceptibility measurements evolved from the process of calibrating the balance. The variables of the system and the choice of an acceptable standard were considered in view of attaining maximum precision and accuracy.

The investigation of the cluster compounds should establish the nature of the magnetic ground state in the (2+), (3+), and (4+) M_6X_{12} ions of niobium and tantalum. Additional information about the bonding in the cluster units can be obtained from knowledge of their temperature independent paramagnetism. Coupled with x-ray crystal structure, vibrational and electronic spectra, and chemical behavior, the magnetic properties of the Ta, Nb, and W subhalides would lead to a more complete description of their molecular and electronic structure. This would allow a test for theoretical predictions and aid in the fundamental understanding of the forces that hold these polynuclear units together.

Mononuclear tungsten(IV) complexes

The existence of some controversy concerning the magnetic properties of $WCl_4(C_5H_5N)_2$ and $WBr_4(C_5H_5N)_2$ and the availability of both a susceptibility instrument and these compounds led to this investigation.

Peacock and Kennedy (30) first studied the magnetic properties of these compounds and reported a temperature dependent magnetic moment. They reported the presence of a Néel temperature at 100°K for $WCl_4(C_5H_5N)_2$ and proposed that the large value of θ was due to antiferromagnetic exchange. Effective magnetic moments of 2.06 and 2.03 B.M. were reported at 291°K for the chloride and 288°K for the bromide, respectively. Brown (31) reported a much larger curvature in the χ_M versus 1/T plots but observed no Néel temperature down to liquid helium. Effective moments calculated from the limiting slope of the χ_M versus 1/T plots at the higher temperatures were 1.6 and 2.1 B.M. for the chloride and bromide, respectively.

Fowles (32) has investigated the magnetic susceptibilities of some nitrile complexes of tungsten(IV) halides and reported behavior similar to the pyridine complexes. Effective moments at room temperature varied from 1.84 to 2.07 B.M.

Hull and Stiddard (33) have reported the preparation, infra-red spectra, and magnetic susceptibilities of tungsten(IV) and molybdenum(IV) chloride and bromide complexes with 2,2'-dipyridyl. The two nitrogen atoms in these complexes are constrained to the cis configuration. The effective magnetic moments for the tungsten complexes were 1.64 and 1.69 B.M. for the chloride and bromide, respectively. Allen and Fowles (34) have reported the infra-red spectra and magnetic susceptibilities of some Mo(IV) chloride complexes. They claimed that the triphenylphosphine derivative $MoCl_4 \cdot 2P\emptyset_3$ had the trans configuration while the complexes of acetonitrile and 2,2'-bipyridyl had the cis configuration. The χ_M versus 1/T plots have shown curvature for all reported data on cis isomers, but the similar plot for $MoCl_4 \cdot 2P\emptyset_3$ was linear.

The magnetic properties of d^2 ion complexes can be predicted from ligand field theory considerations. An expression for the magnetic moment has been presented by Kamimura (35) as a function of spin-orbit coupling constant, low symmetry field parameter, and temperature. The assumptions of the Kotani theory (36) were used for this calculation but Kamimura, Koide, Sekiyama, and Sugano (37) have shown that those assumptions are not valid for 4d and 5d elements. Perturba-

tion of the strong field basis functions simultaneously by spin-orbit coupling and electron repulsion yielded eigenfunctions and eigenvalues appropriate to these heavy elements in a cubic field. Perturbation by a low symmetry field potential was not carried out in their calculations.

Occupation of thermally accessible states higher than the ground state has been suggested (31) to explain the magnetic behavior of these d^2 ions. The low symmetry field potential would split the energy levels arising from spin-orbit coupling. Figgis (38) has proposed that some of the levels resulting from this splitting could be lowered to within a few hundred cm^{-1} of the ground state.

The purpose of this investigation was then to carefully measure the magnetic susceptibility of these d^2 ions and interpret their behavior in view of available theory.

EXPERIMENTAL

Materials

In this work, all compounds which were susceptible to hydrolysis and air oxidation were contained in evacuated vessels or inert atmospheres during preparation and experimentation. In addition, all materials used in their preparation were rigorously dried and stored in evacuated containers. Whenever this was not possible, the materials were purified immediately before use. Storage and handling of all solid materials were done in a dry-box under argon atmosphere. The dry-box was maintained at a dew point of ca. -65°C by pumping a constant flow of argon (dried over Linde 4A Molecular Sieves) through the box. All vessels were evacuated to ca. 10^{-5} Torr before being sealed. Reactions were carried out in Pyrex, Vycor, and tantalum vessels.

Tantalum metal

Tantalum powder obtained from the Fansteel Metallurgical Corporation, Metal Products Division, was used in the preparation of all tantalum(V) halides. Spectrographic analysis of this metal indicated the presence of the following elements in parts per million: Nb, 90; Fe, 150; W, 50; Mo, 40; Ti, 10; Zr, 10; Ni, 50; Si, 50; C, 370; O, 1600; N, 60; H, 36.

Aluminum metal

Aluminum of 99.999 nominal percent purity was obtained in block form from laboratory stock. The block was machined into turnings for use in the reduction of tantalum(V) halides. Analysis of the turnings showed iron to be present in less than 16 ppm.

Halogens

General grade chlorine was distilled from a lecture size cylinder. Reagent grade bromine was dried by treatment for several days with well out-gassed phosphorus(V) oxide in an evacuated flask. The bromine was then vacuum distilled into a clean flask from which it was again vacuum distilled as needed.

Organic solvents

All organic solvents used in this work were spectro-grade reagents obtained from Eastman Company. The liquids were thoroughly dried before use by successively vacuum distilling them onto out-gassed barium(II) oxide and phosphorus (V) oxide. The reagent was frozen and the flask out-gassed at *ca.* 10^{-5} Torr. The liquids were then vacuum distilled into clean flasks containing Molecular Sieves for storage.

Niobium, tantalum and tungsten cluster compounds

The following compounds were prepared, analyzed, and made available by John L. Meyer (24).

Dodeca-μ-chloro-hexatantalum trichloride hexahydrate

Anal: Calcd. for $Ta_6Cl_{12}Cl_3 \cdot 6H_2O$: Ta, 62.92; Cl, 30.82; H_2O, 6.26. Found: Ta, 62.99; Cl, 30.94; H_2O (by difference), 6.1.

Tris(tetraethylammonium)hexachlorododeca-μ-chloro-hexatantalum Anal: Calcd. for $[(C_2H_5)_4N]_3[(Ta_6Cl_{12})Cl_6]$: Ta, 51.34; Cl, 30.18; C, 13.63; H, 2.86. Found: Ta, 51.39; Cl, 30.16; C, 13.43; H, 3.03.

Bis(tetraethylammonium)hexachlorododoce-μ-chloro-hexatantalum Anal: Calcd. for $[(C_2H_5)_4N]_2[(Ta_6Cl_{12})Cl_6]$: Ta, 54.71; Cl, 32.16; C, 9.68; H, 2.03. Found: Ta, 54.81; Cl, 32.23; C, 9.78; H, 2.04.

Bis(tetraethylammonium)hexabromododeca-μ-chloro-hexatantalum Anal: Calcd. for $[C_2H_5)_4N]_2[(Ta_6Cl_{12})Br_6]$: Ta, 48.23; C, 8.54; H, 1.79; X/Ta, 3.00; AgX (for one specific sample), 150.0 mg. Found: Ta, 48.4; C, 8.51; H, 2.06; X/Ta, 2.97; AgX (for one specific sample), 152.6 mg.

Bis(tetraethylammonium)hexabromododeca-μ-bromo-hexatantalum Anal: Calcd. for $[(C_2H_5)_4N]_2[(Ta_6Br_{12})Br_6]$: Ta, 38.99; Br, 51.65; C, 6.90; H, 1.45. Found: Ta, 38.68;

Br, 51.27; C, 6.65; H, 1.50.

Bis(tetraphenylarsonium)hexachlorododeca-μ-chloro-hexatantalum Anal: Calcd. for $[(C_6H_5)_4As]_2[(Ta_6Cl_{12})Cl_6]$: Ta, 43.59; Cl, 25.62; C, 23.15; H, 1.62. Found: Ta, 43.07; Cl, 25.46; C, 22.95; H, 1.62.

The following compounds were prepared, analyzed, and made available by Peter B. Fleming (25,26).

Dodeca-μ-chloro-hexaniobium dichloride octahydrate Anal: Calcd. for $Nb_6Cl_{12}Cl_2 \cdot 8H_2O$: Nb, 46.53; Cl, 41.44; H_2O, 12.03. Found: Nb, 46.53; Cl, 41.53; H_2O (by difference), 11.94.

Dodeca-μ-bromo-hexaniobium dibromide octahydrate Anal: Calcd. for $Nb_6Br_{12}Br_2 \cdot 8H_2O$: Nb, 30.60; Br, 61.49; H_2O, 7.91. Found: Nb, 30.55; Br, 60.62; H_2O (by difference), 8.83.

Bis(tetraphenylarsonium)hydroxotetrachloroaquododeca-μ-chloro-hexaniobium Anal: Calcd. for $[(C_6H_5)_4As]_2$ $[(Nb_6Cl_{12})(OH)Cl_4(H_2O)]$: Nb, 28.92; Cl, 29.43; C, 29.91; H, 2.30; O, 1.66. Found: Nb, 28.99; Cl, 29.23; C, 29.22; H, 2.45; O, 1.46.

Bis(tetraethylammonium)hexachlorododeca-μ-chloro-hexaniobium Anal: Calcd. for $[(C_2H_5)_4N]_2[(Nb_6Cl_{12})Cl_6]$:

Nb, 38.28; Cl, 43.83; C, 13.20; H, 2.27. Found: Nb, 38.44; Cl, 43.52; C, 13.73; H, 2.81.

Tris(tetraethylammonium)hexachlorododeca-μ-chloro-hexaniobium Anal: Calcd. for $[(C_2H_5)_4N]_3[(Nb_6Cl_{12})Cl_6]$: Nb, 35.14; Cl, 40.23; C, 18.17; H, 3.81. Found: Nb, 35.47; Cl, 40.08; C, 18.48; H, 4.14.

The following compounds were prepared, analyzed, and made available by Ronald D. Hogue.[1]

Bis(tetraethylammonium)hexachloroocta-μ_3-chloro-hexatungsten Anal: Calcd. for $[(C_2H_5)_4N]_2[(W_6Cl_8)Cl_6]$: W, 59.31; Cl, 26.69; C, 10.33; H, 2.17. Found: W, 59.23; Cl, 26.60; C, 10.65; H, 2.23.

Bis(tetraethylammonium)hexabromoocta-μ_3-chloro-hexatungsten Anal: Calcd. for $[(C_2H_5)_4N]_2[(W_6Cl_8)Br_6]$: W, 51.87; X/W, 2.33; C, 9.04; H, 1.90. Found: W, 51.63; X/W, 2.27; C, 9.31; H, 1.94.

The following compounds were prepared, analyzed, and made available by Theodore M. Brown.[2]

---

[1]Hogue, R. D., Ames, Iowa. On the preparation of tungsten halide cluster compounds. Private communication. 1967.

[2]Brown, T. M., Tempe, Arizona. On the characterization of tetrahalobis(pyridine)tungsten(IV) complexes. Private communication. 1966.

Tetrachlorobis(pyridine)tungsten(IV) Anal: Calcd. for $WCl_4(C_5H_5N)_2$: W, 38.00; Cl, 29.31; N, 5.79; Cl/W, 4.00; N/W, 2.00. Found: W, 37.71; Cl, 29.04; N, 5.63; Cl/W, 3.99; N/W, 1.96.

Tetrabromobis(pyridine)tungsten(IV) Anal: Calcd. for $WBr_4(C_5H_5N)_2$: W, 27.79; Br, 48.31; N, 4.23; Br/W, 4.00; N/W, 2.00. Found: W, 27.55; Br, 47.76; N, 4.10; Br/W, 3.99; N/W, 1.95.

The phase $TaCl_{2.83}$ was prepared, analyzed, and made available by James B. Hamilton.[1]

The phase $TaCl_{2.83}$ Anal: Calcd. for $TaCl_{2.83}$: Ta, 64.33; Cl, 35.67. Found: Ta, 64.75, 64.63; Cl/Ta (chloride by difference), 2.81.

Synthesis

Temperature gradient furnaces contained a split porcelain core each half of which was wound separately. Thus, the two ends of the furnace could be controlled at different temperatures. Equilibration at a specific temperature was achieved by using a one inch bore thick-walled aluminum liner in a single wound furnace. The temperature was controlled

[1]Hamilton, J. B., Ames, Iowa. On the investigation of the tantalum chloride system. Private communication. 1966.

to $\pm$ 2°C using a Minneapolis Honeywell, Brown Electronik temperature proportionating controller.

Tantalum(V) halides

Tantalum(V) chloride and bromide were prepared from direct combination of the elements by passing the halogen over the metal heated to 400°C. Purification was effected by sublimation under 5-10 mm. pressure of argon to prevent entrainment of impurities. The temperature was maintained at about ten degrees below the melting point of the tantalum(V) halide (m.p., $TaCl_5$, 221°C; $TaBr_5$, 272°C). A significant amount of residue always remained after sublimation. The crystalline tantalum(V) halide was stored in a screw-capped bottle in the dry-box.

Tantalum(IV) bromide

Tantalum(IV) bromide was prepared by aluminum metal reduction of the tantalum(V) bromide at 250°C in an aluminum (III) bromide melt. In this procedure 1.2 grams of aluminum turnings were combined with 92 grams of tantalum(V) bromide. The reactants were placed in a Pyrex tube ca. 14 inches long having a constriction about one-third of the distance from one end. The tube was filled in the dry-box, evacuated to ca. 10^{-5} Torr on a vacuum manifold, and sealed. It was then

placed in a horizontal position in the furnace with all the reactants in the longest section of the tube. After ten days a dark crystalline product was obtained. The excess tantalum(V) bromide and the aluminum(III) bromide were removed by sublimation at 225°C for 24 hours. The yield was about 60 grams of tantalum(IV) bromide with some crystals large enough to be retained on a #60 mesh sieve.

The phase $TaBr_{2.83}$

The phase $TaBr_{2.83}$ was prepared according to Boatman (5) by the disproportionation of tantalum(IV) bromide at temperatures between 400-450°C. The best results were obtained at ca. 405°C with sufficient $TaBr_5$ present to maintain its equilibrium pressure over the solid $TaBr_4$. In a typical preparation, 15 grams of tantalum(IV) bromide and 5 grams of tantalum(V) bromide were sealed in an evacuated Pyrex tube ca. 3 inches long and 0.5 inch in diameter. The reaction vessel was placed in a vertical position in the furnace with an aluminum liner to smooth out thermal gradients. A temperature of 405 $\pm$ 2°C was maintained over the sample with the upper portion slightly warmer than the bottom. After twenty-five days a brown powder remained. The material was transferred in the dry-box to another tube ca. 8 inches long. The

excess tantalum(V) bromide was removed by sublimation at 225°C for twenty-four hours. Analytical data for two different preparations are given below.

Anal: Calcd. for $TaBr_{2.83}$: Ta, 44.48; Br, 55.52. Found: (1) Ta, 44.31, 44.56; (2) Ta, 44.44, 44.48.

Dodeca-μ-bromo-hexatantalum tribromide

The compound $Ta_6Br_{12}Br_3$ ($TaBr_{2.50}$) was prepared by two methods. The transport method described by the two step reaction 1 yielded a product which contained some of the $TaBr_{2.83}$ phase.

$$Ta(s) + 4TaBr_5(g) \overset{630^{\circ}C}{\rightarrow} 5TaBr_4(g)$$
$$15TaBr_4(g) \overset{450^{\circ}C}{\rightarrow} Ta_6Br_{15}(s) + 9TaBr_5(g) \qquad (1)$$

Heat treatment in a 500/25°C gradient removed the higher halide yielding a clean product. The second method involved equilibration of $Ta_6Br_{12}Br_2$ ($TaBr_{2.33}$) with $TaBr_5$ in a Pyrex tube at ca. 460°C for fifteen days. The excess tantalum(V) bromide was removed by sublimation at 225°C for twenty-four hours.

Analytical data for material prepared by both methods are given below.

Anal: Calcd. for Ta_6Br_{15}: Ta, 47.53; Br, 52.47. Found: (1) Ta, 47.26, 47.22; (2) Ta, 47.04, 47.08; Br,

52.31, 51.83; Br/Ta, 2.52, 2.49.

Dodeca-μ-bromo-hexatantalum dibromide

The compound $Ta_6Br_{12}Br_2$ ($TaBr_{2.33}$) was prepared by aluminum metal reduction of tantalum(V) bromide in a 400/280°C thermal gradient for three days. The excess tantalum(V) bromide and the aluminum(III) bromide were removed by sublimation and the product was heat treated in a 450/25°C gradient for thirty hours. The higher temperature was then raised to 550°C for an additional twenty-four hours. Initial heat treatment at 550°C tended to produce some tantalum metal in the product. Analytical data for a typical preparation are given below.

Anal: Calcd. for Ta_6Br_{14}: Ta, 49.25, Br, 50.75. Found: Ta, 49.38, 49.48; Br/Ta (bromide by difference), 2.32.

Tantalum(IV) chloride

Tantalum(IV) chloride was prepared in a manner similar to that of the bromide. Aluminum metal reduction of tantalum(V) chloride in an aluminum(III) chloride melt was carried out in a temperature gradient of 230/200°C for about two weeks. Excess tantalum(V) chloride and aluminum(III) chloride were removed from the product by sublimation at 200°C for twenty-four hours.

Dodeca-μ-chloro-hexatantalum trichloride

The compound $Ta_6Cl_{12}Cl_3$ ($TaCl_{2.50}$) was prepared by disproportionation of tantalum(IV) chloride in a 425/290°C gradient for ten days. The product contained some of the $TaCl_{2.83}$ phase. Heat treatment in a 550/25°C gradient for three days followed by washing with absolute methanol yielded a clean product. Analytical data for the product are given below.

Anal: Calcd. for Ta_6Cl_{15}: Ta, 67.12; Cl, 32.88. Found: Ta, 67.08, 67.10; Cl/Ta (chloride by difference), 2.50.

Mercury(II)tetrathiocyanatocobaltate(II)

The compound $Hg[Co(NCS)_4]$ was prepared by the method of Figgis and Nyholm (39), who recommended its use as a magnetic susceptibility standard. Analysis for the magnetic cobalt ion gave the following results.

Anal: Calcd. for $Hg(Co(NCS)_4)$: Co, 11.98. Found: Co, 12.15, 12.14.

An emission spectrum of the material showed the following elements to be present in parts per million: Cu, 10; Mn, 1; Ni, 100; Rh, 5.

Diammonium hexaaquonickel(II) sulfate

The compound $(NH_4)_2Ni(H_2O)_6(SO_4)_2$ was prepared by mixing equimolar solutions of $NiSO_4$ and $(NH_4)_2SO_4$ in water. The solution was allowed to evaporate slowly at room temperature until large crystals had formed. The crystals were washed with distilled water, dried at room temperature, and ground to a fine powder. The powder was placed in a tube, evacuated to ca. 10^{-5} Torr, and out-gassed for two hours to remove adsorbed water. Analysis gave the following results.

Anal: Calcd. for $(NH_4)_2Ni(H_2O)_6(SO_4)_2$: Ni, 14.86. Found: 14.95, 14.93, 14.93.

Analytical Procedures

Analysis of air sensitive compounds was effected by transferring weighed samples contained in screw-capped bottles to hydrolysis cells or closed beakers in the dry-box.

Tantalum

Tantalum was determined gravimetrically as the oxide Ta_2O_5. After the samples were hydrolyzed in aqueous ammonia, the solutions were heated on a hot plate to ensure complete hydrolysis and oxidation of tantalum(IV) oxide to tantalum(V) oxide. The solutions were cooled to room temperature and acidified with nitric acid to ca. pH 1. The precipitate was

filtered on medium retention filter paper and washed thoroughly with dilute nitric acid. The paper was charred and the oxide ignited at 650°C in a muffle furnace.

The oxide was also produced by the "H-tube" method as described by Schäfer and Dohmann (40). In this method the compound was heated to 100-110°C for about twenty-four hours with nitric acid in a sealed "H" tube.

When it was not necessary to obtain tantalum and halide analyses from the same sample, the sample was placed in a tared crucible. Concentrated nitric acid was added and then carefully boiled off. Two or three repetitions of this treatment produced the desired oxide which was then ignited.

Tungsten

Tungsten was determined gravimetrically as the oxide WO_3 by the tared crucible method described for tantalum. The oxide was ignited at 500-550°C.

Halogens

Halogens were determined by potentiometric titration with silver nitrate or by gravimetric precipitation of the silver halide. The amount of halide was determined in the solutions after the metal oxide had been removed by filtration.

Iron

Iron present in the anhydrous tantalum halides at the trace level was determined by the Ames Laboratory Analytical Service Group, Iowa State University of Science and Technology, Ames, Iowa.

Physical Measurements

X-ray diffraction

X-ray powder patterns were obtained with a 114.59 mm. Debye-Scherrer camera. Finely powdered samples were packed and sealed into 0.2 mm. Lindemann glass capillaries. Samples were exposed to copper $K\alpha$ radiation for twenty to thirty hours.

Spectra

Near infra-red spectra were obtained on solutions using a Cary Model 14 recording spectrophotometer and one centimeter quartz cells. The wave length range investigated was 600-2100 mμ. Reflectance spectra were obtained with a Beckman Model DU spectrophotometer equipped with the Beckman 2580 reflectance attachment. Potassium bromide was used as dilutant and reference material. The sample was contained in a cell provided with a fused silica window and sealed from the atmosphere by an "O" ring.

Far infra-red spectra were obtained using a Beckman IR-11 grating spectrophotometer in a double beam operation on Nujol mulls. The mulled sample was sandwiched between polyethylene windows and sealed with an "O" ring.

Magnetic Susceptibility

Faraday balance construction

Magnetic susceptibility measurements were obtained using a Faraday balance constructed and calibrated in this laboratory by the author. A Varian V-4007-1 magnet provided with variable-gap, six-inch pole pieces and constant H dH/dZ pole caps was used with a V-2200 power supply. The magnet was mounted on wheels inside of a 2½' x 4½' x 7 3/4' aluminum frame and could traverse the length of the frame along a track. The design facilitated access of the magnet to two different systems at opposite ends of the frame. The position of the magnet along the track was secured by means of a brake assembly mounted under the magnet trailer. The magnet could be rotated on its base by 180 degrees.

Force measurements were obtained with a Cahn, RG, electrobalance to detect weight change between field-on and field-off conditions. The Cahn balance, suspension wire, and sample container were protected from air currents and

moisture condensation by a vacuum enclosure. All components were constructed from non-magnetic stainless steel, brass, copper, or aluminum. All connections were machined and fitted with rubber "O" rings. Centering of the samples in the suspension tube was achieved by means of a three point suspension of the balance housing on brass bolts. The tube was centered between the pole caps of the magnet by sliding the base plate of the balance housing along slotted bolt holes. Access to the Cahn balance was attained by means of a pivoting lid seated on an "O" ring. Visual observation of the sample was provided by a glass viewer on the lid of the vacuum chamber. The sample suspension tube could be disconnected below the base plate by a threaded "O" ring coupling joint. This allowed the vertical position of the sample with respect to the magnet pole caps to be determined. The Cahn balance was supported on two blocks attached to an aluminum plate which could be leveled independently of the balance housing by three set screws. These screws rested on a second plate fixed rigidly to the base of the balance housing. Two holes in the upper plate provided clearance for the sample suspension on loop A (maximum load 1.0 gram) and loop B (maximum load 2.5 grams) of the balance beam. Alignment of

the two loops over the suspension tube was provided by two cone shaped depressions, 2.08 inches apart, in the lower plate to contain one of the set screws. The remaining two screws rested in "V" shaped tracks. The balance was manually shifted from one rest position to the other.

The balance housing was connected to an isolated vacuum pump by means of a port in the base plate. A vacuum valve sealed the balance chamber after the system was evacuated and flushed with helium. The pump could then be shut off to reduce vibrations. Helium at ca. 0.1 Torr was retained in the system as an exchange gas to achieve rapid thermal equilibrium between the sample and the cryostat. The helium was purified by passing it through Linde 4A Molecular Sieves immersed in liquid nitrogen.

Temperature variation and measurement

The sample temperature was measured with a copper-constantan thermocouple suspended above the sample container. The thermocouple was calibrated at several temperatures between liquid nitrogen and room temperature using organic slush baths. The results were plotted to provide a graph of E.M.F. versus temperature. The temperature of a specific susceptibility measurement was then determined from the E.M.F. generated by the thermocouple.

Variation of temperature was achieved by using liquid nitrogen and an isopentane slush contained in a narrow-tail glass dewar. The sample was cooled to 77°K with liquid nitrogen after measurements at room temperature had been obtained. One to two hours were allowed for the sample to reach thermal equilibrium before the susceptibility was measured. Measurements at 113°K were obtained using an isopentane slush. The bath was then allowed to warm to room temperature which required ca. 24 hours. Measurements could be taken at selected intervals and the temperature determined from the thermocouple voltage. Whereas the rate of temperature change was ca. 1 degree per 8 minutes, less than 5 minutes was required to obtain the measurement. Thus, it was assumed that continual thermal equilibrium was maintained within the limits of the temperature measurement. Measurements on a sample having a temperature independent moment provided a means to determine the temperature difference between sample and thermocouple during warming. Nickel ammonium sulfate hexahydrate which has been recommended (41) as a magnetic susceptibility standard was measured at several temperatures. The actual temperature was calculated from the relationship: $\chi g = (3065/T + 0.5) \times 10^{-6}$ emu/g. The dif-

ference between observed and calculated temperature was less than one percent in all cases. It was concluded that the slow rate of warming with the use of helium at ca. 0.1 Torr provided a satisfactory method for temperature variation. The isopentane was frozen and cooled to 77°K with liquid nitrogen to obtain temperatures between 113°K and 77°K. The solid was allowed to warm slowly in the same manner as before. A metal dewar should be used for this procedure as one glass dewar was broken during warming of the frozen isopentane.

Force measurements

The change in weight detected by the Cahn balance was measured with a variable resistance used in a bridge circuit. The bridge was balanced by the resistance to produce zero voltage output from the circuit to a Leads & Northrop, Model 8934, d.c. null detector. The resistance was calibrated with class "M" weights so that the difference between two readings yielded the weight change in milligrams.

Field measurements

The reproducibility of the magnetic field was determined to be less than 0.2 percent deviation from the mean average. The measurements were obtained over a time period of three months. The magnetic field strength between homogeneous field pole caps was measured with an H_2O reference N.M.R.

probe and a Varian, Model F-8, Nuclear Fluxmeter.

The method of Honda and Owen (42) for determination of field dependence of the magnetic susceptibility was used in this investigation. The interaction of a substance with a magnetic field generates a force expressed by Equation 2.

$$f = m\chi_g H \, dH/dZ + c\sigma \, dH/dZ \qquad (2)$$

where: f = force acting on the substance, dynes,

m = mass of the substance, grams,

χ_g = gram susceptibility, emu/gram,

H = magnetic field, oersted,

dH/dZ = field gradient along Z axis, oersted/cm.,

c = concentration of ferromagnetic impurity, ppm.,

σ = saturation magnetization of the impurity, dyne-cm./oersted.

Dividing all terms in Equation 2 by the force constant $H \, dH/dZ$, denoted as F_i, yields Equation 3.

$$\Delta f_i / \Delta F_i = m\chi_g + c\sigma \, 1/\Delta H_i \qquad (3)$$

The subscript refers to a specific field setting and Δ implies the difference between the term at H_i and H_o. Since f_o, F_o, and H_o are not necessarily equal to zero the difference Δ represents more accurately the magnitude of the term due to magnetic interaction. The term $\Delta f_i / \Delta F_i$ in Equation 3

is the apparent susceptibility. Plotting $\Delta f_i/\Delta F_i$ versus $1/\Delta H_i$ for several values of the field H_i yields an intercept equal to the product of the true paramagnetic susceptibility with the mass of the sample. The slope $c\sigma$ would be zero if no impurity was present because paramagnetism has no field dependence. The current input to the magnet coils was related to a dial setting on the power supply. This dial setting was then reproduced to obtain a specific field H_i.

The method of Honda and Owen requires that the product of the magnetic field and the field gradient be constant over the region of the sample. Special pole caps designed to yield a region of constant H dH/dZ were purchased from Varian Associates, Incorporated. The magnetic field in the region of the pole caps was measured with a Hall element. The probe was mounted on a carriage suspended between the pole caps and the position was measured with a micrometer.

A three dimensional graph of field strength versus distance from the origin was used to determine the magnet constants and the optimum sample size and position. The coordinates were arbitrarily chosen with Z as the vertical axis, X as the axis through the pole pieces, and Y as the axis parallel to the faces of the pole caps and perpendicular

to the Z axis. The origin was set at the pole cap minimum on the Z axis, the center of the pole caps on the Y axis, and half way between the pole caps on the X axis. It was determined that the sample container should not exceed 10 mm. in diameter and 40 mm. in length. The bottom of the container should not extend lower than 10 mm. above the minimum pole gap which coincided with the maximum magnetic field strength. The force constant H dH/dZ was obtained by plotting the square of the field versus the distance from the origin along the Z axis. The slope of the line was equal to $d(H^2)/dZ$ or twice the magnitude of H dH/dZ. The term H dH/dZ was observed to be constant from 5 to 50 mm. above the origin. Values of F_i for five field settings are listed in Table 1 of the calibration section.

Sample container

The sample container was machined from Teflon rod to form a cylindrical bucket 10 mm. in length and 7 mm. in diameter. A threaded cap on the bucket permitted a tight seal to protect air sensitive samples from exposure during loading. The container was suspended from the Cahn balance on a thin tungsten wire. The center of the sample was located 20 mm. above the origin on the Z axis. The force

on the container and suspension was observed to be constant over the temperature range of 77 to 300°K. One container was used for all samples and periodic measurements of its susceptibility were made to insure that the container corrections were accurate. A cleaning solution of equal volumes of nitric and sulfuric acid was used to wash the container after a sample was removed. The container was rinsed with distilled water and then acetone after removal from the boiling acid mixture.

Operational procedure

The weights of the sample and container were determined prior to magnetic measurements. The weight of the sample was obtained again after the measurements to determine if evacuation had caused a decrease in the sample mass. Air sensitive samples were loaded in the dry-box. The Teflon capsule was exposed to the atmosphere for 30-60 minutes during weighing and loading into the balance. No decomposition of the sample was detected, even for the most reactive compounds. The balance chamber was evacuated to ca. 10^{-5} Torr and outgassed for 3-5 hours before the helium exchange gas was introduced.

The weight of the sample and container was balanced with the variable resistance and null detector at H_o. The resist-

ance dial reading was recorded and the procedure was repeated at five field settings between six and twelve kilo-oersted. The weight was balanced again at H_o so that corrections could be applied for drift in the balance. The difference in weight between the sample in a field H_i and H_o multiplied by 0.980 dyne per milligram yielded the magnetic interaction force Δf_i.

Calibration

Calibration of the magnet constants ΔF_i and $1/\Delta H_i$ consisted of several steps. Field measurements provided one set of values for these constants. Force measurements on a gold metal sample provided a second set of values for ΔF_i using Equation 3, the reported susceptibility of gold, and the assumption that no ferromagnetic impurity was present. The values of the magnet constants are listed in Table 1.

Table 1. Force constants and reciprocal field values for Faraday balance with a pole gap of 1.000 ± 0.001 inch and center of sample at Z = 2.00 cm.

Dial setting	$\Delta F_i \times 10^{-6}$ A	$\Delta F_i \times 10^{-6}$ B	$1/\Delta H_i \times 10^5$ A
10-100	7.81	7.84	8.53
9-100	6.38	6.39	9.48
8-100	4.75	4.72	11.0
7-100	3.38	3.30	13.1
6-100	2.35	2.25	15.8

A. Calculated from field measurements.

B. Calculated from gold metal, $\chi_g = -0.143 \times 10^{-6}$ emu/gram, reference (43).

The magnitude of the two sets of values for ΔF_i are in reasonable agreement, but the relative values within a set differ significantly. Donoghue (43) has described a procedure for establishing the internal consistency of the magnet constants. Thus, a sample of high purity was measured and the force constants were adjusted to yield colinearily for a plot of $\Delta f_i/\Delta F_i$ versus $1/\Delta H_i$. A paramagnetic and diamagnetic sample were then measured and the apparent susceptibility $\Delta f_i/\Delta F_i$ was plotted versus $1/\Delta H_i$ using the adjusted force constants. The gold sample was used for the first step in the procedure. The paramagnetic salt $Hg[Co(NCS)_4]$ and diamagnetic Teflon were used for the second part. The nature of the force equation demands that the slope of the Honda-Owen plot be positive or zero but never negative. The force constants determined from field measurements yielded a negative slope for the Teflon sample. The values obtained from the gold sample yielded an essentially zero slope for both the paramagnetic and diamagnetic samples.

Some components of the power supply required replacement which changed the field strength of the specified dial settings. Rather than repeat the field measurements, the new force constants were determined by measuring a standard sample.

An investigation of magnetic susceptibility standards by Simmons (41) has indicated that nickel ammonium sulfate hexahydrate was the most satisfactory of several common standards. With this standard material consistently reproducible results were obtained and observations agreed with the reported temperature dependence of the susceptibility. Calculation of the absolute susceptibility from field measurements agreed with the literature within less than one percent. The salts $(NH_4)_2Fe(SO_4)_2 \cdot 6H_2O$, $CuSO_4 \cdot 5H_2O$, and $Hg(Co(NCS)_4)$ were considered to be unsatisfactory.

The force constants obtained from the nickel salt were verified to be an internally consistent set by measurements on diamagnetic Teflon. The final step in the procedure involved measurements on a sample of high purity, adding a minute quantity of ferromagnetic iron, and repeating the measurements. Thus the slope of the Honda-Owen plot (Eq. 3) should increase while the intercept remains unchanged. The relative values of $1/\Delta H_i$ were adjusted such that the intercept remained constant. The Teflon container was used for this step and iron was added by rubbing the container between soiled fingers. The susceptibility then was independent of impurity concentration. The magnet constants obtained by

this internally consistent procedure are listed in Table 2. The force constants were taken as the average of several measurements refined by least squares to give the best fit to all the data. The reciprocal field values were obtained using ca. 12 ppm. iron contamination.

Table 2. Magnet constants for Faraday balance with pole gap of 1.000 ± 0.001 inch and center of sample at Z = 2.00 cm.

Dial Setting	$\Delta F_i \times 10^{-6}$ [a]	$1/\Delta H_i \times 10^5$
10-100	8.485	9.00
9-100	6.905	10.0
8-100	5.107	11.5
7-100	3.582	13.5
6-100	2.449	16.1

[a] Determined from force measurements on $(NH_4)_2Ni(SO_4)_2 \cdot 6H_2O$ with $\chi_g = (3065/T + 0.5) \times 10^{-6}$ emu/g, reference (41).

The magnetic susceptibility of this salt was measured at several temperatures between 77°K and room temperature. The experimental and calculated values are compared in Table 3.

The compound $Hg(Co(NCS)_4)$ was prepared as a magnetic susceptibility standard by Figgis and Nyholm (39). The susceptibilities which they reported were relative to water as a reference standard. They later reported (44) a value using

Table 3. Temperature dependence of magnetic susceptibility for $(NH_4)_2SO_4 \cdot NiSO_4 \cdot 6H_2O$ (χ_g(calc) = (3065/T + 0.5) x 10^{-6} emu/g.)

Temperature (^oK)	$\chi_g x 10^{-6}$ emu/g calc.	exp.
297.0	10.30	10.35
243	12.59	12.57
160	19.10	19.06
136	22.45	22.57
113	27.00	27.02
77	39.55	39.49

$CuSO_4 \cdot 5H_2O$ as a reference. A number of susceptibility investigations reported in the literature have been based on use of this cobalt salt as a standard. In view of the work by Simmons (41), the susceptibility of $Hg(Co(NCS)_4)$ was measured at several temperatures using the magnet force constants in Table 2. The results are compared with the calculated values in Table 4. It was the contention of Simmons that the temperature dependence of $Hg(Co(NCS)_4)$ did not correspond to the values reported by Figgis and Nyholm. The same conclusion may be inferred from the data given in Table 4.

Table 4. Temperature dependence of magnetic susceptibility for $Hg(Co(NCS)_4)$

Temperature	$\chi_g \times 10^{-6}$ emu/g		
	calc (1)[a]	calc (2)[b]	exp.
294.8	16.3	15.8	16.04
246	19.4	18.8	19.42
231	20.7	20.0	20.46
164	28.6	27.7	28.57
134	34.6	33.5	35.50
113	40.5	39.2	42.26
77	57.2	55.4	60.50

[a] $\chi_g = (498/T + 10) \times 10^{-6}$, reference (39).

[b] $\chi_g = (482/T + 10) \times 10^{-6}$, reference (44).

Data Processing

The data obtained with the Faraday balance were processed on an IBM 360 computer using Equation 3 according to the method of Honda and Owen. The method of least squares was used to obtain the best fit to five values of $\Delta f_i/\Delta F_i$ and $1/\Delta H_i$. The gram susceptibility was calculated from the intercept after correction for the container susceptibility was applied. The output list consisted of the temperature, reciprocal temperature, gram susceptibility, and molar susceptibility. The slope and intercept of Equation 3 were printed for each data set along with the uncertainty of the molar susceptibility. A plot of χ_M versus 1/T could be

obtained when desired with the use of the appropriate Fortran message. The molar susceptibilities of samples exhibiting temperature dependent paramagnetism were used to calculate a magnetic moment for the compound. The magnetic moment of a paramagnetic compound can be related to its magnetic susceptibility by the Van Vleck expression, Equation 4 (45, p. 135).

$$\chi_M = (N\beta^2\mu^2/3kT) + \chi_D + \chi_{TIP} \qquad (4)$$

where: χ_M = molar magnetic susceptibility, emu/mole,

N = Avogadro number,

β = magnitude of the Bohr magnetron, erg/gauss,

μ = paramagnetic moment, Bohr magnetrons,

k = Boltzman constant,

T = absolute temperature,

χ_D = molar diamagnetic susceptibility, emu/mole,

χ_{TIP} = Van Vleck temperature independent paramagnetism, emu/mole.

Experimentally, a paramagnetic compound whose susceptibility varies linearly with reciprocal temperature is said to obey the Curie law. The magnetic moment of such a compound is obtained from the slope of a plot of χ_M versus $1/T$ by the application of Equation 4. The intercept yields the sum of the diamagnetic and temperature independent paramagnetic

susceptibilities. The magnetic susceptibility of a great many paramagnetic compounds deviates from the requirements of the Curie law in a way which may be described by a simple modification of the law, the Curie-Weiss law given in Equation 5.

$$\chi_M = (C/T-\theta) + \chi_D + \chi_{TIP} \qquad (5)$$

where θ is a constant and C is $N\beta^2\mu^2/3k$ as defined for Equation 4. Under some circumstances the origin and magnitude of θ can be accounted for in terms of exchange interactions which tend to order the spins on neighboring paramagnetic ions. However, for the majority of paramagnetic substances which exhibit Curie-Weiss behavior θ is merely an empirical quantity indicating the magnitude of departure from Curie law behavior. Unless magnetic dilution studies are carried out or measurements to temperatures below the Néel or Curie temperatures are performed, one cannot definitely assign θ as a representation of magnetic exchange. The non-linearity of χ_M as a function of 1/T may arise from thermal population of states above the ground state such that the magnetic moment varies with temperature. When a deviation from Curie law behavior occurs the parameter θ in Equation 5 may be varied until a plot of χ_M versus $1/T-\theta$ becomes linear. The moment

can be calculated from the slope of the plot and ($\chi_D + \chi_{TIP}$) can be obtained from the intercept. A moment determined in this manner has significance only if it has been established that θ arises from magnetic exchange. When the origin of θ is unknown one can only calculate μ_{eff} at a specific temperature. The expression for the effective magnetic moment is given by Equation 6.

$$\mu_{eff} = 2.828[(\chi_M - \chi_D)T] \tag{6}$$

where the constant 2.828 was obtained from $(3k/N\beta^2)^{\frac{1}{2}}$ by insertion of the appropriate values of k, N, and β.

When θ is very small compared to the temperature range investigated curvature in the χ_M versus 1/T plot may be observed only at the lowest temperatures. The intercept obtained by extrapolation of the linear portion of the plot then yields a value of ($\chi_{TIP} + \chi_D$). Corrected molar susceptibilities can be obtained according to Equation 7.

$$\chi_M^{corr} = \chi_M - \chi_D - \chi_{TIP} = C/T-\theta \tag{7}$$

Rearrangement of Equation 7 to obtain the reciprocal corrected molar susceptibility given by Equation 8 provides a method for evaluation of θ.

$$1/\chi_M^{corr} = \frac{T}{C} - \frac{\theta}{C} \tag{8}$$

where C is $N\beta^2\mu^2/3k$. Values of μ and θ can be calculated

from the slope and intercept, respectively, of a plot of $1/\chi_M^{corr}$ versus T.

Computer programs were written to calculate the moment from Equation 4 and for variation of θ. The value of θ selected was that which yielded the minimum standard deviation for a least squares analysis of Equation 5.

The magnetic moment can be calculated from the spectroscopic splitting factor g obtained from electron spin resonance also. Equation 9 gives the relationship between the moment and the g factor for a specific total spin quantum number S.

$$\mu = g[S(S+1)]^{\frac{1}{2}} \tag{9}$$

Electron spin resonance measurements detect only temperature dependent paramagnetism whereas bulk susceptibility measurements detect the total magnetism of the material.

RESULTS AND DISCUSSION

The magnetic properties of a series of cluster compounds were investigated to elucidate the nature of their electronic configuration. Diamagnetic core corrections used in calculating the corrected molar susceptibility will be considered first. Since the $M_6X_{12}^{3+}$ ions were paramagnetic while the $M_6X_{12}^{4+}$ and $M_6X_{12}^{2+}$ ions were diamagnetic, compounds of the (3+) cluster ion will be discussed next. The temperature independent paramagnetic susceptibilities of the cluster compounds are then considered for all the ions. Magnetic and spectral properties of the discrete cluster ions will then be utilized in the characterization of the phases $TaCl_{2.83}$, $TaBr_{2.83}$, and the non-equilibrium tribromide phase, all of which contain the cluster unit. Chemical properties of these species will also be used in their characterization. Finally the magnetic susceptibilities and infra-red spectra of some d^2 tungsten(IV) halide mononuclear complexes will be discussed in terms of their molecular and electronic configuration.

Diamagnetic Core Corrections

Diamagnetism is present in all substances whether the material exhibits paramagnetism or not. The general procedure

for dealing with diamagnetism in paramagnetic compounds is to calculate its magnitude from additive atomic constants. A measured susceptibility is then corrected to give a value which represents only the paramagnetic susceptibility of the compound. When the diamagnetic component of the susceptibility is very small compared to the paramagnetic component, accurate determination of its magnitude is not essential. However, the diamagnetism of the cluster compounds can be of the same order of magnitude as the paramagnetism. In order to evaluate the magnetic properties of such compounds it becomes important to obtain a more accurate estimate of the diamagnetic susceptibility.

Selwood (46, page 78) lists the diamagnetic susceptibilities of a number of ions which can be used in correcting measured susceptibilities for diamagnetism. Values determined for these atomic constants were based on the assumption that the core electrons were localized on the particular atom. For ionic compounds the diamagnetism can be calculated from such tables of atomic constants which are additive. However, most compounds contain varying degrees of covalency causing delocalization of electrons. Hameka (47) has concluded that it is generally not possible to express molecular

diamagnetism accurately as a sum of atomic contributions since interatomic terms are of major importance. As an example Kaczmarczyk and Kolski (48) have shown that the diamagnetism in boron cluster compounds was significantly larger than the value calculated from atomic constants. Electrons in molecular orbitals of the boron cluster generate a diamagnetism in the same manner as the π electrons of organic aromatic compounds.

The bonding in the metal cluster ions has been described in terms of a molecular orbital scheme by Cotton and Haas (20). The $M_6X_{12}^{2+}$ ion according to their model would have sixteen atomic electrons delocalized over the metal octahedron in eight molecular orbitals. The diamagnetism of an electron in such a large molecular orbital would surely be greater than for an electron localized in an atomic orbital. An estimate of the diamagnetic susceptibility can be obtained from Equation 10 (49, p. 14).

$$\chi_D = \frac{-Ne^2}{6mc^2} \sum_n \bar{r}_n^2 \qquad (10)$$

where: N = Avogadro number,

e = charge on an electron,

m = mass of an electron,

c = velocity of light,

$\bar{r}_n^2$ = square of the mean radius of the n^{th} electron.

If exact wave functions were available for all the electrons in the molecule one could calculate $\bar{r}$ for each electron and, hence, the molecular diamagnetism. Since the necessary wave functions are not available another means must be used to obtain χ_D. A method used by Schneider and Mackay (27) involved extrapolation of the atomic constants for Nb^{5+} and Nb^{4+} to obtain values for $Nb^{2.67+}$, $Nb^{2.50+}$, and $Nb^{2.33+}$ which correspond to the oxidation states of niobium in the (4+), (3+), and (2+) cluster ions, respectively. Their approach neglected delocalization of the bonding electrons into molecular orbitals while their entire characterization of the $Nb_6X_{12}^{n+}$ ions was based on a molecular orbital scheme.

Perhaps a closer approximation can be obtained by assuming the mean radius of each electron in a molecular orbital to be the radius of a sphere passing through the center of the six metal atoms. The size of the metal octahedron has been determined for several compounds by x-ray crystallography. For more accurate calculations tetragonal distortions which have been observed in some cluster compounds would have to be taken into account. The geometrical shapes of the molecular orbitals leading to different symmetries would also lead to

different effective radii. While this is not an exact method based on sound theoretical principles, it seems a better empirical approach than using atomic constants for a molecular problem. Insertion of the appropriate values of the constants in Equation 10 and addition of a term for the atomic diamagnetism of the core electrons of niobium(V), tantalum(V), molybdenum(VI), or tungsten(VI) yields Equation 11.

$$\chi_D = -2.83 \times 10^{10} \sum_n \bar{r}_n^2 + 6\chi_D^{core} \qquad (11)$$

The atomic diamagnetism for the six metal atoms obtained by the extrapolation technique are listed in Table 5 for the niobium, tantalum, molybdenum, and tungsten clusters. The radius of the sphere passing through the metal atoms $\bar{r}$, the number of electrons in molecular orbitals n, and the molecular diamagnetism calculated from Equation 11 are listed for comparison. It can be seen from Table 5 that the molecular diamagnetism exceeds the extrapolated atomic values by ca. 100 emu/mole for all the cluster ions. While these values of the diamagnetic susceptibilities are not exact, they most likely represent the best available values and will be used for all corrections reported in this work. No correction has been introduced for the delocalized electrons of the bridging

Table 5. Atomic and molecular diamagnetic susceptibilities for the six metal atoms in some cluster ions

Cluster ion	$-\chi_D$(atomic) (10^{-6})emu/mole	$\bar{r}$ (10^{-8})cm	n #electrons	$-\chi_D$(molecular + core) (10^{-6})emu/mole
$Nb_6F_{12}^{3+}$	129[a]	1.97[b]	15	220[a]
$Nb_6X_{12}^{2+}$	134	2.05[b]	16	244
$Nb_6X_{12}^{3+}$	129	2.05	15	232
$Nb_6X_{12}^{4+}$	124	2.05	14	220
$Ta_6X_{12}^{2+}$	164	2.05	16	274
$Ta_6X_{12}^{3+}$	158	2.05	15	262
$Ta_6X_{12}^{4+}$	154	2.05	14	250
$Mo_6Cl_8^{4+}$	161	1.86[b]	24	276
$W_6Br_8^{4+}$	222	1.86	24	312

[a]Diamagnetism of six metals only, halogens not included.

[b]Metal-metal distances of 2.80A, 2.90A, and 2.63A were taken as average values to obtain the three values of $\bar{r}$ listed.

halides which certainly must contribute more to the diamagnetism of the cluster ion than they would in a localized atomic orbital. The overlap of an sp^2d hybridized orbital on the metal with a p orbital on the bridging halide would not form a molecular orbital in the sense of those described for the metal cluster. However, the effective radius of the electrons on the halide ion would be enlarged due to delocalization into the metal orbital by the formation of the covalent bond. The size of this contribution to the diamagnetic susceptibility of the cluster ion is not so easily estimated as that part arising from electrons in metal molecular orbitals. The diamagnetic corrections for cations, anions, and ligands involved in this work other than the metal ions of the cluster compounds are listed in Table 6.

Paramagnetic Cluster Compounds

The $M_6X_{12}^{3+}$ ions form compounds which exhibit paramagnetism of the magnitude indicating one unpaired electron per cluster unit. Table 7 lists the magnetic moments of some (3+) cluster compounds along with values of θ and the spectroscopic splitting factor g determined from electron spin resonance studies. The moment calculated from Equation 9 was included when a value of g was available. Only the

Table 6. Diamagnetic core corrections applied to determine $\chi'_M = \chi_M - \chi_D$

$-\chi_D$(cations) (10^{-6})emu/mole		$-\chi_D$(anions) (10^{-6})emu/mole		$-\chi_D$(ligands) (10^{-6})emu/mole	
$(C_2H_5)_4N^+$	108	OH^-	12	H_2O	13
$(C_6H_5)_4As^+$	225	F^-	11	CH_3CN	27
NH_4^+	12	Cl^-	26	C_5H_5N	49
Nb^{5+}	9	Br^-	36	$(C_6H_5)_3P$	167
Nb^{4+}	14	I^-	52		
Ta^{5+}	14	SO_4^-	40		
Ta^{4+}	19				
W^{6+}	13				
W^{5+}	19				
W^{4+}	25				

Table 7. Magnetic properties of some $M_6X_{12}^{3+}$ compounds of niobium and tantalum

Compound	θ (^oK)	μ_{eff}[a] (B.M.)	μ (B.M.)	g	μ(calc)[b] (B.M.)
$(Et_4N)_3Nb_6Cl_{12}Cl_6$	0	1.97	1.65 ± 0.02	1.949	1.69
$(Ph_4As)_2Nb_6Cl_{12}Cl_4(OH)(H_2O)$	0	1.78	1.46 ± 0.01		
$(Et_4N)_2Nb_6Cl_{12}Cl_5(DMSO)_2$	0	1.94	1.50 ± 0.02		
$Nb_6F_{12}F_3$	-1	1.93	1.67 ± 0.02[c]		
$(Et_4N)_3Ta_6Cl_{12}Cl_6$	0	1.87	1.62 ± 0.02	1.922	1.66
$Ta_6Cl_{12}Cl_3 \cdot 6H_2O$	-110	1.71		1.897	1.64
$Ta_6Cl_{12}Cl_3$	-50	1.73			
$Ta_6Br_{12}Br_3$	-125	1.73			

[a]Calculated from Equation 6 at 298^{o}K.

[b]Calculated from $g[S(S+1)]^{\frac{1}{2}}$ with $S = \frac{1}{2}$.

[c]Determined from linear part of χ_M versus 1/T plot, ($T > 90^oK$).

effective moment calculated at 298°K was included for $Ta_6Cl_{15}\cdot 6H_2O$, Ta_6Cl_{15}, and Ta_6Br_{15} since very large values of θ were observed for those compounds. A value of zero for θ indicates Curie law behavior. Susceptibility values of these compounds at several temperatures are listed in Tables 1A-8A of the Appendix.

The magnetic moments of 1.65 and 1.62 B.M. for $(Et_4N)_3Nb_6Cl_{18}$ and $(Et_4N)_3Ta_6Cl_{18}$, respectively, are lower than the spin-only value of 1.73 B.M. for a single electron. Reduction of the magnetic moment via spin-orbit coupling is common for 4d and 5d elements where the spin-orbit coupling coefficient is large. Since the single electron resides in an a_{2u} orbital singlet level, a contribution to the moment from orbital angular momentum can arise only through a second order mixing of excited state functions into the ground term via spin-orbit coupling. Consequently reduction of the moment is not expected to be large. The spin-orbit coupling coefficient is larger for tantalum than for niobium, thus one would expect the tantalum compound to have the lower moment. However, the energy separation between the ground state and the levels coupled with it via the spin-orbit interaction is greater in the tantalum compound. This should

lessen the effect of the larger spin-orbit coupling coefficient for tantalum so that the close agreement between the two moments is not unreasonable.

Electron spin resonance (esr) hyperfine structure for the $Nb_6Cl_{12}^{3+}$ ion in solution was observed by Mackay (27). The symmetrical resonance signal and the even spacing of the hyperfine splitting indicated no anisotropy in the cluster unit and symmetrical delocalization of the single electron over the region of all six niobium atoms. The esr spectra of solid $(Et_4N)_3Nb_6Cl_{18}$ and $(Et_4N)_3Ta_6Cl_{18}$ were symmetrical and the moments calculated from g factors were in close agreement with those obtained from susceptibility measurements. The observed Curie law behavior of these compounds was consistent with an isolated symmetrical ion having all six coordination sites on the cluster occupied with non-bridging identical ligands. The Curie law behavior for $(Ph_4As)_2Nb_6Cl_{12}Cl_4(OH)(H_2O)$ indicated that asymmetry in the coordination sphere of the six ligands does not alter the energy levels of the ground state significantly. The absence of magnetic exchange would suggest that no bridging exists between cluster units in the crystalline solid. The low moment of 1.46 B.M. most likely can be attributed to contamination by the diamagnetic

$Nb_6Cl_{12}^{4+}$ ion.

A product obtained from the reaction of $(Et_4N)_3Nb_6Cl_{18}$ in dimethylsulfoxide (DMSO) with one equivalent of $AgClO_4$ gave the following analytical results.[1]

Anal: Calcd. for $[(C_2H_5)_4N]_2[(Nb_6Cl_{12})Cl_5][(CH_3)_2SO]_2$: Nb, 35.3; Cl, 38.2; C, 15.2; H, 3.32. Found: Nb, 35.3; Cl, 38.4; C, 15.4; H, 3.49.

Since the formula of this complex suggested asymmetry in the coordination sphere, the susceptibility was measured to compare with the previously mentioned behavior of $(Ph_4As)_2Nb_6Cl_{12}Cl_4(OH)(H_2O)$. Curie law behavior was observed and a moment of 1.50 B.M. was obtained. In this case it is possible that the sample contained an impurity of $Nb_6Cl_{12}^{2+}$, which would lower the observed moment since it is diamagnetic. Such an impurity may have resulted from reduction of the $Nb_6Cl_{12}^{3+}$ unit in DMSO, which is known to quantitatively effect reduction of $Nb_6Cl_{12}^{4+}$ to $Nb_6Cl_{12}^{3+}$.[1]

The magnetic susceptibilities of $Nb_6Cl_{15}\cdot 7H_2O$ and $Ta_6Cl_{15}\cdot 7H_2O$ have recently been reported by Schäfer and Spreckelmeyer (50). The values for $Ta_6Cl_{15}\cdot 7H_2O$ agree favor-

---

[1]Grindstaff, W. K., Ames, Iowa. On the preparation of substituted niobium halide cluster compounds. Private communication. 1967.

ably with those obtained in this work; however, measurements at only three temperatures were reported. The magnitude of the susceptibilities for the niobium compound was greater than that of the tantalum compound at all temperatures. Variation of θ to make the plot of χ_M versus $1/T-\theta$ linear for $Nb_6Cl_{15}\cdot 7H_2O$ using Schäfer's data yielded a value of *ca.* -200^oK. The intercept of the linear plot yielded a value of *ca.* -1100×10^{-6} emu/mole which was unreasonably large since χ_D(calc) equals only -625×10^{-6} emu/mole.

The esr spectrum of solid $Ta_6Cl_{15}\cdot 6H_2O$ indicated that anisotropy was present in the cluster unit. The compound exhibited deviation from Curie law behavior with a value of -110^oK for θ. The apparent distortion of the cluster could cause alterations in the ordering and separation of the molecular energy levels. Thermal population of levels close to the ground state could then cause deviation from Curie law behavior. Curie-Weiss behavior arises from magnetic exchange interaction, which in the case of the large cluster ions would most likely occur via superexchange through bridging ligands.

A g factor of 1.897 for $Ta_6Cl_{15}\cdot 6H_2O$ yields by Equation 9 a value of 1.64 B.M. for μ compared to 1.71 B.M. for μ_{eff}

calculated from Equation 6. The close agreement between μ and μ_{eff} could be regarded as an indication that χ_{TIP} is small. The larger difference between μ and μ_{eff} for $(Et_4N)_3$ Ta_6Cl_{18} reflects a large value of χ_{TIP}. However, the presence of diamagnetic (2+) and (4+) cluster ions as an impurity in $Ta_6Cl_{15}\cdot 6H_2O$ could cause the value of μ_{eff} to be low. Comparison of μ and μ_{eff} would then be invalid. In any case, there appears to be a significant difference between the environments of the $Ta_6Cl_{12}^{3+}$ ion in $(Et_4N)_3$ Ta_6Cl_{18} and $Ta_6Cl_{15}\cdot 6H_2O$.

The crystal structure of $Ta_6Cl_{14}\cdot 7H_2O$ reported by Burbank (12) described the cluster as an elongated octahedron with two chloride ions and four water molecules occupying the coordination sites as indicated by the formula $[Ta_6Cl_{12}Cl_2$ $(H_2O)_4]\cdot 3H_2O$. The chlorides were trans to each other along the elongated axis. One might expect $Ta_6Cl_{15}\cdot 6H_2O$ to have three chlorides and three water molecules occupying the coordination sites by analogy to $Ta_6Cl_{14}\cdot 7H_2O$. The apparent distortion of the metal octahedron in $Ta_6Cl_{15}\cdot 6H_2O$ indicated by esr studies would then be consistent with this model according to the rules set forth by Burbank (12). His contention was that four negative ligands lead to flattening of

the cluster, two negative ligands lead to elongation, and six negative ligands leave the equilibrium symmetry undisturbed. Presumably three and five negative ligands distort the cluster in some manner also. Burbank also proposed that the tantalum cluster is subject to large deformations while the niobium cluster is not. The basis for such a proposal comes from two sources. First, Robin and Kuebler (21) contended that splitting of some of the absorption maxima in the electronic spectra of tantalum cluster ions was caused by distortion of the metal octahedron. They claimed the splitting was absent in the spectra of the analogous niobium ions. All ions were measured in aqueous solution. Mackay (27) showed that it was possible to assign a one to one correspondence in the absorption maxima of the niobium and tantalum ions. McCarley and Espenson (15) showed that the spectrum of $Ta_6Cl_{12}^{4+}$ reported by Robin and Kuebler (21) was actually the spectrum of $Ta_6Cl_{12}^{3+}$ which along with the observation of Mackay spoils their argument for distortion. The second source of information was the crystal structures of Nb_6Cl_{14} (10) and Ta_6I_{14} (11). The difference between the long and short metal-metal distances was 0.06A for the niobium compound and 0.275A for tantalum. However it is possi-

ble that this large difference is caused more by the different halogen atoms than by the metal atoms in the two cases.

If one assumes that deviation from Curie law behavior arises from distortion of the metal octahedron, it would follow that the compounds $(Ph_4As)_2Nb_6Cl_{16}(OH)(H_2O)$ and $(Et_4N)_2Nb_6Cl_{17}(DMSO)_2$ are not distorted. However, if the niobium cluster is not subject to large deformation, the fact that θ is ca. -200^oK for $Nb_6Cl_{15}\cdot 7H_2O$ and only -100^oK for $Ta_6Cl_{15}\cdot 7H_2O$ (50) cannot be rationalized in terms of a distorted metal octahedron. There appears to be insufficient evidence to prove that the niobium cluster is not subject to large deformations. One must consider magnetic exchange as the cause of deviation from Curie law behavior also. Since $(Ph_4As)_2Nb_6Cl_{16}(OH)(H_2O)$ and $(Et_4N)_2Nb_6Cl_{17}(DMSO)_2$ are most likely represented by fully coordinated non-bridging models, magnetic exchange should be weak and unimportant in these compounds.

The structures of Nb_6Cl_{14} (10) and Ta_6I_{14} (11) involve intercluster bridging by both terminal and inner halogen atoms as indicated by the formulation $(M_6X_{10}X_{2/2})X_{2/2}X_{4/2}$. Since these two compounds are diamagnetic no exchange takes place but they do serve to demonstrate bridging in cluster

compounds. The bridging by two different types of halide would be a more reasonable explanation for distortion of the cluster since all six coordination sites are occupied by the same kind of ligand. Schäfer (9) described the crystal structure of $NbF_{2.50}$ as $Nb_6F_{12}F_{6/3}$ indicating three dimensional bridging between undistorted cluster units by the three terminal fluorides. Again all six coordination sites are occupied but distortion is absent since the bridging is the same in all directions. It has been shown from x-ray data that Ta_6Cl_{15} and Ta_6Br_{15} (51) have the same structure as Nb_6F_{15} but a complete single crystal x-ray analysis has not been reported. The susceptibility of all three compounds exhibits deviation from Curie law behavior with θ values of $-1^{o}K$ for Nb_6F_{15}, $-50^{o}K$ for Ta_6Cl_{15}, and $-125^{o}K$ for Ta_6Br_{15}. The molar susceptibility corrected for diamagnetism as a function of reciprocal temperature is shown in Figure 1 for Nb_6F_{15}, Ta_6Cl_{15}, and Ta_6Br_{15}.

One can attribute the observed behavior to an increase in exchange interaction with increasing atomic number of the halogen which is consistent with magnetic exchange observed in other transition metal halide compounds (52, p. 146). The magnetic exchange should increase with increasing ease of

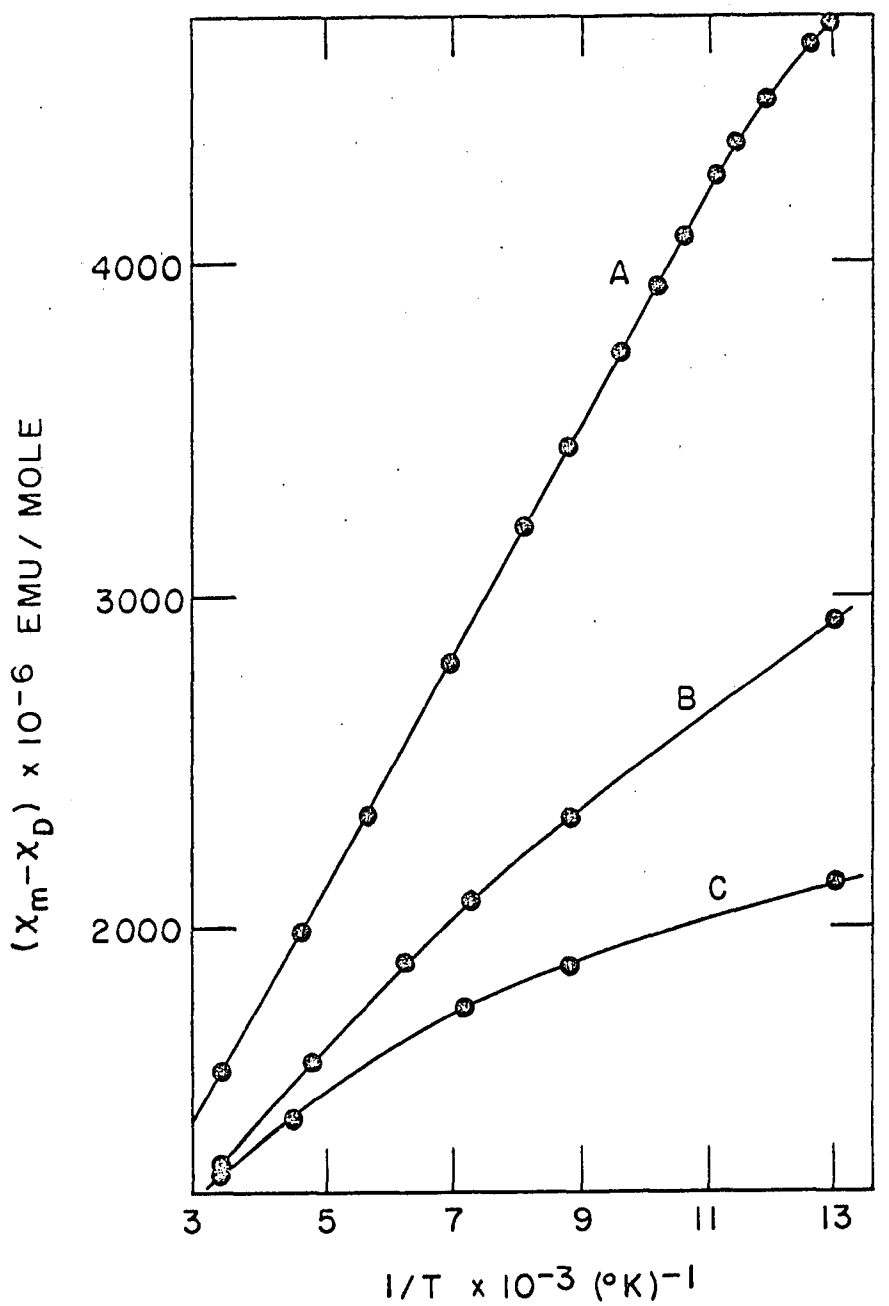

Figure 1. Magnetic susceptibilities of (A) Nb_6F_{15} (B) Ta_6Cl_{15}, (C) Ta_6Br_{15}

polarization of the halide ion (49, p. 168). An electron at one magnetic center must couple with the bonding electrons of the bridging ion which in turn couple with an electron on a second magnetic center. Since polarizability increases from fluoride to bromide the results are consistent with the proposed exchange mechanism.

Non-bridging models for $Ta_6Cl_{15}\cdot 6H_2O$ such as $[(Ta_6Cl_{12})Cl_3(H_2O)_3]\cdot 3H_2O$ and $[(Ta_6Cl_{12})(H_2O)_6]Cl_3$ are not consistent with the magnetic data. X-ray crystal structure data (9,10, 11) previously presented for related compounds suggests that distortion may actually arise due to asymmetric bridging. Models such as $[(Ta_6Cl_{12})Cl_{2/2}Cl_2(H_2O)_2]\cdot 4H_2O$ and $[(Ta_6Cl_{12})Cl_{4/2}Cl(H_2O)]\cdot 5H_2O$ representing one and two dimensional bridging, respectively, are more consistent with the results. Bridging of the cluster ions in this manner could lead to anisotropy in the crystalline solid and magnetic exchange.

A comparison of the molar susceptibilities corrected for diamagnetism as a function of reciprocal temperature is shown in Figure 2 for $(Et_4N)_3Ta_6Cl_{18}$, Ta_6Cl_{15}, and $Ta_6Cl_{15}\cdot 6H_2O$. It is interesting to note that θ is larger for $Ta_6Cl_{15}\cdot 6H_2O$ than for Ta_6Cl_{15}. One would expect the water molecules to produce greater separation of the magnetic ions and reduce

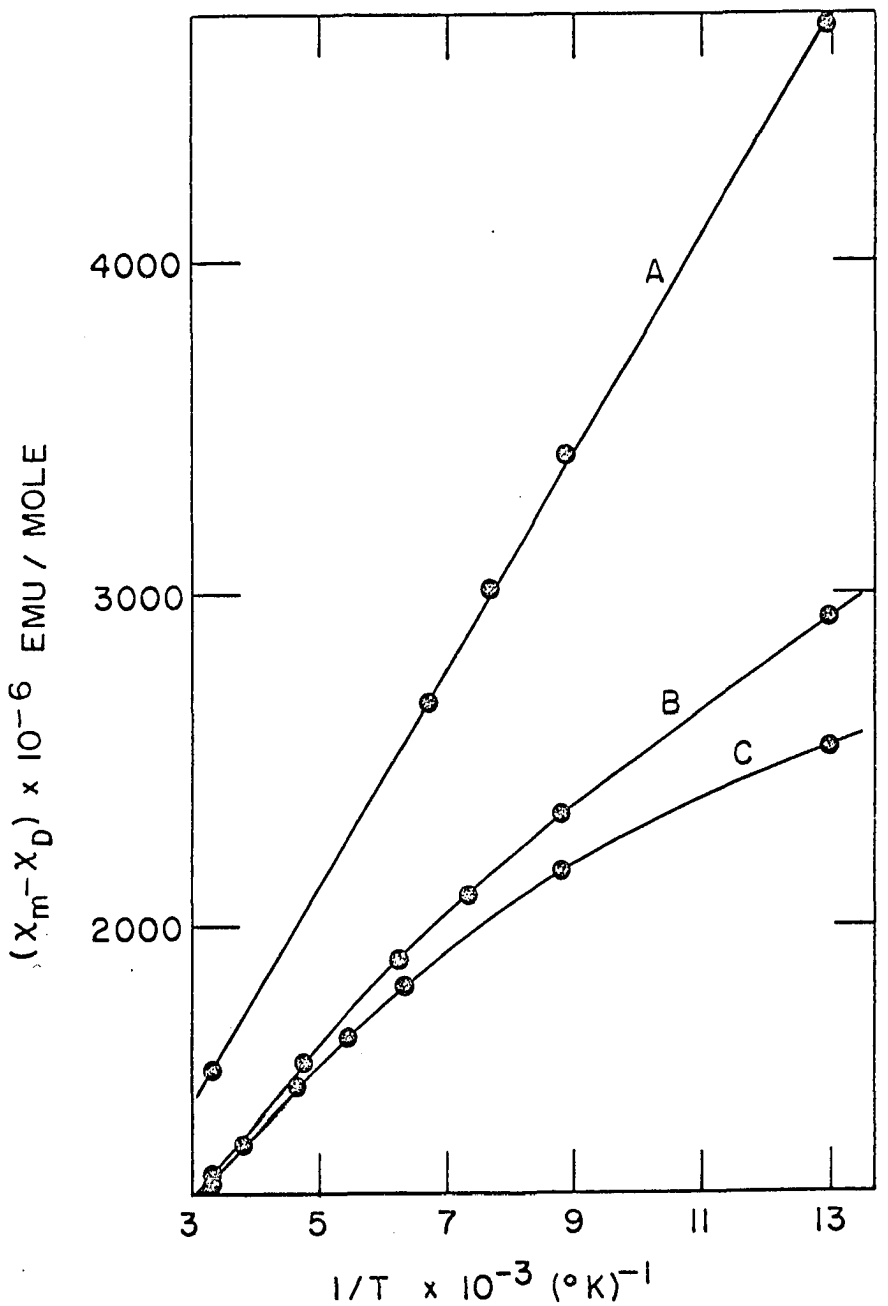

Figure 2. Magnetic susceptibilities of (A) $(Et_4N)_3Ta_6Cl_{18}$, (B) Ta_6Cl_{15}, (C) $Ta_6Cl_{15} \cdot 6H_2O$

magnetic exchange as generally observed upon going from an anhydrous to a hydrated species (46, p. 152). This unusual behavior suggests that magnetic exchange is not the only factor causing deviation from Curie law behavior in $Ta_6Cl_{15}\cdot 6H_2O$.

Before concluding this discussion on the paramagnetic (3+) cluster ions a word about the paramagnetism of $Nb_6Cl_{14}\cdot 7H_2O$ and $Ta_6Cl_{14}\cdot 7H_2O$ reported by Krylov (28) is in order. Molar susceptibilities of $Nb_6Cl_{14}\cdot 7H_2O$ (28) and $Nb_6Cl_{15}\cdot 7H_2O$ reported by Schäfer (50) were the same within $\pm$ 15×10^{-6} emu/mole at all temperatures. Perhaps a more accurate formula would be $Nb_6Cl_{12}Cl_2(OH)\cdot 6H_2O$ indicating the (3+) cluster ion if the reported analytical data for niobium and chloride are correct. It is certainly incorrect to formulate the compound as the (2+) cluster in view of its paramagnetism and deviation from Curie law behavior. Comparison of $Ta_6Cl_{14}\cdot 7H_2O$ (28) and $Ta_6Cl_{15}\cdot 7H_2O$ (50) showed a much larger difference in the molar susceptibilities but clearly indicated the presence of a significant amount of $Ta_6Cl_{12}^{3+}$. The tantalum compound could probably be formulated as a mixture of $Ta_6Cl_{14}\cdot 8H_2O$ and $Ta_6Cl_{12}Cl_2(OH)\cdot 6H_2O$. Slight temperature dependence in the susceptibilities of diamagnetic $Nb_6Cl_{14}\cdot$

$8H_2O$ and $Ta_6Cl_{14}\cdot 8H_2O$ reported by Schäfer (50) can be attributed to contamination by the (3+) ion. The same explanation holds for the weak moments of ca. 0.5 B.M. for $Ta_6Cl_{14}\cdot 10H_2O$, $Ta_6Br_{14}\cdot 8H_2O$, $Ta_6Cl_{12}(SO_4)_2\cdot 7H_2O$, and $Ta_6Br_{14}(SO_4)_2\cdot 7H_2O$ observed by Hughes (29).

Temperature Independent Paramagnetism

Temperature independent paramagnetism arising from the high frequency term in the susceptibility expression derived by Van Vleck (53, p. 277) was observed to be present in all the cluster ions. The high frequency term is given by Equation 12 when $(E_o - E_n \gg kT)$.

$$\chi_{TIP} = -2N \sum_{n,m} (\phi_o,m|\mu_i|\phi_{n,m})^2/jm(E_o-E_n) \qquad (12)$$

where: n and m are quantum numbers,

ϕ_o,m = wave function of the ground state,

$\phi_{n,m}$ = wave function of an excited state,

$\mu_i = \beta(\bar{L}_i+2\bar{S}_i)$, i denotes a coordinate,

j_m = multiplicity of the ground state,

E_o-E_n = energy separation between the ground and excited state.

Since E_n is greater than E_o the term E_o-E_n will be negative and cancel the minus sign in the expression making χ_{TIP}

positive. The minus sign is sometimes omitted by writing the energy separation term as E_n-E_o. The summation is over all states above the ground state. For an upper state to contribute to the susceptibility, its symmetry representation and that of the ground state must be such that the matrix element $(\phi_{o,m}|\mu_i|\phi_{n,m})$ is non-zero. In order for this to occur the product representation $\Gamma(\phi_{o,m})\cdot\Gamma\mu_i\cdot\Gamma(\phi_{n,m})$ must contain the totally symmetric representation A_1. When E_o-E_n is very large the upper level will contribute very little to the susceptibility even when the matrix element is non-zero. Investigation of the temperature independent paramagnetism of a series of cluster compounds should then provide information about the symmetry and energy separation of the excited states of the cluster ions.

Values of χ_{TIP} for a number of niobium, tantalum, and tungsten cluster compounds are listed in Table 8 along with the oxidation state of the cluster n and the calculated diamagnetic susceptibility. Susceptibilities at specific temperatures are listed in Tables 1A-19A of the Appendix. The value of χ_{TIP} was determined from the intercept of a plot of χ_M versus 1/T according to Equation 4 when Curie law behavior was observed. For compounds exhibiting Curie-Weiss behavior,

Table 8. Temperature independent paramagnetism of some niobium, tantalum, and tungsten cluster compounds

Compound	n+	$-\chi_D \times 10^{-6}$ emu/mole	$\chi_{TIP} \times 10^{-6}$ emu/mole
$(Et_4N)_2Nb_6Cl_{18}$	4	904	618 ± 15
$(Et_4N)_3Nb_6Cl_{18}$	3	1024	652 ± 21
$(Et_4N)_2Nb_6Cl_{17}(DMSO)_2$	3	994	664 ± 20
Nb_6F_{15}	3	385	470 ± 26
$Nb_6Cl_{14}\cdot 8H_2O$	2	612	516 ± 13
$Nb_6Br_{14}\cdot 8H_2O$	2	832	642 ± 6
$(Ph_4As)_2Ta_6Cl_{18}$	4	1168	472 ± 44
$(Et_4N)_2Ta_6Cl_{18}$	4	934	501 ± 23
$(Et_4N)_2Ta_6Cl_{12}Br_6$	4	994	526 ± 12
$(Et_4N)_2Ta_6Br_{18}$	4	1114	544 ± 26
$Ta_6Cl_{14}(OH)_2$	4	538	340 ± 10
$(Et_4N)_3Ta_6Cl_{18}$	3	1054	497 ± 29
Ta_6Cl_{15}	3	552	332 ± 15
Ta_6Br_{15}	3	782	462 ± 10
$Ta_6Cl_{15}\cdot 6H_2O$	3	630	170 ± 12
$(Et_4N)_4Ta_6Cl_{18}$	2	1174	540 ± 30
$(Et_4N)_2W_6Cl_8Cl_6$	4	876	331 ± 14
$(Et_4N)_2W_6Cl_8Br_6$	4	916	295 ± 24

the value of χ_{TIP} was obtained from the intercept of Equation 5 after selection of an appropriate value of θ to produce a linear function. The value of χ_{TIP} thus obtained is valid only if θ is due to magnetic exchange. One must use caution in the interpretation of χ_{TIP} when Curie law behavior is not observed. The high frequency term does not remain independent of temperature when the ground state configuration changes due to thermal population of upper states (i.e., when $E_o - E_n \simeq kT$). Values of χ_D were obtained from Tables 5 and 6 using the value of the molecular diamagnetism for the metal octahedron. Table 9 lists reported values of χ_{TIP} for some cluster compounds along with the reference to the work. Reported values were adjusted to include the molecular contribution to the diamagnetism of the metal octahedron.

The results can be compared to investigate the effect of the metal, the halogen, and the oxidation state upon the magnitude of χ_{TIP}. Selected compounds from Tables 8 and 9 are compared in Table 10 to show trends in the magnitude of χ_{TIP}. The niobium compounds clearly exhibit larger values of χ_{TIP} than the analogous tantalum compounds. Correlation of the absorption maxima in the electronic spectra of niobium and tantalum cluster ions indicates that $E_o - E_n$ should be

Table 9. Reported values of χ_{TIP} corrected for molecular diamagnetism

Compound	n+	$\chi_{TIP} \times 10^{-6}$ emu/mole	Reference
$(Et_4N)_2Nb_6Cl_{18}$	4	552 ± 69	27
$(Et_4N)_3Nb_6Cl_{18}$	3	691 ± 23	27
$Nb_6Cl_{15}\cdot 7H_2O$	3	455[a]	50
$Nb_6Cl_{14}(OH)\cdot 6H_2O$	3	300[a]	28
Nb_6Cl_{14}	2	568	50
$Nb_6Cl_{14}\cdot 8H_2O$	2	528	50
$Nb_6Cl_{14}\cdot 7H_2O$	2	840	21
$Ta_6Cl_{12}(SO_4)_2\cdot 7H_2O$	4	516	29
$Ta_6Br_{12}(SO_4)_2\cdot 7H_2O$	4	623	29
Ta_6Cl_{15}	3	452	50
Ta_6Br_{15}	3	440	2
$Ta_6Cl_{15}\cdot 7H_2O$	3	343	50
$Ta_6Cl_{14}\cdot 8H_2O$	2	408	50
$Ta_6Cl_{14}\cdot 10H_2O$	2	358	29
$Ta_6Br_{14}\cdot 8H_2O$	2	508	29
$Mo_6Cl_8Cl_4$	4	427	54
$Mo_6Cl_8Cl_4$	4	310	55
$(H_3O)_2Mo_6Cl_{14}\cdot 6H_2O$	4	284	55
$(NH_4)_2Mo_6Cl_{14}\cdot H_2O$	4	337	55

[a]Obtained from extrapolation of two highest temperatures.

Table 10. Comparison of χ_{TIP} for some similar cluster compounds

Compound	$-\chi_D \times 10^{-6}$	Compound	$-\chi_D \times 10^{-6}$
(a)		(e)	
$(Et_4N)_2Nb_6Cl_{18}$	618 ± 15	$Ta_6Cl_{12}Cl_2(OH)_2$	340 ± 10
$(Et_4N)_2Ta_6Cl_{18}$	501 ± 23	$Ta_6Cl_{12}Cl_3 \cdot 6H_2O$	170 ± 12
$(Et_4N)_3Nb_6Cl_{18}$	652 ± 21	$Ta_6Cl_{12}Cl_2 \cdot 8H_2O$	408
$(Et_4N)_3Ta_6Cl_{18}$	497 ± 29	(f)	
(b)		$(Et_4N)_3Nb_6Cl_{12}Cl_6$	652 ± 21
$(Et_4N)_2Ta_6Cl_{18}$	501 ± 23	$(Ph_4As)_2Nb_6Cl_{16}(OH)(H_2O)$	594 ± 45
$(Et_4N)_3Ta_6Cl_{18}$	497 ± 29	$(Et_4N)_2Nb_6Cl_{17}(DMSO)_2$	664 ± 20
$(Et_4N)_4Ta_6Cl_{18}$	540 ± 30	$Nb_6Cl_{12}Cl_3 \cdot 7H_2O$	300
(c)		(g)	
$(Ph_4As)_2Ta_6Cl_{12}Cl_6$	472 ± 44	$(Et_4N)_3Ta_6Cl_{18}$	497 ± 29
$(Et_4N)_2Ta_6Cl_{12}Cl_6$	501 ± 23	$Ta_6Cl_{12}Cl_{6/2}$	332 ± 15
$(Et_4N)_2Ta_6Cl_{12}Br_6$	526 ± 12	$(Et_4N)_2Ta_6Br_{18}$	554 ± 26
$(Et_4N)_2Ta_6Br_{12}Br_6$	544 ± 26	$Ta_6Br_{12}Br_{6/2}$	462 ± 10

Table 10. (Continued)

Compound	$-\chi_D \times 10^{-6}$	Compound	$-\chi_D \times 10^{-6}$
(d)		(h)	
$Nb_6Cl_{14} \cdot 8H_2O$	516 ± 13	$(Et_4N)_2Nb_6Cl_{18}$	618 ± 15
$Nb_6Br_{14} \cdot 8H_2O$	642 ± 6	$(Et_4N)_2Ta_6Cl_{18}$	501 ± 23
$Ta_6Cl_{14} \cdot 8H_2O$	408	$Mo_6Cl_8Cl_4$	427
$Ta_6Br_{14} \cdot 8H_2O$	508	$(Et_4N)_2W_6Cl_{14}$	331 ± 14

smaller for niobium. It can be seen from Equation 12 that a decrease in the energy separation between the ground state and the excited states leads to an increase in χ_{TIP} as observed. Certain absorption maxima in the electronic spectra also exhibit a shift to lower energy upon oxidation of the cluster ions from (2+) to (3+) to (4+). Accordingly, one might expect the (4+) ion to exhibit the largest value of χ_{TIP}. Comparison of three analogous tantalum compounds in part b of Table 10 shows that the $Ta_6Cl_{12}^{2+}$ ion has the largest value of χ_{TIP} while the (3+) and (4+) ion are essentially the same. Within experimental error all three ions have the same value for χ_{TIP}. The small difference in χ_{TIP} for the three compounds and the large uncertainty in the reported values prevents one from placing much significance on the differences between these results. The fact that the symmetry of the ground state changes as electrons are removed could account for the failure to observe an increase in χ_{TIP} with oxidation of the cluster ion. The values of χ_{TIP} for $(Et_4N)_2Nb_6Cl_{18}$ and $(Et_4N)_3Nb_6Cl_{18}$ were the same within experimental error as seen from Table 8. The compound $(Et_4N)_4Nb_6Cl_{18}$ could not be obtained for susceptibility measurements.

Part c of Table 10 compares the values of χ_{TIP} for some derivatives of the tantalum (4+) cluster ion. Replacement of the tetraethylammonium cation by the larger tetraphenylarsonium cation appeared to have no effect on the magnitude of χ_{TIP} within experimental error. The ligand field strength of the chloride ion is known to be greater than the bromide ion as indicated by its position in the spectrochemical series. One would expect then that E_o-E_n be greater in the chloride derivatives of the cluster ions than for the respective energy separations in the bromide derivatives. The electronic spectra of the chloride and bromide cluster ions show that equivalent absorption maxima are at lower energy for the bromide. One can then predict that χ_{TIP} of the bromide derivatives would be larger than the values of the similar chlorides. Replacement of the six terminal chlorides with bromide ions and then all eighteen chlorides exhibits an increase in χ_{TIP} as seen in part c of Table 10. However, the uncertainty in the data was greater than the difference in the magnitude of χ_{TIP}. A better example of the influence on χ_{TIP} exerted by the halide can be found in comparison of the (2+) hydrates shown in part d of Table 10. The bromide derivatives of both niobium and tantalum have values of χ_{TIP}

which are ca. 100 emu/mole greater than the analogous chlorides.

Distortion of the metal octahedron, bridging between clusters, and asymmetry in the coordination sphere may effect the symmetry and separation of the molecular energy levels and therefore, the magnitude of χ_{TIP}. Part e of Table 10 shows a marked difference in χ_{TIP} for the tantalum chloride cluster hydrates with n = 2, 3, and 4. The compound $Ta_6Cl_{12}Cl_2(OH)_2$ was obtained by maintaining a dynamic vacuum for several days on the product of the (4+) cluster ion $Ta_6Cl_{12}Cl_4 \cdot 9H_2O$ which had been crystallized from aqueous solution.

Anal: Calcd. for $Ta_6Cl_{12}Cl_2(OH)_2$: Ta, 67.18; Cl, 30.71; Cl/Ta, 2.33. Found: Ta, 66.71, Cl, 30.60; Cl/Ta, 2.34; OH (by difference), 2.69.

These results indicate that the (4+) hydrate must be unstable toward hydrolysis under dynamic vacuum. Hydrolysis of this nature may explain the $M_6Cl_{14}(OH) \cdot 6H_2O$ (28) compounds discussed in the previous section.

In compliance with the tendency of the cluster ions to maintain complete occupation of the six coordination sites the (4+) compound could be formulated as $Ta_6Cl_{12}Cl_{4/2}(OH)_2$.

This arrangement of two dimensional bridging would most likely lead to distortion of the metal octahedron as proposed for $[Ta_6Cl_{12}Cl_{4/2}Cl(H_2O)]\cdot 5H_2O$ in the (3+) cluster compound. The (2+) cluster hydrate is distorted according to x-ray studies (12) and may be written as $[(Ta_6Cl_{12})(H_2O)_4Cl_2]\cdot 4H_2O$ with no halide bridging between cluster units. The magnitude of χ_{TIP} is lower for the hydrated compounds as compared to the compounds $(Et_4N)_{6-n}Ta_6Cl_{18}$ where the oxidation state of the cluster unit is the same. A descent in symmetry of the O_h point group as a consequence of distortion within the metal octahedron should alter the symmetry and separation of the molecular energy levels participating in the high frequency term of the susceptibility. It can be concluded that distortion of the cluster ion does alter these levels and reduces the magnitude of χ_{TIP}. The extremely low value of 170×10^{-6} emu/mole for χ_{TIP} in $Ta_6Cl_{15}\cdot 6H_2O$ cannot be assigned much significance unless the origin of θ has been discerned. It is indicated in Table 9 that χ_{TIP} for $Nb_6Cl_{15}\cdot 7H_2O$ was obtained by extrapolation of the susceptibilities at the two highest temperatures. As mentioned in the previous section, magnetic exchange appears not to be the only cause of deviation from Curie law behavior in this compound. Part f of

Table 10 indicates that asymmetry in the coordination sphere of the cluster ion has little or no effect on the magnitude of χ_{TIP}. A very low value of χ_{TIP} for $Nb_6Cl_{15}\cdot 7H_2O$ may reflect a deformation in the metal octahedron. However, the values of χ_{TIP} for $Nb_6Cl_{15}\cdot 7H_2O$ and $Ta_6Cl_{15}\cdot 6H_2O$ must be considered suspect until the condition ($E_o-E_n \gg kT$) has been shown to be valid.

Part g of Table 10 compares χ_{TIP} for the compounds $Ta_6Cl_{12}Cl_{6/3}$ and $Ta_6Br_{12}Br_{6/3}$ with $(Et_4N)_3Ta_6Cl_{18}$ and $(Et_4N)_2Ta_6Br_{18}$. All four compounds should be undistorted and coordinated by six similar ligands. The compounds $M_6X_{12}X_{6/3}$ where bridging between cluster ions is present clearly show a reduction in the magnitude of χ_{TIP}. Since they exhibit deviation from Curie law behavior the significance of the values obtained for χ_{TIP} is less certain. The compounds $Nb_6Cl_{14}\cdot 8H_2O$ and $Ta_6Cl_{14}\cdot 8H_2O$ have larger values of χ_{TIP} than $Nb_6Cl_{15}\cdot 7H_2O$ and $Ta_6Cl_{15}\cdot 6H_2O$ where deviation from Curie law behavior is observed. Reduction of χ_{TIP} in Nb_6Cl_{14} compared to $(Et_4N)_2Nb_6Cl_{18}$ and $(Et_4N)_3Nb_6Cl_{18}$ may be explained by the small deformation of the metal octahedron observed from x-ray studies of Nb_6Cl_{14} (10). Slight distortion may be present in Ta_6Cl_{15} and Ta_6Br_{15} although preliminary x-ray

studies (51) indicate they are isomorphous with the symmetrical $Nb_6F_{12}F_{6/3}$ (9). It is not clear what effect if any that magnetic exchange may have on the high frequency term of the susceptibility.

Comparison of the (4+) cluster ions of niobium, tantalum, molybdenum, and tungsten chloride is shown in part h of Table 10. It can be seen that χ_{TIP} for the M_6Cl_8 cluster units is about two-thirds that of the M_6X_{12} units. The niobium and molybdenum ions have values of χ_{TIP} ca. 100×10^{-6} emu/mole greater than the corresponding tantalum and tungsten ions. Mackay (27) proposed that χ_{TIP} was greater in $Nb_6Cl_{12}^{4+}$ than in $Mo_6Cl_{12}^{4+}$ because E_o-E_n determined from electronic spectra was greater for the molybdenum cluster. Until accurate M.O. wave functions are available and the matrix elements $(\phi_{o,m}|\mu_i|\phi_{n,m})$ are calculated one cannot assume as did Mackay (27) that the non-zero matrix elements are of the same order of magnitude for the M_6X_{12} and M_6X_8 cluster ions.

Before concluding this section it is important to comment on the one reported value of χ_{TIP} which is totally inconsistent with all other data. The value of χ_{TIP} for $Nb_6Cl_{14}\cdot7H_2O$ reported by Robin and Kuebler (21) was ca. 320×10^{-6} emu/mole greater than that reported here or by

Schäfer (50). Robin observed a measured susceptibility of $+240 \times 10^{-6}$ emu/mole over the temperature range of 42-290°K. A negative value of the same magnitude would yield a value of 360×10^{-6} emu/mole for χ_{TIP} which is ca. 170 emu/mole lower than Schäfer's value. Since all of the compounds studied yielded a negative intercept except Nb_6F_{15} where χ_D was small, it must be assumed that the sign of the force change was incorrectly determined. In no case has a value as large as 850×10^{-6} emu/mole reported by Robin and Kuebler (21) been observed for χ_{TIP} in a cluster compound.

Characterization of the Phases $TaCl_{2.83}$ and $TaBr_{2.83}$

The phases $TaCl_{2.83}$ and $TaBr_{2.83}$ were shown by x-ray powder patterns to be isomorphous; see Table 20A in the Appendix for "d" spacings. Originally the $TaBr_{2.83}$ phase was proposed to be $Ta_6Br_{12}Br_5$ (5) for the following reasons. When this phase was combined with water the $Ta_6Br_{12}^{2+}$ ion was identified in solution by its electronic spectrum and the red-brown insoluble residue was identified as tantalum(IV) oxide. Observation that the $Ta_6X_{12}^{4+}$ ion decomposed in a neutral aqueous solution suggested that the $Ta_6X_{12}^{5+}$ ion also would be unstable in solution. A slow step rupture of the (5+) cluster ion could produce reducing fragments which could

in turn yield $Ta_6X_{12}^{2+}$ ions by rapid reduction of other (5+) ions.

A search for a suitable solvent which would dissolve the compound without decomposition was unsuccessful. It was observed that $TaBr_{2.83}$ either reacted with a selected solvent or was substantially insoluble in it. Dimethylsulfoxide reacted to yield both the $Ta_6Br_{12}^{2+}$ and $Ta_6Br_{12}^{3+}$ ions while N,N'-dimethylformamide produced the $Ta_6Br_{12}^{2+}$ ion the same as water. Methanol alone yielded the 2+ ion, but in a solution of hydrogen chloride in methanol the red (4+) ion was obtained. Acetone yielded the (4+) ion in the presence of air. When $TaBr_{2.83}$ was combined with acetone under vacuum a solution of the $Ta_6Br_{12}^{3+}$ ion was obtained, and about 20% of the total tantalum remained in the insoluble residue. Some of the acetone reacted with the compound to produce a colorless organic product which was separated from the acetone by fractional distillation at ca. 62°C. An infra-red spectrum failed to reveal the identity of this product. The $TaBr_{2.83}$ appeared to be essentially insoluble in acetonitrile.

In order to observe electronic transitions in the $TaBr_{2.83}$ phase the reflectance spectrum of the solid was measured. The resulting spectrum disclosed two broad bands

centered around 375 and 900 mμ. The band centered around 900 mμ appeared to contain absorption maxima at 935 and 840 mμ with a shoulder of lower intensity at ca. 750 mμ. The reflectance spectrum of $Ta_6Br_{12}Br_2$ was significantly different having absorption maxima at 790 and 675 mμ. The minimum absorbance between the two broad bands was observed at 585 mμ in the $TaBr_{2.83}$ phase and at 525 mμ in $Ta_6Br_{12}Br_2$. The reflectance spectrum of the black $Ta_6Br_{12}Br_3$ was similar to that of $TaBr_{2.83}$ except for the shoulder at 750 mμ which was less prominent.

An experiment was designed where the reflectance spectrum of $TaBr_{2.83}$ was measured after exposure of a sample to the atmosphere for varying periods of time. The quartz window on the sample cell was removed to allow exposure and then replaced in order to measure the spectrum. The reflectance spectra of anhydrous $TaBr_{2.83}$ and the material after exposure to the atmosphere for 12, 36, and 108 hours are shown in Figure 3. The peak at 840 mμ increased in intensity and shifted to 850 mμ while the one at 935 mμ showed little change and appeared as a shoulder on the major absorption maximum. The shoulder at 750 mμ increased in intensity and shifted to a discrete peak at 730 mμ. In the absorption

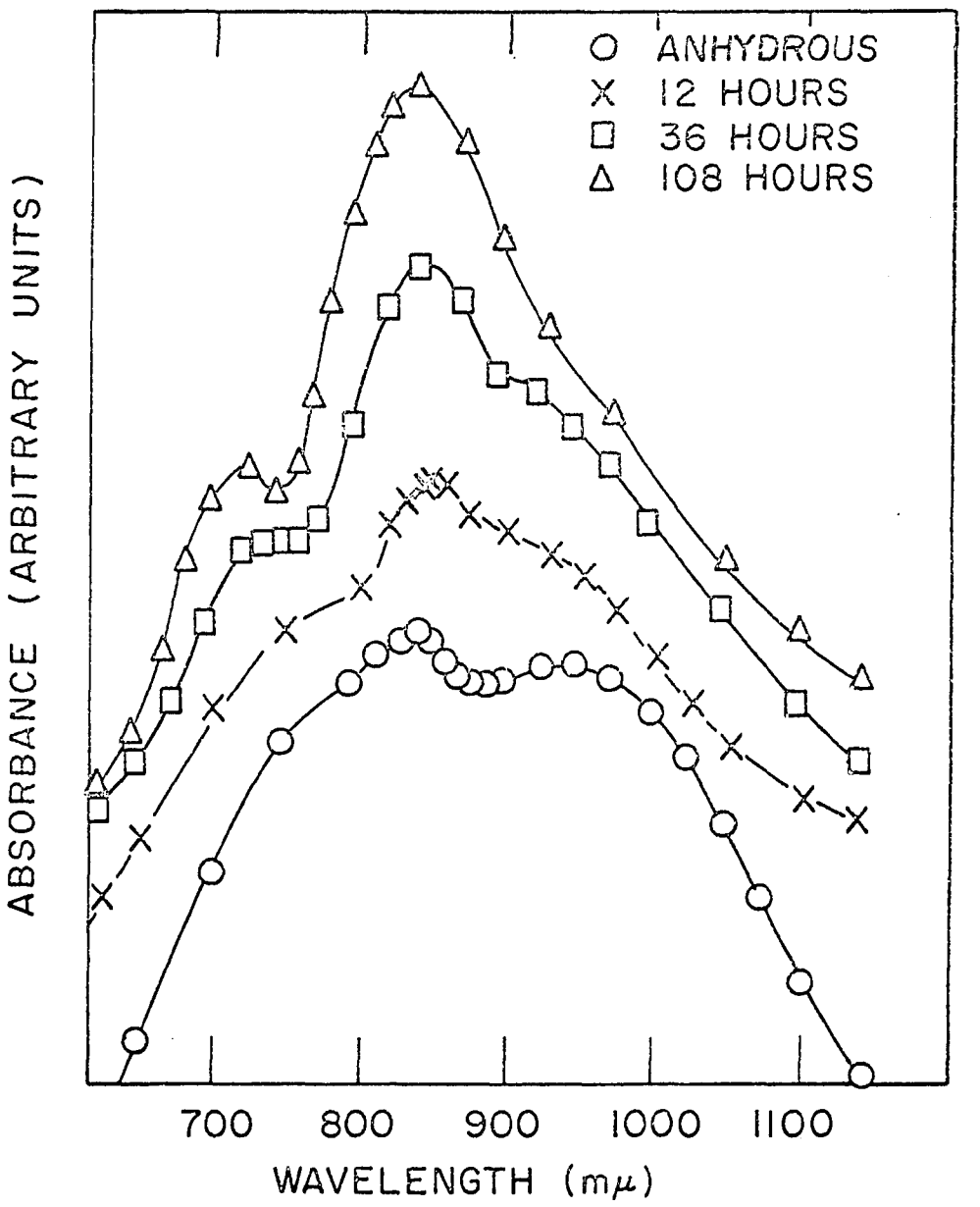

Figure 3. Reflectance spectrum of $TaBr_{2.80}$ exposed to air

spectrum of aqueous $Ta_6Br_{12}^{3+}$ a strong band is found at 868 mμ and a lower intensity peak at 713 mμ. The similarity found on comparing the spectrum of anhydrous $TaBr_{2.83}$ with that of $Ta_6Br_{12}Br_3$, or that of aqueous $Ta_6Br_{12}^{3+}$ with the air-exposed $TaBr_{2.83}$ indicated that the (3+) species is the cluster ion present in the $TaX_{2.83}$ phase. Since the composition of $TaX_{2.83}$ lies between that of TaX_4 and $Ta_6X_{12}X_3$, and both $Ta_6X_{12}^{3+}$ and an easily hydrolyzed tantalum(IV) species appeared to be present, the formula $2Ta_6X_{15}\cdot 3TaX_4$ is proposed to represent the $TaX_{2.83}$ phase more accurately than $Ta_6X_{12}X_5$.

Observed behavior of $TaX_{2.83}$ in water can be readily understood in view of the proposed formulation according to Equation 13.

$$Ta_6X_{12}^{3+} + Ta(IV) = Ta_6X_{12}^{2+} + Ta(V) \qquad (13)$$

The $Ta_6X_{12}^{2+}$ ion dissolves to yield a green solution and the tantalum(V) species is hydrolyzed to the white oxide. Since there are three equivalents of tantalum(IV) and only two equivalents of $Ta_6X_{12}^{3+}$, one equivalent of tantalum(IV) is hydrolyzed to the red-brown oxide. Separation of the insoluble oxides from the green solution of $Ta_6X_{12}^{2+}$ was then used to determine the quantities of tantalum in different valence states. A weighed sample of $TaBr_{2.83}$ was placed in a flask

and mixed with distilled water. The soluble and insoluble portions of the mixture were separated by filtration and analyzed for tantalum. The insoluble residue contained 23.9 percent by weight of the total tantalum while the soluble portion contained 75.75 percent. The values of 20 percent and 80 percent for the insoluble and soluble portions, respectively, are predicted for the formulation $2Ta_6X_{15}\cdot 3TaX_4$. The Br/Ta molar ratio for the mixed valence formulation was calculated to be 2.80. The Br/Ta ratio of 2.83 found by analyses could reflect the presence of some excess $TaBr_4$ in the product. Thus in an effort to remove excess $TaBr_4$ a sample of $TaBr_{2.83}$ was washed with acetonitrile in an evacuated system and analyzed. The following results were obtained.

Anal: Calcd. for $TaBr_{2.80}$: Ta, 44.71; Br, 55.29. Found: Ta, 44.82; Br, 54.60.

The quantitative oxidation of $Ta_6Cl_{12}^{2+}$ to $Ta_6Cl_{12}^{3+}$ by iron(III) was reported by Espenson and McCarley (15). They also observed that the oxidation of the (3+) ion to the (4+) ion required an excess of iron(III) ca. 10^3 times that of the cluster ion. Reaction of material, which gave analysis corresponding to $TaCl_{2.81}$, with solutions containing iron(III) was used to determine the oxidation state of the components.

A weighed sample of $TaCl_{2.81}$ was placed in a beaker under an argon atmosphere. An aliquot of iron(III) solution was added to the sample and the mixture stirred overnight. A red-brown solid product (shown to be a derivative of the $Ta_6Cl_{12}^{4+}$ ion) was removed by filtration and the solution diluted to a known volume. Two aliquots were placed in volumetric flasks, 1,10-phenanthroline was added to one of the solutions, and they were diluted to volume. The absorbance of the $Fe(o\text{-phen})_3^{2+}$ complex was measured at 512 mμ using the other solution without the indicator as a reference solution. The concentration of iron(II) was determined by comparison with the absorbance of standard solutions. The number of moles of $2Ta_6Cl_{15}\cdot 3TaCl_4$ was obtained using a formula weight of 4202 g/mole. This was compared to the number of moles of iron(II) formed in the reaction. Equations 14 and 15 represent the proposed reduction of iron(III).

$$Ta_6Cl_{12}^{3+} + Fe(III) = Ta_6Cl_{12}^{4+} + Fe(II) \qquad (14)$$

$$Ta(IV) + Fe(III) = Ta(V) + Fe(II) \qquad (15)$$

One mole of $2Ta_6Cl_{15}\cdot 3TaCl_4$ should produce five moles of iron(II) when a large excess of iron(III) was present and three moles of iron(II) when the quantity of iron(III) was limited. The results of several determinations are listed in

Table 11. Sample 1 was reacted with a deficiency of iron(III) and essentially all the reagent was reduced to iron(II). The solution was shown to contain $Ta_6Cl_{12}^{3+}$ by spectrophotometric detection of the ion. Samples 2 and 3 were treated with a slight excess of iron(III). All the tantalum(IV) and $Ta_6Cl_{12}^{3+}$ were oxidized in sample 2 so the iron(III) solution was diluted before reaction with sample 3. Some oxidation of $Ta_6Cl_{12}^{3+}$ according to Equation 14 was observed but lowering the concentration of iron(III) retarded this reaction. The fact that the $Ta_6Cl_{12}^{3+}$ ion was in the solid state and not in solution would probably negate the concentration ratio conditions established by Espenson (15). Samples 4 and 5 were reacted with a large excess of iron(III). The number of moles of iron(II) found corresponded to the total number of moles of tantalum(IV) and $Ta_6Cl_{12}^{3+}$ within ten percent. The red-brown solid product collected by filtration was dissolved in methanol, and shown to contain the $Ta_6Cl_{12}^{4+}$ ion by measuring the electronic spectrum of the solution. Thus it was concluded that the experimental results supported the mixed valence formulation $2Ta_6X_{15}\cdot 3TaX_4$ more strongly than the $Ta_6X_{12}X_5$ model. The phase shall henceforth be termed $TaX_{2.80}$. At this point it was of interest to consider evidence bearing on

Table 11. Data from reaction of iron(III) with $TaCl_{2.81}$

Sample number	Sample weight	Moles(10^{-5}) $TaCl_4$	Moles(10^{-5}) Ta_6Cl_{15}	Total # moles(10^{-5})	Moles(10^{-5}) Fe(III) added	Moles(10^{-5}) Fe(II) found
1	0.1354	9.66	6.44	16.1	9.30	9.28
2	0.1281	9.15	6.10	15.2	18.6	15.8
3	0.1160	8.28	5.52	13.8	18.6	11.7
4	0.1951	13.9	9.28	23.2	93.0	21.2
5	0.1505	10.7	7.16	17.9	93.0	19.8

the structural features of the mixed valence species. Cotton and Lippard (56) reported the mixed valence compound $(C_9H_7NH^+)_2(Re_3Br_9)(ReBr_6^{2-})$ containing both a trimeric rhenium cluster unit and the $ReBr_6^{2-}$ ion. In a similar manner one could formulate a model for $TaX_{2.80}$ as $(Ta_6X_{12}^{3+})_2(TaX_6^{2-})_3$. The model $(TaX_2^{2+})_3(Ta_6X_{12}X_6^{3-})_2$ could be a reasonable choice, also, in view of the $[(C_2H_5)_4N^+]_3[Ta_6Cl_{12})Cl_6^{3-}]$ derivative prepared by Meyer (24). The halide acceptor strength of $Ta_6X_{12}X_3$ versus TaX_4 would of course be significant in determining which model would be favored. The alternative to a distinct molecular species of course would be a mixed crystal formulation of the type found by Schäfer (8) for $NbCl_3$ over its homogeneity range. The trihalide was described as a layer lattice with closest packed anions. The homogeneity range was explained by replacement of trimeric clusters of niobium atoms in the interstices with dimeric clusters. The large hexameric cluster of tantalum atoms would not fit into the interstices of closest packed halogen atoms so a scheme different from Schäfer's model would have to be devised. The structural features of the solid must account for the low solubility of the $TaBr_{2.80}$ phase even in solvents like methanol or water. A sample of $TaBr_{2.80}$ also appeared to be

insoluble in an aluminum(III) bromide melt at ca. 250°C and unreactive toward liquid iodine at 150°C.

In order to elucidate the structural nature of the $TaX_{2.80}$ phase, the magnetic susceptibilities and infra-red spectra of the chloride and bromide were investigated. The results are compared with information obtained from similar studies of the discrete cluster ions and their derivatives.

The magnetic susceptibilities of $TaCl_{2.80}$ and $TaBr_{2.80}$ were measured from 77°K to room temperature. Both compounds were found to be paramagnetic, but exhibited a slight deviation from Curie law behavior at lower temperatures as shown in Figure 4. The spectroscopic splitting factor g was determined for these solids at room temperature by electron spin resonance. A value of 1.91 for g was obtained for both the chloride and the bromide. This corresponded to the values of 1.897 for $Ta_6Cl_{15}\cdot 6H_2O$ and 1.922 for $[(C_2H_5)_4N]_3[(Ta_6Cl_{12})Cl_6]$, but is lower than the value of 1.95 for $Ta_6Br_{15}\cdot 6H_2O$. The resonance signal was anisotropic for $Ta_6Cl_{15}\cdot 6H_2O$ but isotropic for the $TaX_{2.80}$ compounds. The isotropic g-factors indicated the absence of distortion within the cluster unit. The various models can be evaluated by comparison of their magnetic moments determined from bulk susceptibility and

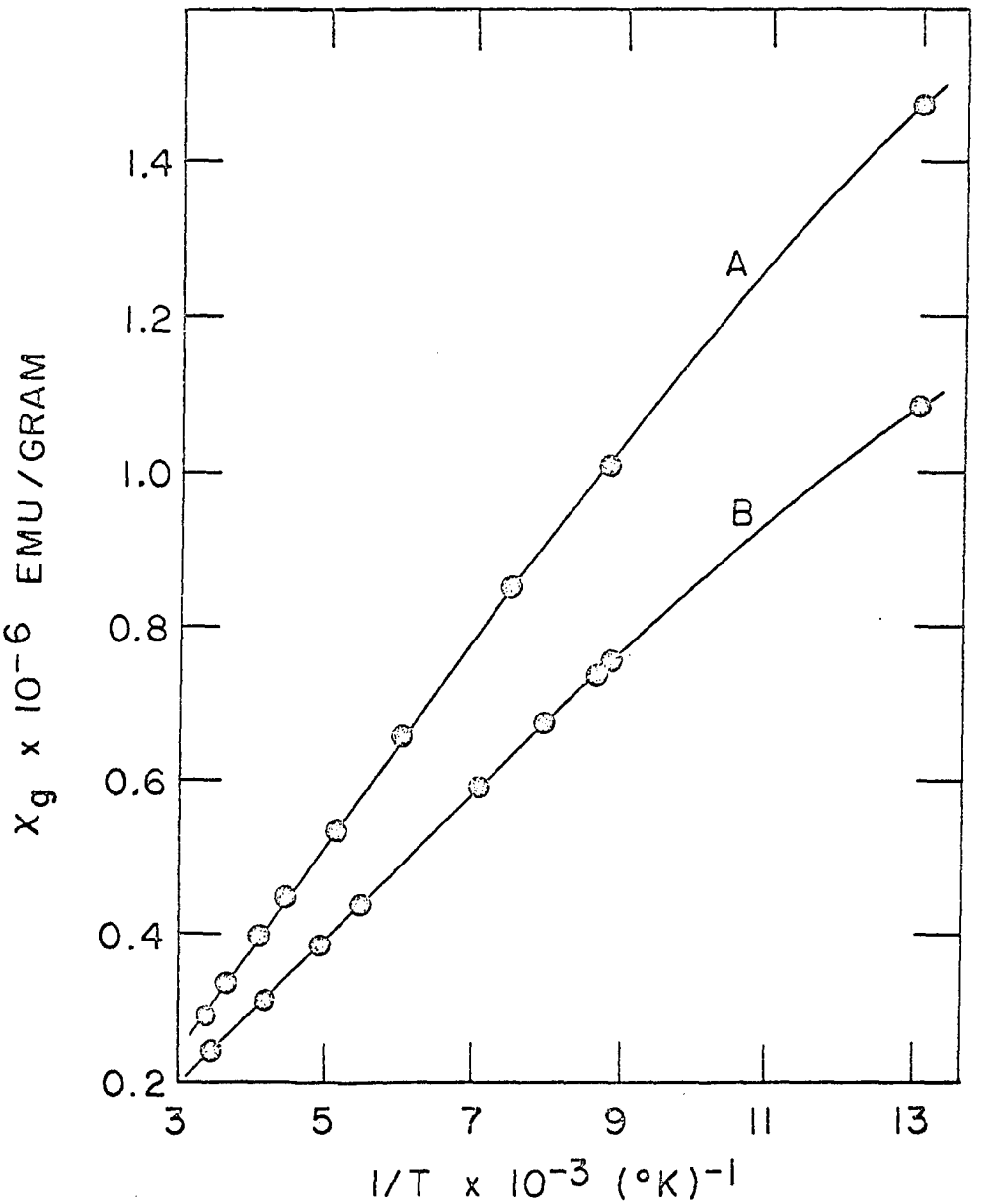

Figure 4. Magnetic gram susceptibilities of (A) $TaCl_{2.81}$ and (B) $TaBr_{2.80}$

electron spin resonance measurements. Treatment of the magnetic data depends upon the molecular configuration of the compound. The magnetic moment can be calculated from the molar susceptibility which depends on the molecular weight of the compound. The molar susceptibility obtained for the $Ta_6X_{12}X_5$ model was different than that obtained for $2Ta_6X_{15} \cdot 3TaX_4$. The models $(Ta_6X_{12}^{3+})_2(TaX_6^{2-})_3$, $(TaX_2^{2+})_3(Ta_6X_{18}^{3-})_2$, and the mixed crystal model would all yield the same molar susceptibility. Rationalization of the magnetic properties of the components for these models can then be used to select the most accurate representation.

The magnetic moment can be calculated from the g factor if one assumes the total spin quantum number S is one half for both the (5+) and (3+) cluster unit. The Cotton-Haas (20) molecular orbital scheme indicates this would be a correct assumption. The product $g(S(S+1))^{\frac{1}{2}}$ yields a moment of 1.65 B.M. for the $Ta_6X_{12}X_5$ model as compared to a moment of 1.42 B.M. determined from susceptibility data. In view of the large difference between the moments determined from esr and susceptibility data, it was concluded that the $Ta_6X_{12}X_5$ model is not an accurate representation of the $TaX_{2.80}$ phase.

In order to compare esr and bulk susceptibility data for

the $(Ta_6X_{12}^{3+})_2(TaX_6^{2-})_3$ model, it was necessary to use the moment of the anion μ_a as well as that of the cation μ_c. The total magnetic moment would then be expressed as $(2\mu_c^2 + 3\mu_a^2)^{\frac{1}{2}}$. The value of μ_c was determined from the g-factor to be 1.65 B.M. and μ_a was reported by Torp (57) to be 0.20 B.M. No resonance would be observed for TaX_6^{2-} at the frequency and field strengths investigated, thus, the g-factor was assumed to be due only to the (3+) cluster ion. The calculated moment was determined to be 2.36 B.M. The moments obtained from susceptibility data were 2.29 B.M. and 2.56 B.M. for the chloride and bromide, respectively. The susceptibility data are presented in Tables 21A and 22A of the Appendix. A plot of χ_M versus $1/T-\theta$ was made linear by variation of the parameter θ. Values of θ were $-16^{\circ}K$ and $-23^{\circ}K$ for the chloride and bromide, respectively. The intercept of the linear plot was then determined and used to correct the molar susceptibility as described in the experimental section. The moment was calculated from the slope of the linear plot.

The $(TaX_2^{2+})_3(Ta_6X_{18}^{3-})_2$ model can be treated in a manner similar to that of $(Ta_6X_{12}^{3+})_2(TaX_6^{2-})_3$. The value of μ_a for the anion would be 1.65 B.M. but μ_c for the cation has not been evaluated. If the order of the crystalline lattice

was such that the tantalum(IV) ion existed in a site of nearly octahedral symmetry, the moment should be close to zero. Distortions producing lower symmetry could increase the moment of the cation. In this regard McCarley and Boatman (58) have reported moments of 0.69 and 0.43 B.M. for the adducts $TaCl_4(C_5H_5N)_2$ and $TaBr_4(C_5H_5N)_2$, respectively. The total moment calculated from the g-factor and an arbitrary value of 0.50 B.M. for the moment of a distorted octahedral tantalum(IV) cationic species would yield a value of 2.49 B.M. for the compound. The result was not significantly different from the previous model to allow differentiation between the two. Consideration of the deviation from Curie law behavior leads one to conclude that the $(TaX_2^{2+})_3(Ta_6X_{18}^{3-})_2$ model is unlikely by comparison to the Curie law behavior of $(Et_4N)_3Ta_6Cl_{12}Cl_6$. The $(TaX_2^{2+})_3(Ta_6X_{18}^{3-})_2$ model has an attractive aspect, however, in that closest packing of the large anions with cations in the interstices provides a means of describing the crystal structure. The $(Ta_6X_{12}^{3+})_2(TaX_6^{2-})_3$ model fails to provide a means of arranging the crystalline lattice such that all six coordination sites on the cation are occupied. All available crystal structure data indicate the six terminal sites on the

M_6X_{12} cluster unit are always occupied (9,10,11,12).

The mixed crystal model must involve bridging of the cluster ions through halogens and possibly halo-tantalum(IV) species to provide occupation of the six coordination sites. This bridging would provide a means for magnetic exchange in these compounds similar to the bridging in the $Ta_6X_{12}X_{6/3}$ compounds. Magnetic dilution should be enhanced by the large halo-tantalum(IV) species. Values of -16^oK and -23^oK for θ in $TaCl_{2.80}$ and $TaBr_{2.80}$ compared to -50^oK and -125^oK in Ta_6Cl_{15} and Ta_6Br_{15}, respectively, are in agreement with this expectation. The mixed crystal model actually should be viewed as intermediate between the $(TaX_2^{2+})_3(Ta_6X_{18}^{3-})_2$ and $(Ta_6X_{12}^{3+})_2(TaX_6^{2-})_3$ models.

The infra-red spectra between 50 and 850 cm^{-1} arising from molecular vibrations were used to obtain information about the molecular configuration of the $TaX_{2.80}$ phases. The absorption maxima for the lower tantalum chlorides and bromides are listed in Tables 12 and 13. Certain bands in the spectra have been assigned to vibrations of the M_6X_{12} moiety by Meyer (24). Absorption maxima near 140, 290, and 330 cm^{-1} for the chloride and 140, 190, and 230 cm^{-1} for the bromide were considered internal vibrations with the 140 cm^{-1} band assigned to a metal-metal mode. A band near 140 cm^{-1} was

Table 12. Infra-red spectra of the lower tantalum chloride phases

$TaCl_4$ (cm^{-1})[a]	$TaCl_{3.03}$ (cm^{-1})	$TaCl_{2.80}$ (cm^{-1})	$TaCl_{2.50}$ (cm^{-1})
386 S	387 W	400 M	
	372 W		
363 S	356 VS	359 S	
		338 VS	331 VS
	311 M	303 W	300 M
	271 W		280 VW
	249 S	250 S	254 M
247 VS		242 S	
	234 S		235 S
	227 S		
212 VW	191 W		191 VW
172 M		177 W	173 W
	164 M		166 VW
	140 W	142 W	143 M
127 M			137 W
	108 VW	117 VW	
100 S	93 VW	95 VW	93 V

[a]Relative intensities; VS = very strong, S = strong, M = medium, W = weak, VW = very weak.

Table 13. Infra-red spectra of the lower tantalum bromide phases

$TaBr_4$ (cm^{-1})[a]	$TaBr_{3.15}$ (cm^{-1})	$TaBr_{2.80}$ (cm^{-1})	$TaBr_{2.50}$ (cm^{-1})	$TaBr_{2.33}$ (cm^{-1})
268 S		272 S	271 M	
253 S		242 S		237 S
	231 VS	233 VS	230 VS	228 VS
220 W	212 W			212 S
		197 S	197 S	192 W
174 VS	184 S			182 S
159 M		165 W	164 M	159 M
	154 VS	150 VS	152 S	147 M
	128 M		144 S	133 S
		122 W		120 W
116 W		115 W		
	106 VW	106 W	108 W	107 M
	101 W	98 W	100 VW	100 W
91 M	92 M	92 VW	94 W	93 W
73	68 W		79 W	84 W
	66 W	62 M	63 M	63 VW
57 VW	56 M			
	48 VW	51 VW	48 VW	48 W

[a]Relative intensity; VS = very strong, S = strong, M = medium, W = weak, VW = very weak.

observed for all the chlorides except $TaCl_4$ but not for the bromides. The phases $TaBr_{2.50}$ and $TaBr_{2.33}$ exhibited maxima at 144 and 147 cm^{-1}, respectively, while all the phases of the bromide system except $TaBr_4$ showed a band at 150 ± 4 cm^{-1}. In order to gain a more complete view of the molecular configuration of the $TaX_{2.80}$ phase it was desirable to have the vibrational spectrum of each of the components involved. An infra-red spectrum of Rb_2TaBr_6 was obtained for evaluation of the $(Ta_6Br_{12}^{3+})_2(TaBr_6^{2-})_3$ model. The compound was prepared according to the method described by Torp (57) and identified from its x-ray powder pattern. Absorption maxima at 212 (VS), 110 (S), 60 (M), and 56 (W) cm^{-1} were observed. The absence of a band near 212 cm^{-1} in $TaBr_{2.80}$ leads one to believe that the $TaBr_6^{2-}$ ion is not present in the phase or is highly distorted. The spectrum of $TaBr_4$ contains several bands which can be correlated to bands in the $TaBr_{2.80}$ phase. A comparison of the absorption maxima for $TaBr_4$, $TaBr_{2.50}$, $TaBr_{2.80}$, Rb_2TaBr_6, $(Ta_6Br_{12})_2(PtBr_6)_3$, and $(Et_4N)_3Ta_6Br_{18}$ is shown in Figure 5. The hexabromoplatinate(IV) derivative was obtained by mixing aqueous solutions of $Ta_6Br_{12}Br_3$ and H_2PtBr_4 followed by slow evaporation and crystallization. Comparison of d spacings obtained from an x-ray powder pattern with those

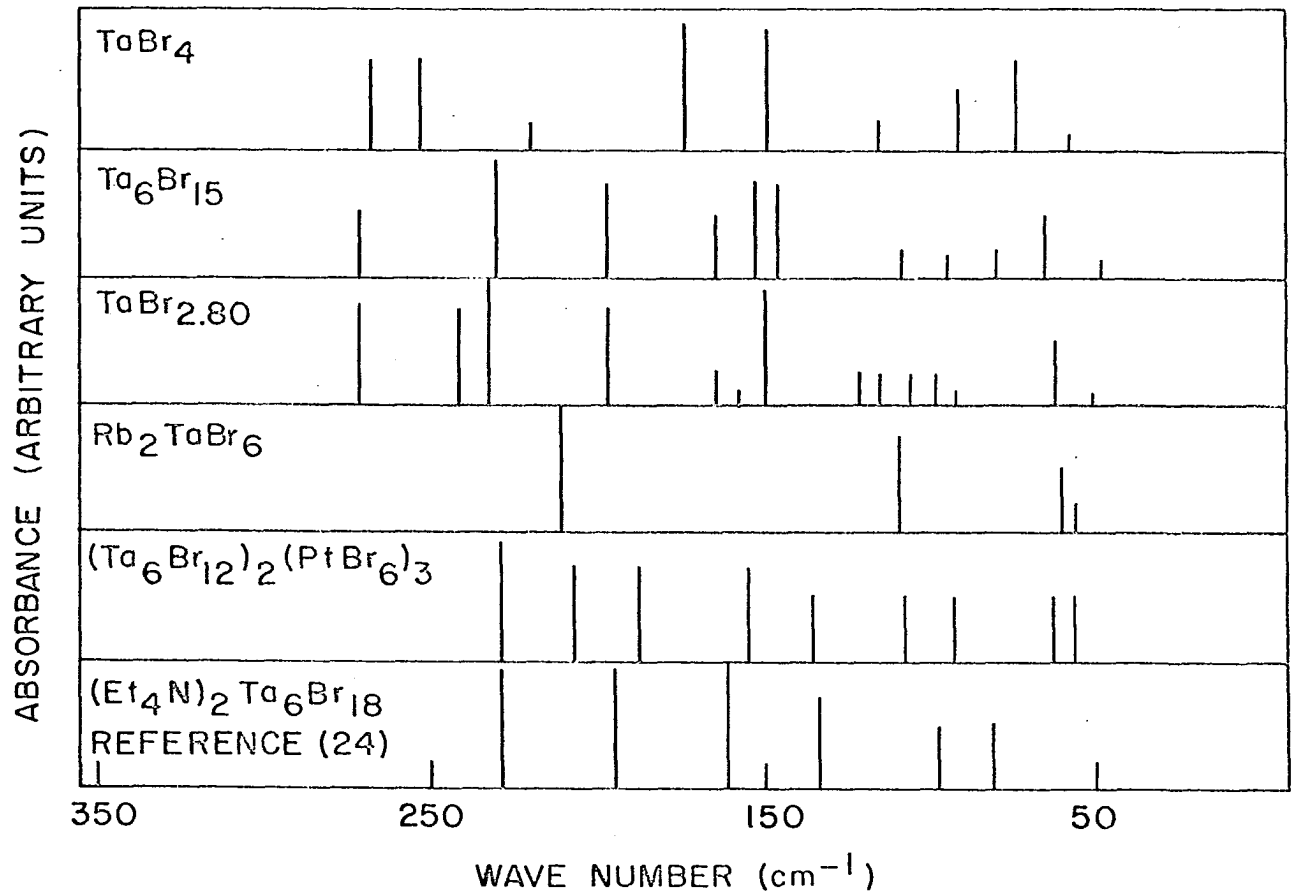

Figure 5. Infra-red spectra of some tantalum bromide compounds related to the $TaBr_{2.80}$ phase

of $TaBr_{2.80}$ is shown in Table 20A of the Appendix. Although x-ray patterns of the two materials were similar a one to one correspondence was not obtained. The weight percent of tantalum in the compound was found to be 34.5 compared to a calculated value of 35.5. Because no water bands were observed in the infra-red spectrum of the product from 50-4000 cm^{-1} the crystals were considered to be anhydrous. Bands at 208 (S), 108 (M), 63 (M), and 56 (M) are near to those of Rb_2TaBr_6 and were assigned to the hexabromoplatinate(IV) ion. Bands at 230 (VS), 188 (S), 155 (S), 135 (M), and 93 (M) were assigned to the Ta_6Br_{12} cluster since they are near the absorption maxima observed for $(Et_4N)_2Ta_6Br_{18}$ by Meyer (24). Comparison of the $TaBr_{2.80}$ and $(Ta_6Br_{12})_2(PtBr_6)_3$ spectra clearly indicate that the $(Ta_6Br_{12})_2(TaBr_6)_3$ model is not an accurate description of the molecular structure. Bands at 272, 233, 197, 164, 150, 106, 98, 92, 62, and 51 cm^{-1} in $TaBr_{2.80}$ correspond closely to bands in the spectrum of $TaBr_{2.50}$. Bands at 272, 242, 115, and 92 correspond to absorption maxima in $TaBr_4$ also. Correlation of the infra-red spectra therefore lends support to the proposed mixed valence species $2Ta_6Br_{15}\cdot 3TaBr_4$ for the $TaBr_{2.80}$ phase. A similar correlation can be obtained for the $TaCl_{2.80}$ phase,

however, the chloride system was studied in less detail. Vibrations due to the tantalum(IV) species in the $TaX_{2.80}$ phase would certainly be altered from those in TaX_4 since the structure of the tetrahalide would be changed according to the model. One cannot then expect the spectrum of $TaX_{2.80}$ to be a super-position of the spectra of TaX_4 and $TaX_{2.50}$.

While x-ray studies would be required to definitely assign the positions of the atoms in the $TaCl_{2.80}$ and $TaBr_{2.80}$ phases, the evidence presented shows that the constituency of these phases can be represented by the mixed valence formulation $2Ta_6X_{15}\cdot 3TaX_4$. The chemical behavior and the electronic spectrum disclose the presence of $Ta_6X_{12}^{3+}$ and tantalum(IV) species in the material. Paramagnetism confirms the presence of $Ta_6X_{12}^{3+}$ ions and the magnetic exchange provides evidence for bridging between the cluster units. Spectral and magnetic properties lead to the conclusion that a mixed crystal model with halide ions and halo-tantalum(IV) species bridging the cluster units is the best representation of the $TaX_{2.80}$ phase.

Non-Equilibrium Tribromide Phase

Observation from x-ray powder patterns that the tribromide was an intermediate in the formation of $TaBr_{2.80}$ led

to further investigation of this species. Boatman (59) reported the tribromide to be a mixture of several substances based on x-ray powder data. Electronic spectra from reflectance measurements on the solid tribromide and $Ta_6Br_{12}Br_2$ showed the $Ta_6Br_{12}^{2+}$ ion to be present in the tribromide. Extraction of the tribromide with acetonitrile and then dry methanol left a green product on the frit of the extractor which yielded a Br/Ta molar ratio of 2.32 upon analysis. Boatman thus concluded that the tribromide was a mixture of $Ta_6Br_{12}Br_2$ and higher bromide species. Schäfer (2) reported a stable tribromide species which had a range of homogeneity with the Br/Ta molar ratio varying from 3.1 to 2.9. The x-ray powder pattern of this material was very similar to that of the niobium trichloride phase (6) containing trimeric and dimeric metal clusters. Comparison of the x-ray powder pattern data indicated that the tribromide reported by Schäfer (2) was different than that observed by Boatman (59). The tribromide investigated in this work gave x-ray diffraction data in agreement with that obtained by Boatman. No product was obtained which yielded powder pattern data in agreement with that reported by Schäfer.

The tribromide material was prepared by aluminum reduc-

tion of tantalum(V) bromide in a 410/320°C thermal gradient. The product was green and yielded the $Ta_6Br_{12}^{2+}$ ion when dissolved in water. Treatment of the tribromide in a 550/25°C thermal gradient yielded $Ta_6Br_{12}Br_2$. A sample having a composition corresponding to $TaBr_{3.15}$ was determined to be diamagnetic with $(10^6)\chi_g$ values of -0.109, -0.123, and -0.141 emu/gram at 77, 114, and 298°K, respectively. A sample having a composition corresponding to $TaBr_{3.16}$ was reported by Schäfer (2) to have a diamagnetic susceptibility of -0.1×10^{-6} emu/gram from 90-295°K. In contrast a sample corresponding to $TaBr_{2.90}$ (2) yielded $(10^6)\chi_g$ values of +0.56, +0.12, and -0.03 emu/gram at 90, 195, and 297°K, respectively. The temperature dependence of this material was similar to that of $TaBr_{2.80}$, but the magnitude of the susceptibilities was smaller for $TaBr_{2.90}$.

Occasionally preparations of $TaBr_{2.80}$ from $TaBr_4$ were suspended before reaction was complete. In these cases mixtures were evident from x-ray powder pattern data and elemental analyses. All compositions between $TaBr_3$ and $TaBr_{2.8}$ were shown to contain mixtures of the tribromide and the $TaBr_{2.80}$ phase. Comparison of x-ray powder pattern data for compositions corresponding to $TaBr_{3.01}$ and $TaBr_{3.43}$ showed a

one to one correspondence of their major lines. The "d" spacings are given in Table 23A of the Appendix. Although the lines of $TaBr_4$ might be expected in the powder pattern of the sample with composition $TaBr_{3.43}$, they were not observed. It should be noted that the constant "d" spacings for the two compositions do not indicate any significant homogeneity range for this phase.

A sample of tantalum trichloride was prepared by reaction of tantalum metal with tantalum(V) chloride in a 630/300 ^{o}C thermal gradient for seven days. The product appeared black, was insoluble in water, and gave the following analytical results.

Anal: Calcd. for $TaCl_{3.00}$: Ta, 62.98; Cl, 37.02. Found: Ta, 62.55; Cl, 37.18; Cl/Ta, 3.03.

X-ray powder pattern data are listed in Table 23A of the Appendix also. Comparison of "d" spacings showed this compound to be the same as the trichloride reported by Schäfer (1), but structurally different from the tribromide reported in this work.

The far infra-red spectra of compositions corresponding to $TaCl_{3.03}$ and $TaBr_{3.15}$ are compared to those of other lower halides in Tables 12 and 13 of the previous section. Two

strong bands at 183 ± 1 and 130 ± 3 cm^{-1} in $TaBr_{3.15}$ and $TaBr_{2.33}$ are absent in $TaBr_{2.80}$ and $TaBr_{2.50}$. In the chloride system major bands at 142 ± 2, 238 ± 4, and 252 ± 3 cm^{-1} were observed in $TaCl_{2.50}$, $TaCl_{2.80}$, and $TaCl_{3.03}$ which possibly indicates a similarity in some of the metal-halogen vibrational modes of these compounds. Significantly, the very strong band at 331 ± 7 cm^{-1} assigned to an internal mode of the M_6Cl_{12} moiety (24) is absent in $TaCl_{3.03}$. However a very strong band does appear at 356 cm^{-1}. Other correlations might be made but insufficient data are available to make them meaningful at this time.

On the basis of results presented here and those reported by Boatman (59) it is proposed that the tribromide can be represented by the formulation $Ta_6Br_{14}\cdot 2TaBr_5$. This mixed valence species has a Br/Ta molar ratio of 3.00 and as noted above does not appear to have a significant homogeneity range. Failure to remove all $TaBr_5$ or $TaBr_4$ from the sample $TaBr_{3.43}$ may account for the higher composition observed. Reaction of Ta_6Br_{14} with $TaBr_5$ at 350°C for three days followed by removal of excess $TaBr_5$ at 225°C yielded an observable quantity of tribromide determined from an x-ray powder pattern. This reaction suggests that $TaBr_5$ may be taken up by Ta_6Br_{14}

via acid-base interaction, e.g. possibly $[Ta_6Br_{12}][TaBr_6]_2$, although this phase cannot be the final equilibrium phase formed under these conditions. Since the tribromide is readily soluble in water and $TaBr_5$ can be extracted free from Ta_6Br_{14} with acetonitrile, the structural nature of this material most likely differs from that of $TaBr_{2.80}$ and $TaBr_{2.50}$, which are thought to be insoluble because of intercluster bridging by the outer halogen atoms.

Mononuclear Tungsten(IV) Complexes

The magnetic susceptibilities of $WCl_4(C_5H_5N)_2$ and $WBr_4(C_5H_5N)_2$ were measured from room temperature down to 77°K as described in the experimental section. Susceptibilities between 77 and 51°K were obtained by Mr. John D. Greiner, Jr. of this laboratory by the Faraday method also. Both complexes exhibited deviation from Curie law behavior as shown in Figure 6. Susceptibility data for these complexes are listed in Tables 24A and 25A of the Appendix. A Néel temperature near 100°K as reported by Peacock and Kennedy (30) was not observed; in this respect the results agreed with those reported by Brown (31). Comparison of $(\chi_M-\chi_D)$ versus 1/T for $WCl_4(C_5H_5N)_2$ between reported values and those reported here are shown in Figure 7.

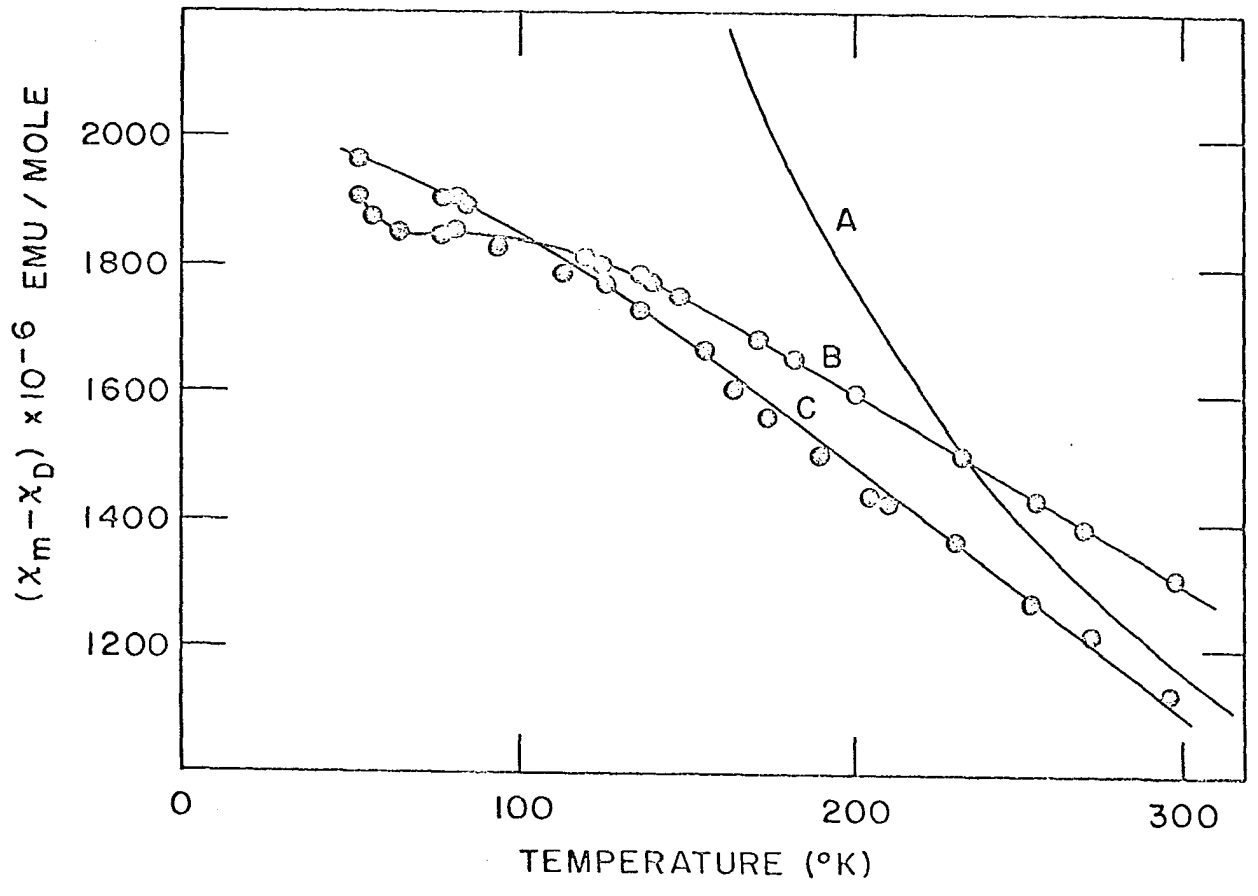

Figure 6. Magnetic susceptibilities of (A) Curie law, (B) $WCl_4(C_5H_5N)_2$, (C) $WBr_4(C_5H_5N)_2$

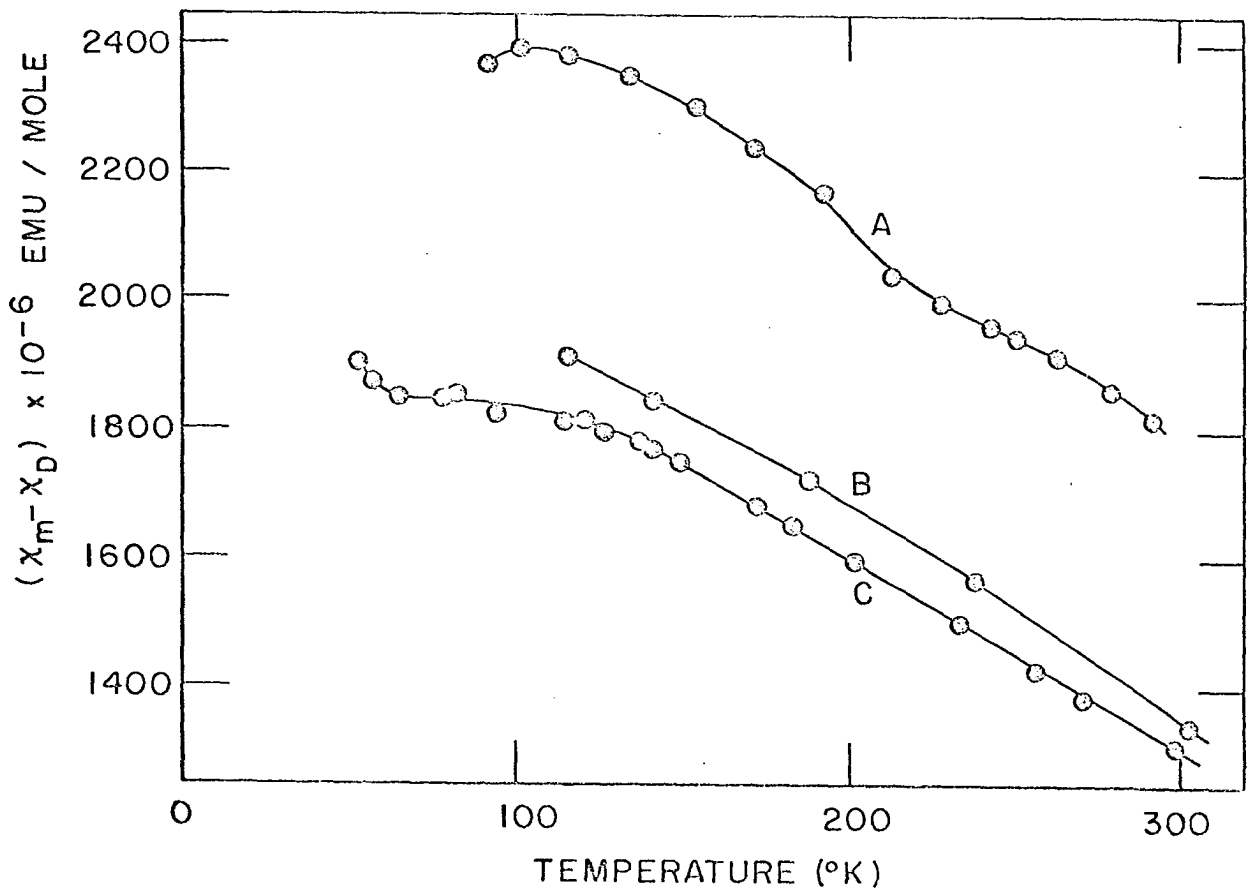

Figure 7. Magnetic susceptibilities of $WCl_4(C_5H_5N)_2$, (A) Peacock (30), (B) Brown (31), (C) this work

Peacock and Kennedy prepared their complexes from K_2WCl_6 and K_2WBr_6 by direct reaction with excess pyridine. The products were washed with acetone and then water. The chloride was reported to be orange and the bromide yellow-green. Brown prepared the complexes from WCl_4 and WBr_4 by direct reaction with pyridine yielding tan chloride and yellow-green bromide products. The complexes were prepared and handled under vacuum or in an inert atmosphere.

Table 14 compares the analytical data for the complexes prepared by Peacock and Kennedy (30) with those by Brown for preparation 1 (31) and preparation 2 (this work). The Cl/W molar ratio of 3.74 reported by Peacock suggests the presence of some tungsten(III) halide complex. Fowles *et al.* (32) reported the formation of $WCl_3(C_5H_5N)_3$ when $WCl_4(CH_3CN)_2$ was reacted with excess pyridine. A significant quantity of tungsten(III) present in the product would explain the large susceptibilities reported for $WCl_4(C_5H_5N)_2$ by Peacock (30). The analytical data indicate also that room temperature effective moments of 2.06 and 2.03 B.M. for the chloride and bromide, respectively, do not accurately represent the tungsten(IV) complexes. The conclusion that $WCl_4(C_5H_5N)_2$ exhibited a Néel temperature was based on one susceptibility

Table 14. Comparison of analytical data for $WCl_4(C_5H_5N)_2$ and $WBr_4(C_5H_5N)_2$

Compound	Reference	% W calcd.	% W found	% X calcd.	% X found	% C_5H_5N calcd.	% C_5H_5N found	X/W found
$WCl_4(C_5H_5N)_2$	(30)	38.00	38.8	29.31	28.0	32.69	34.3	3.74
	(31)	38.00	37.63	29.31	29.13	32.69	32.43	4.01
	(page 17)	38.00	37.71	29.31	29.04	32.69	31.8[a]	3.99
$WBr_4(C_5H_5N)_2$	(30)	27.79	28.1	48.31	48.2	23.90	21.7	3.82
	(31)	27.79	27.52	48.31	47.83	23.90	23.82	4.00
	(page 17)	27.79	27.55	48.31	47.76	23.90	23.2[a]	3.99

[a]Calculated from percent nitrogen determined.

value of 91°K which was lower than the value at 100°K by 0.92 percent. This would hardly seem to be adequate evidence for such a conclusion since it is less than the uncertainty of their measurements.

Brown (31) reported μ_{eff} values at 300°K of 1.81 B.M. for the chloride complex and 1.70 B.M. for the bromide complex. These values are slightly higher than the respective values of 1.77 and 1.67 B.M. obtained in this work, but the agreement is within the uncertainty of the measurements. Effective moments and infra-red spectra for tungsten(IV) chloride and bromide complexes with 2,2'-dipyridyl (dipy) were reported by Hull and Stiddard (33). The two nitrogen atoms in these complexes are constrained to the cis configuration so that comparison with the pyridine (py) complexes can be used to determine their configuration. A value of 1.69 B.M. for μ_{eff} at room temperature for WBr_4(dipy) agrees well with the pyridine complex reported here. A value of 1.64 B.M. for WCl_4(dipy) is quite low if the configuration is the same in $WCl_4 \cdot 2py$ and WCl_4(dipy).

Absorption maxima in the far infra-red spectrum of $WCl_4 \cdot 2py$ and $WBr_4 \cdot 2py$ are compared in Table 15 with those reported by Hull and Stiddard (33) for the 2,2'-dipyridyl

Table 15. Infra-red spectra of some tungsten(IV) halide complexes from 50-850 cm^{-1}

$WCl_4 \cdot 2py$ (cm^{-1})	I[b]	$WCl_4(dipy)$[a] (cm^{-1})	$WBr_4 \cdot 2py$ (cm^{-1})	I[b]	$WBr_4(dipy)$[a] (cm^{-1})
793	W		787	W	
768	M		753	M	
683	M		682	M	
			639	M	
608	W		609	W	
			565	M	
445	M	413	442	M	413
323	S[c]	319[c]	253	S[c]	258[c]
311	S[c]	300[c]	220	S[c,d]	227[c]
253	W				215
220	M[d]				
193	M[d]		201	S[d]	
164	M[e]		122	M[e]	
133	M[e]		92	M[e]	
90	W[e]		63	W[e]	

[a]Reference (33).

[b]Relative intensities; S = strong, M = medium, W = weak.

[c]Metal-halogen stretching mode.

[d]Metal-pyridine stretching mode.

[e]Metal-halogen bending mode.

complexes. All bands above 400 cm^{-1} are assigned to pyridine vibrations. Bands at 319 and 300 cm^{-1} for WCl_4(dipy) correspond to metal-halogen stretching modes of 323 and 311 cm^{-1} observed for $WCl_4 \cdot 2py$. Bands at 258 and 227 cm^{-1} for WBr_4(dipy) correspond to those at 253 and 220 cm^{-1} observed for $WBr_4 \cdot 2py$. These values can be compared to the only infrared-active metal-halogen stretching mode at 306 cm^{-1} for Rb_2WCl_6 and at 220 cm^{-1} for Rb_2WBr_6 (30). Accordingly, one might expect the bands at 227 and 215 cm^{-1} for WBr_4(dipy) to represent metal-halogen stretching modes. These values also correspond to the expected frequency shift due to a change in the reduced mass by replacing chloride with bromide. The band at 258 cm^{-1} for WBr_4(dipy) and 253 cm^{-1} for $WBr_4 \cdot 2py$ are comparable to a very strong band at 246 cm^{-1} for $ZrBr_4 \cdot 2py$ and 258 cm^{-1} for $ZrBr_4$(dipy) which have been assigned (60) to metal-bromide stretching modes. Since the metal-bromide and metal-nitrogen modes have nearly the same frequencies, coupling could possibly cause one or both of these frequencies to be shifted. Accordingly, the bands at 253 and 220 cm^{-1} have been assigned to metal-bromide stretching modes in Table 15. An increase in intensity of the 220 cm^{-1} band upon comparison of $WBr_4 \cdot 2py$ to $WCl_4 \cdot 2py$ has been

interpreted as an accidental degeneracy of a metal-bromide and metal-nitrogen stretching mode. The infra-red spectrum of solid 2,2'-dipyridyl showed bands at 647(VW), 614(W), 430(VW), 403(VS), 167(VS), 94(S), and 70(M) cm^{-1}, none of which can account for the 258, 227, and 215 cm^{-1} bands in WBr_4(dipy). Insufficient data are available at present to confirm molecular configuration of these complexes, but $WCl_4 \cdot 2py$ and WCl_4(dipy) appear to be more similar than their magnetic moments imply.

Allen and Fowles (34) reported that $MoCl_4$(dipy) and $MoCl_4 \cdot 2P(C_6H_5)_3$ yielded a linear plot of χ_M versus 1/T from 90-293°K. They claimed the triphenylphosphine ($P\emptyset_3$) complex had the trans configuration based on its infra-red spectrum which exhibited two bands very close together at 342 and 334 cm^{-1}. The dipyridyl complex which is confined to the cis configuration exhibited bands at 334 and 311 cm^{-1}. Plotting the susceptibility data of Allen and Fowles (34) revealed that $MoCl_4 \cdot 2P\emptyset_3$ was indeed linear in χ_M versus 1/T, but $MoCl_4$(dipy) was curved with a θ value of ca. 30°K. These results suggested that the cis and trans configurations exhibit a difference in their magnetic properties if $MoCl_4 \cdot 2P\emptyset_3$ was actually in the trans form. Beattie and Webster

(61) as well as Harrah (62) reported the infra-red spectrum of $MoCl_4 \cdot 2P\emptyset_3$ to be in agreement with that reported by Allen and Fowles (34). Carmichael, Edwards, and Walton (63) reported susceptibility data for $MoCl_4$(dipy) at twelve temperatures between 81-302°K with a value of 3°K for θ and a linear plot of χ_M versus 1/T over this temperature range.

Due to the proposed trans configuration for $MoCl_4 \cdot 2P\emptyset_3$, the analogous $WCl_4 \cdot 2P\emptyset_3$ was prepared according to the method of Allen and Fowles (34) for the molybdenum complex. Solutions of $WCl_4 \cdot 2(C_3H_7CN)$ (32) and $P(C_6H_5)_3$, when mixed in dry chloroform in an evacuated flask, yielded yellow-orange crystals. The crystals were separated by decantation under vacuum and transferred in the dry-box to an extractor. They were washed free of excess triphenylphosphine by extraction with dry cyclohexane in which the complex was insoluble. Analysis for carbon and hydrogen gave the following results.

Anal: Calcd. for $WCl_4[P(C_6H_5)_3]_2$: C, 50.86; H, 3.56. Found: C, 50.71, 50.67; H, 3.81, 3.74.

The complex appeared to be hydrophobic and unreactive toward the atmosphere but was stored and handled in the dry-box.

The magnetic susceptibilities of $WCl_4 \cdot 2P\emptyset_3$, $WCl_4 \cdot 2py$, Cs_2WCl_6 (30), and K_2WCl_6 (30) are compared in Figure 8. The

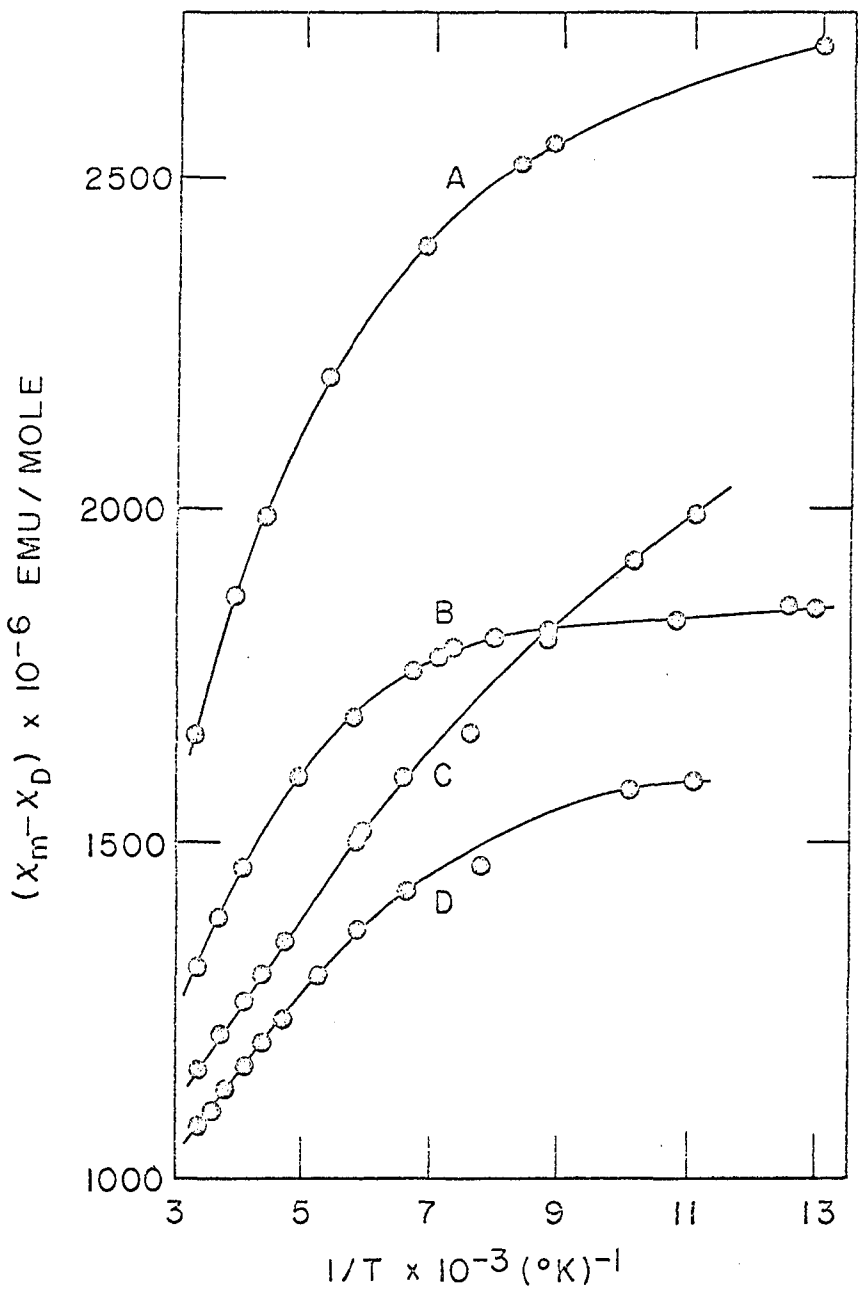

Figure 8. Magnetic susceptibilities of (A) $WCl_4 \cdot 2P\emptyset$, (B) $WCl_4 \cdot 2py$, (C) Cs_2WCl_6 (30), (D) K_2WCl_6 (30)

data for Cs_2WCl_6 and K_2WCl_6 are given so that the behavior of octahedral complexes can be compared to the substituted derivatives of lower symmetry. Susceptibility data for $WCl_4 \cdot 2P\emptyset_3$ are given in Table 26A of the Appendix. Although the susceptibility of $WCl_4 \cdot 2P\emptyset_3$ is a non-linear function of reciprocal temperature, it does not approach temperature independent behavior near 77°K like $WCl_4 \cdot 2py$. The susceptibilities of $WCl_4 \cdot 2P\emptyset_3$ and $WBr_4 \cdot 2py$ are nearly linear functions of temperature down to 77°K.

The infra-red spectrum of $WCl_4 \cdot 2P\emptyset_3$ is compared to the spectra of $WCl_4 \cdot 2py$ and solid $P(C_6H_5)_3$ in Table 16. Peaks at 324 and 316 cm^{-1} for $WCl_4 \cdot 2P\emptyset_3$ were obtained by analysis of a poorly resolved doublet which could be extrapolated to center at 320 cm^{-1}. The band at 292 cm^{-1} is assigned to a metal-phosphorus stretching mode since it is absent in $WCl_4 \cdot 2py$ and $P(C_6H_5)_3$. Ray and Westland (60) assigned bands at 343(S), 324(VS), 303(W) and 278(S) cm^{-1} to metal-chloride stretching modes for the 1,2-bis(diphenylphosphino)ethane complex $HfCl_4$(diph). The phosphorus atoms are confined to the cis configuration in a manner similar to the nitrogen atoms in 2,2'-dipyridyl. Comparison of the absorption maxima in the spectrum of $WCl_4 \cdot 2P\emptyset_3$ with those for $HfCl_4$(diph) discloses

Table 16. Infra-red spectra of $WCl_4(C_5H_2N)_2$, $WCl_4[P(C_6H_5)_3]_2$, and $P(C_6H_5)_3$

$WCl_4(C_5H_5N)_2$		$WCl_4[P(C_6H_5)_3]_2$		$P(C_6H_5)_3$	
(cm^{-1})	I[a]	(cm^{-1})	I[a]	(cm^{-1})	I[a]
608	M	617	W	615	W
		549	S	540	S
		518	VS	510	VS
		503	VS	497	VS
489	VW	488	VS	490	VS
445	M	447	S		
		429	M	429	M
		420	VW	419	M
394	VW	397	VW	398	W
323	S[b]	324	S[b]		
311	S[b]	316	S[b]		
		292	M[c]		
253	W	253	W	252	W
220	M[d]	226	W	213	W
193	M[d]	193	VW	196	M
				186	M
164	M[e]	163	M[e]		
		145	M		
133	M[e]	134	VW		
90	W[e]	120	VW		

[a]Relative intensities; VS = very strong, S = strong, M = medium, W = weak, VW = very weak.

[b]Metal-halogen stretching mode.

[c]Metal-phosphine stretching mode.

[d]Metal-pyridine stretching mode.

[e]Metal-halogen bending mode.

some significant differences with only the band at 324 cm^{-1} being observed for both complexes. The band at 278 cm^{-1} for HCl_4(diph) might belong to a metal-phosphorus stretching mode since it is absent in the analogous diarsine complex (60). It was concluded that infra-red spectra of $WCl_4 \cdot 2P\emptyset_3$ did not provide sufficient evidence to definitely confirm a trans configuration. The assignment by Allen and Fowles (34) of a trans configuration to $MoCl_4 \cdot 2P\emptyset_3$ is subject to question because the band arising from metal-halogen is split by 8 cm^{-1}; only one band is allowed for a trans complex. $WCl_4 \cdot 2P\emptyset_3$ was too insoluble to obtain dipole moment data which could establish configuration as done by Chatt and Rowe (64) for some rhenium halide phosphine complexes.

The magnetic susceptibilities of $WCl_4 \cdot 2py$ and $WBr_4 \cdot 2py$ below 20°K were obtained from mutual inductance measurements by Jelinek[1]. Both complexes exhibited a sharp increase in their susceptibilities near liquid helium temperatures but not of the order observed for ferromagnetic substances. The susceptibilities of $WBr_4 \cdot 2py$ were too small to be detected by the instrument at temperatures above 4.2°K. Susceptibility

---

[1]Jelinek, F., Ames, Iowa. On the low temperature susceptibilities of $WCl_4(C_5H_5N)_2$ and $WBr_4(C_5H_5N)_2$. Private communication. 1966.

data for $WCl_4 \cdot 2py$ and $WBr_4 \cdot 2py$ are listed in Table 17.

Table 17. Magnetic susceptibilities of $WCl_4(C_5H_5N)_2$ and $WBr_4(C_5H_5N)_2$ below 20°K

Temperature °K	$\chi_M \times 10^2$ emu/mole $WCl_4(C_5H_5N)_2$[a]	$WCl_4(C_5H_5N)_2$[b]	$WBr_4(C_5H_5N)_2$[b]
1.3	1.18		.440
1.4		1.085	
1.75	0.98		
1.88		0.964	
2.00	0.86		
2.25	0.78		
2.80	0.62	0.806	
2.98			.303
3.20	0.58		
3.55		0.630	
3.60	0.53		
4.2	0.50	0.490	<0.20
6.7	0.39		
7.3	0.35		
10.0	0.30		
18.0	0.22		>0.17

[a]Preparation #1, reference (31).

[b]Preparation #2, (this work).

A plot of χ_M versus 1/T for $WCl_4 \cdot 2py$ was linear within the uncertainty of the measurements from 2-52°K. The slope of this plot yielded a value of 0.34 B.M. for the magnetic moment of the ground state configuration provided of course that no paramagnetic impurity was present. Susceptibilities at only two temperatures were obtained for $WBr_4 \cdot 2py$ but a moment of ca. 0.14 B.M. was calculated from them. Reduction of the magnetic moment in 5d elements with a less than half filled ground level is expected due to antiparallel coupling between the spin and orbital angular momentum of the unpaired electrons.

In order to discuss the ground state configuration of these d^2 ion complexes, one must make some assumptions about the forces acting on the two unpaired electrons. The free ion has a ^3F ground state under Russell-Saunders LS coupling (65, p. 9). Ernshaw et al. (66) have suggested that an octahedral ligand field in 5d transition metal complexes is strong enough to overcome the Russell-Saunders coupling and lead to a t_{2g}^2 configuration. Electron repulsions within the t_{2g}^2 level lead to a $^3T_{1g}$ state at lowest energy if the sum of the repulsion parameters 3B + C is greater than the single electron spin-orbit coupling constant ξ. Kotani (36) con-

sidered the case where 3B + C is much greater than ζ which applies to the 3d transition elements. Kamimura et al. (37) determined the energy levels arising from the t_{2g}^2 configuration when 3B + C is nearly equal in magnitude to ζ. This situation was proposed to represent the 4d and 5d transition elements more accurately. The degeneracy and ordering of the energy levels obtained by Kamimura et al. (37) were the same as those of Ballhausen (65, p. 121) from application of spin-orbit coupling as a perturbation on the $^3T_{1g}$ state. The two approaches presumably differ only in the energy separation between non-degenerate levels.

Stevens (67) has discussed the splitting of the $^3T_{1g}$ state by an axial component of the ligand field. The low-symmetry field parameter δ was introduced to represent the energy separation between the ^3E and $^3A_2$ levels resulting from splitting of the $^3T_{1g}$ state. A positive value was assigned to δ when the $^3A_2$ state was of lower energy and a negative value when the ^3E state was lowest. Ballhausen (65, p. 232) has shown how spin-orbit coupling can partially remove the degeneracy of the ^3E and $^3A_2$ states. The resulting levels have a total angular momentum represented by M_J values of $\pm$ 2, $\pm$ 1, and 0 in units of $h/2\pi$. There are three non-

degenerate levels with M_J equal to zero, two doubly degenerate levels with M_J equal to $\pm$ 1, and one double degenerate level with M_J equal to $\pm$ 2. An atom whose ground state has the quantum number M_J equal to zero is in a non-magnetic state and has a moment equal to zero. Atoms having a ground state with M_J equal to $\pm$ 1 and $\pm$ 2 have a finite magnetic moment so that the magnetic properties of complex will depend on the ordering and separation of the energy levels. The energy separation of the levels is a function of the magnitude of $3B + C$, ξ, and δ. Ordering of the non-degenerate and doubly degenerate levels depends upon the sign of δ and perhaps the relative magnitude of $3B + C$, ξ, and δ. A ligand field component of lower than axial symmetry (i.e., lower than tetragonal or trigonal symmetry) could possibly remove all remaining degeneracy of the levels. Alteration of the magnetic moment can also arise from delocalization of magnetic electrons away from the metal ion. Figgis *et al.* (68) have treated this problem by introducing a delocalization factor k into the magnetic moment operator of the form $(k\bar{L} + 2\bar{S})\beta$.

The d^2 tungsten(IV) complexes under consideration here have a positive value for λ which is equal to $\xi/2$ while δ may be positive or negative. Kamimura (35) has presented a

lengthy and complex expression for the magnetic moment of the d^2 ion as a function of λ, δ, and temperature. When the low symmetry field component is removed (i.e., $\delta = 0$) this expression should reduce to the cubic field equation given by Kotani (36). It was observed that certain squared terms in Kamimura's equation must be raised to the fourth power before Kotani's equation could be obtained by setting δ equal to zero. Computer evaluation of Kamimura's magnetic moment expression was reported by Terezakis and Carlin (69) but the inconsistency of the squared terms was not mentioned. They reported that the theoretical expression of Kamimura (35) could not be fitted to experimental data by varying λ and δ. The magnetic moment expression, with the squared terms raised to the fourth power, was evaluated on an IBM 360 computer by the author from 2-300°K. The results did not agree with the experimental values either in magnitude or in temperature dependence. The magnetic moment exhibited only slight change for large variations of both λ and δ. Values of 100, 600, 1100, 1600, and 2100 cm^{-1} were used with λ positive and δ negative. Positive values of δ produced a negative square root in some of the terms and could not be evaluated. Energy level diagrams (35) showed a doubly degenerate level at low-

est energy when δ was negative and a non-degenerate level lowest for δ positive.

Theoretical treatments of the d^2 ion presently available appear inadequate to provide a quantitative description of the magnetic properties of the tungsten(IV) complexes. One can, however, draw some conclusions of a qualitative nature from the experimental data in terms of possible ground state configurations. The magnetic moment of 0.34 B.M. for $WCl_4 \cdot 2py$ is constant below 50°K and rises to a value of ca. 1.3 B.M. at 300°K. Since the moment is not zero at lower temperatures a level corresponding to M_J equal to zero is not likely to be lowest. Proof by trace element analyses and esr measurements that paramagnetic impurities were not present would be valuable in confirming that the low temperature moment is not zero. The fact that the moment increases with increasing temperature suggests that one or more levels having greater angular momentum than the ground state are being thermally populated. While the moment increases at higher temperatures which tends to increase χ_M, thermal agitation inhibits alignment of the moment with the external field, thus reducing the susceptibility. It is possible that these opposing factors are the reason for χ_M exhibiting a linear

relationship to temperature above 150°K. When the moment becomes constant below 50°K the susceptibility exhibits a normal 1/T relationship. One might expect a maximum in the χ_M versus 1/T plot where the influence of temperature on the susceptibility is equivalent to that of the changing moment. However, the small energy separation between the ground and excited levels (E_o - E_n) makes the high frequency term of the susceptibility very large. A value of *ca.* 1700×10^{-6} emu/mole can be estimated for χ_{TIP} of $WCl_4 \cdot 2py$ below 50°K from a χ_M versus 1/T plot. Population of the excited levels reduces the magnitude of the high frequency term based on an estimate determined from extrapolation of the limiting slope at 300°K. Reduction of the high frequency term in this manner may compensate for the increase in the low frequency term such that a maximum in χ_M is not observed. Temperature independent susceptibilities comparable to that of $WCl_4 \cdot 2py$ have been reported by Ernshaw *et al.* for some d^4 complexes of rhenium, osmium, and iridium.

The d^4 ion has an energy level configuration similar to that of the d^2 ion in the strong field case except that certain levels are inverted since λ equals $-\xi/2$. Magnetic properties of the octahedral d^4 complex $(NH_4)_2RuCl_6$ (38) are

very similar to those of $WCl_4 \cdot 2py$ down to ca. 70°K, while susceptibilities of Cs_2WCl_6 (30) have a temperature dependence similar to those of $RuCl_4(dipy)$ (38). Thus, it appears that the ground states of d^2 and d^4 ions become similar when the distorted octahedral configuration of one is compared to the undistorted configuration of the other.

The low temperature moment of ca. 0.14 B.M. for $WBr_4 \cdot 2py$ compares reasonably well with that of the analogous chloride, but has not been proven to be constant since χ_M was determined at only two temperatures. The susceptibilities of $WBr_4 \cdot 2py$ and $WCl_4 \cdot 2py$ do appear to have a similar temperature dependence below 4.2°K, however. $WBr_4 \cdot 2py$ exhibits a nearly linear relationship of χ_M to temperature down to 77°K. This suggests that the energy separation between the ground state and first magnetic excited state is smaller than for $WCl_4 \cdot 2py$ where χ_M is linear down to only ca. 150°K. A χ_{TIP} value of ca. 2300×10^{-6} emu/mole below 4.2°K for $WBr_4 \cdot 2py$ supports the contention that $(E_o - E_n)$ is smaller for the bromide. McCarley and Boatman (58) have shown that δ is larger in $TaCl_4 \cdot 2py$ than in $TaBr_4 \cdot 2py$. Since λ should be nearly the same in $WCl_4 \cdot 2py$ and $WBr_4 \cdot 2py$, δ must be responsible for the change in $(E_o - E_n)$.

The susceptibilities of $WCl_4 \cdot 2P\emptyset_3$ cannot be compared to those of $WCl_4 \cdot 2py$ quite so easily. The relative values of δ in the two complexes have not been evaluated and their molecular configurations could possibly be different. The linear relationship of χ_M to temperature for $WCl_4 \cdot 2P\emptyset_3$ extends down to $77^{\circ}K$ but without data at lower temperatures the moment of the ground state cannot be determined. The results of this work clearly show that the problem is still in the embryonic stage and a great amount of information will be required for its solution.

SUMMARY

A Faraday balance was constructed and calibrated in order to investigate the magnetic susceptibilities of some transition metal halide complexes. Measurements were obtained at five field strengths between six and twelve kilo-oersteds over the temperature range of 77°-300°K. $(NH_4)_2Ni(SO_4)_2 \cdot 6H_2O$ was used as a magnetic standard for calibration.

Diamagnetic susceptibilities were calculated for the hexameric niobium, tantalum, molybdenum, and tungsten cluster ions in terms of a molecular orbital scheme. Consideration of molecular diamagnetism due to electron delocalization yielded χ_D values ca. 100×10^{-6} emu/mole larger than those determined from atomic constants.

The $M_6X_{12}^{3+}$ ions of niobium and tantalum exhibited temperature dependent paramagnetism with a moment corresponding to one unpaired electron per cluster ion. Curie law behavior was observed for $(Et_4N)_3M_6Cl_{18}$ compounds while $M_6X_{12}X_{6/2}$ compounds exhibited Curie-Weiss behavior. Curvature in the χ_M versus 1/T plot for $Ta_6Cl_{15} \cdot 6H_2O$ is discussed in terms of inter-cluster bridging via terminal halogens. The $M_6X_{12}^{2+}$, $M_6X_{12}^{4+}$, and $W_6Cl_{12}^{4+}$ ions were observed to be diamagnetic.

Large temperature independent paramagnetic susceptibil-

ities were observed for all oxidation states of the cluster ions. A series of compounds was investigated varying the metal, halogen, and oxidation state of the cluster ion. Generally, χ_{TIP} values of the clusters exhibited these trends: niobium greater than tantalum and bromide greater than chloride. Oxidation of the cluster ion from (2+) to (3+) to (4+) produced very little change in χ_{TIP}.

The phases $TaCl_{2.83}$ and $TaBr_{2.83}$ were characterized in terms of their spectral, magnetic, and chemical properties. Detection of the $Ta_6X_{12}^{3+}$ ion and an easily hydrolyzed tantalum(IV) species led to the mixed valence formulation $2Ta_6X_{15}\cdot 3TaX_4$ with a Br/Ta molar ratio of 2.80. Excess $TaBr_4$ was removed from $TaBr_{2.83}$ by extraction with acetonitrile to obtain the pure phase. Comparison of the far infra-red spectra and magnetic susceptibilities of TaX_4, TaX_3, $TaX_{2.80}$, $TaX_{2.50}$, and $TaBr_{2.33}$ suggested that a mixed crystal model with inter-cluster bridging best represented the $TaX_{2.80}$ phase. The non-equilibrium tribromide phase was formulated as $Ta_6Br_{14}\cdot 2TaBr_5$ according to its physical and chemical properties.

Magnetic susceptibilities of $WCl_4(C_5H_5N)_2$ and $WBr_4(C_5H_5N)_2$ were measured from liquid helium to room

temperatures. Low temperature magnetic moments of 0.34 and 0.14 B.M. for the chloride and bromide, respectively, were attributed to the ground state of the ion. Thermal population of magnetic excited states was proposed to explain an increase in the moment with increasing temperature. Susceptibilities of $WCl_4[P(C_6H_5)_3]_2$ were measured from 77-299°K and observed to have a temperature dependence different from those of $WCl_4(C_5H_5N)_2$. The far infra-red spectra of the complexes suggested a cis configuration for $WCl_4(C_5H_5N)_2$ and $WBr_4(C_5H_5N)_2$. The configuration of $WCl_4[P(C_6H_5)_3]_2$ could not be resolved from its infra-red spectrum although complexes containing this ligand in the trans configuration have been reported. Comparison of the experimental magnetic data to theoretical values yielded poor agreement. Some qualitative conclusions were made concerning the magnetic behavior of the complexes.

SUGGESTIONS FOR FUTURE WORK

Additional x-ray structure data and accurate molecular orbital wave functions would be necessary for a refined theoretical treatment of the molecular diamagnetism of the cluster ions. Accurate values of χ_D must be obtained before comparison of experimental and theoretical values of χ_{TIP} would be practical. Structural information and susceptibility data at lower temperatures for $Ta_6Cl_{15}\cdot 6H_2O$ will be required to explain its deviation from Curie law behavior. Derivatives of the fluoride, bromide, and iodide cluster ions analogous to the chloride derivatives most thoroughly studied in this work should be prepared. Evaluation of χ_{TIP} would be more certain and meaningful with a wider range of compounds.

A liquid helium cryostat should be incorporated into the Faraday balance instrument. Combined with the furnace attachment now available the range of susceptibility measurements would be extended from *ca.* 4 to 1000°K. Investigation of magnetic susceptibilities for the second and third row transition metal sub-halides over this large temperature range might provide insight into the nature of their chemical bonding.

Preparation of a series of tungsten(IV) halide complexes with various ligands should be carried out in order to obtain

complexes in both the cis and trans configuration of the $MX_4 \cdot 2L$ molecule. Dipole moment, x-ray, and infra-red spectral data should be obtained for confirmation of molecular configuration. Magnetic susceptibilities down to liquid helium temperatures should be obtained for these complexes after a thorough analysis has proven their purity. Only then can the magnetic theory of the d^2 ion be evaluated.

ACKNOWLEDGEMENTS

The author wishes to thank Dr. R. E. McCarley for his time and energy in guidance and consultation. Without his generosity, understanding, and tolerance this work would never have been completed.

Thanks go to the members of physical and inorganic chemistry group X for their generous contribution of materials and information; to Mr. Peter Fleming for morale support and high quality compounds; to Mr. John Meyer for encouragement and many cluster complexes; to Mr. James Hamilton and Mr. Ronald Hogue for supplying materials for magnetic studies; and to Mr. Richard Smardzewski for consultation concerning theoretical aspects of this work. I wish to express my gratitude to all members of the group, past and present, for their help and for the social intercourse which made these years of graduate work a pleasure.

Special thanks go to Mr. John D. Greiner, Jr. for his instruction and guidance on the construction and calibration of the Faraday balance. The many hours of discussion in which his experience provided insight into the solution of instrumentation difficulties are greatly appreciated. The author wishes to thank Miss Evelyn Conrad for obtaining infra-red

spectra, Mr. Norman Linder for construction of tantalum reaction vessels by electron beam welding, Miss Leta Mueller for measuring reflectance spectra, and Mr. Edward Maas for oxidation state determinations.

Finally, I wish to express my deepest gratitude to those who provided intellectual stimulation during trying times.

BIBLIOGRAPHY

1. Schäfer, H., Scholz, H., and Gerken, R., Z. anorg. allgem. Chem. 331, 154 (1964).

2. Schäfer, H., Gerken, R., and Scholz, H., Z. anorg. allgem. Chem. 335, 96 (1965).

3. Schäfer, H., Bauer, D., Beckman, W., Gerken, R., Nieder-Vahrenholz, H. G., Niehus, K. J., and Scholz, H., Naturwissenschaften 51, 241 (1964).

4. McCarley, R. E. and Kuhn, P. J., Inorg. Chem. 4, 1482 (1965).

5. McCarley, R. E. and Boatman, J. C., Inorg. Chem. 4, 1486 (1965).

6. Schäfer, H. and Dohmann, K., Z. anorg. allgem. Chem. 300, 1 (1959).

7. Schnering, H. G., Wöhrle, H., and Schäfer, H., Naturwissenschaften 48, 159 (1961).

8. Schäfer, H. and Schnering, H. G., Angew. Chem. 76, 833 (1964).

9. Schäfer, H., Schnering, H. G., Neihus, K. J., and Nieder-Vahrenholz, H. G., J. Less-Common Metals 9, 95 (1965).

10. Simon, A., Schnering, H. G., Wöhrle, H., and Schäfer, H., Z. anorg. allgem. Chem. 339, 155 (1965).

11. Bauer, D., Schnering, H. G., and Schäfer, H., J. Less-Common Metals 8, 388 (1965).

12. Burbank, R. D., Inorg. Chem. 5, 1491 (1966).

13. Schäfer, H. and Bauer, D., Z. anorg. allgem. Chem. 340, 62 (1965).

14. McCarley, R. E., Hughes, B. G., Cotton, F. A., and Zimmerman, R., Inorg. Chem. 4, 1491 (1965).

15. McCarley, R. E. and Espenson, J. H., J. Am. Chem. Soc. 88, 1063 (1966).

16. Sheldon, J. C., Nature 184, 1210 (1959).

17. Gillespie, R. J., Canadian J. Chem. 39, 2336 (1961).

18. Duffey, G. H., Crossman, L. D., and Olsen, D. P., J. Chem. Phys. 38, 73 (1963).

19. Allen, R. J. and Sheldon, J. C., Austral. J. Chem. 18, 277 (1965).

20. Cotton, F. A. and Haas, T. E., Inorg. Chem. 3, 10 (1964).

21. Robin, M. B. and Kuebler, N. A., Inorg. Chem. 4, 968 (1965).

22. Kettle, S. F. A., Theoretical Chimica Acta 2, 211 (1965).

23. Boorman, P. M. and Straughan, B. P., J. Chem. Soc. A11, 1514 (1966).

24. Meyer, J. L. Preparation and infrared spectra of some polynuclear tantalum halide compounds. Unpublished M.S. thesis. Ames, Iowa, Library, Iowa State University of Science and Technology. 1967.

25. McCarley, R. E., Fleming, P. B., and Mueller, L. A., Inorg. Chem. 6, 1 (1967).

26. McCarley, R. E., Dougherty, T. A., and Fleming, P. B., J. Am. Chem. Soc. 89, 159 (1967).

27. Schneider, R. F. and Mackay, R. A., Inorg. Chem. 6, 549 (1967).

28. Krylov, E. I. Naucy. Doklady Vysshei Shkoly, Khim. i Khim. Teknol. 1958, 676 (1958). Original not available; abstracted in Chemical Abstracts 53:5790d. 1959.

29. Hughes, B. G. Some polynuclear tantalum halides and their oxidized derivatives. Unpublished Ph.D. thesis.

Ames, Iowa, Library, Iowa State University of Science and Technology. 1964.

30. Kennedy, C. D. and Peacock, R. D., J. Chem. Soc. 1963, 3392 (1963).

31. Brown, T. M. Preparation and reactions of some lower tungsten halides and halide complexes. Unpublished Ph.D. thesis. Ames, Iowa, Library, Iowa State University of Science and Technology. 1963.

32. Allen, E. A., Brisdon, B. J., Fowles, G. W. A., J. Chem. Soc. 1964, 4531 (1964).

33. Hull, C. G. and Stiddard, M. H. B., J. Chem. Soc. A11, 1633 (1966).

34. Allen, E. A. and Fowles, G. W. A., J. Chem. Soc. 1965, 1636 (1965).

35. Kamimura, H., J. Phys. Soc. Japan 11, 1171 (1956).

36. Kotani, M., J. Phys. Soc. Japan 4, 293 (1949).

37. Kamimura, H., Koide, S., Sekiyama, H., and Sugano, S. J. Phys. Soc. Japan 15, 1264 (1960).

38. Figgis, B. N., J. Inorg. Nucl. Chem. 8, 476 (1958).

39. Figgis, B. N. and Nyholm, R. S., J. Chem. Soc. 1958, 4190 (1958).

40. Schäfer, H. and Dohmann, K. D., Z. anorg. allgem. Chem. 300, 31 (1959).

41. Simmons, V. E. Tetrahedra: magnetic properties, spectra, chemistry, and structures. Unpublished Ph.D. thesis. Boston, Massachusetts, Library, Boston Univerwity Graduate School. 1963.

42. Bates, L. F. Modern magnetism. 3rd ed. Cambridge, England, Cambridge University Press. 1951.

43. Donoghue, J. J., U.S. Atomic Energy Commission Report NAA-SR-117 [North American Aviation, Inc., Downey, Calif.] (1953).

44. Figgis, B. N. and Nyholm, R. S., J. Chem. Soc. 1959, 338 (1959).

45. Kleinberg, J., Argersinger, W. L., and Griswold, E. Inorganic chemistry. Boston, Massachusetts, D. C. Heath and Company. 1960.

46. Selwood, P. W. Magnetochemistry. 2nd ed. New York, New York, Interscience Publishers, Inc. 1956.

47. Hameka, H. F., J. Chem. Phys. 37, 3008 (1962).

48. Kaczmarczyk, A. and Kolski, G. B., Inorg. Chem. 4, 665 (1965).

49. Goodenough, J. B. Magnetism and the chemical bond. New York, New York, Interscience Publishers, Inc. 1963.

50. Spreckelmeyer, B. and Schäfer, H., Less-Common Metals 13, 122 (1967).

51. Schäfer, H., Schnering, H. G., Simon, A., Geigling, D., Bauer, D., Siepman, R., and Spreckelmeyer, B., J. Less-Common Metals 10, 154 (1965).

52. Figgis, B. N. and Lewis, J., Progress in Inorganic Chemistry 6, 37 (1964).

53. Van Vleck, J. H. The theory of electric and magnetic susceptibilities. Oxford, England, Oxford University Press. 1932.

54. Schäfer, H. and Schnering, H., Angew. Chem. 76, 833 (1964).

55. Sheldon, J. C., J. Chem. Soc. 1960, 1007 (1960).

56. Cotton, F. A. and Lippard, S. J., Inorg. Chem. 4, 59 (1965).

57. Torp, B. A. Spectra, magnetic susceptibilities, and structure of some halogen complexes of niobium(IV) and tantalum(IV). Unpublished Ph.D. thesis. Ames, Iowa, Library, Iowa State University of Science and Technology. 1964.

58. McCarley, R. E. and Boatman, J. C., Inorg. Chem. 2, 547 (1963).

59. Boatman, J. C. The equilibrium phase diagrams for the tantalum-tantalum bromide and tantalum-tantalum iodide systems. Unpublished Ph.D. thesis. Ames, Iowa, Library, Iowa State University of Science and Technology. 1964.

60. Ray, T. C. and Westland, A. D., Inorg. Chem. 4, 1501 (1965).

61. Beattie, I. R. and Webster, M., J. Chem. Soc. 1964, 3507 (1964).

62. Harrah, A., Spectrochim. Acta 9, 113 (1962).

63. Carmichael, W. M., Edwards, D. A., and Walton, R. A., J. Chem. Soc. A1, 97 (1966).

64. Chatt, J. and Rowe, G. A., J. Chem. Soc. 1962, 4019 (1962).

65. Ballhausen, C. J. Introduction to ligand field theory. New York, New York, McGraw-Hill Book Company, Inc. 1962.

66. Ernshaw, A., Figgis, B. N., Lewis, J., and Peacock, R. D., J. Chem. Soc. 1961, 3132 (1961).

67. Stevens, K. W. H., Proc. Roy. Soc. A219, 542 (1953).

68. Figgis, B. N., Lewis, J., Mabbs, F. E., and Webb, G. A., J. Chem. Soc. A9, 1411 (1966).

69. Terezakis, E. G. and Carlin, R. L., Inorg. Chem. 6, 2125 (1967).

APPENDIX

Table 1A. Magnetic susceptibilities of $(Et_4N)_3Nb_6Cl_{18}$

Temperature ^oK	$\chi_g(10^6)$ emu/gram	$\chi_M(10^6)$ emu/mole	μ(eff) B.M.
299	0.478	758	1.97
270	0.571	906	1.96
243	0.639	1010	1.91
222	0.735	1170	1.90
175	1.01	1600	1.86
133	1.34	2130	1.78
113	1.71	2710	1.80
77	2.54	4030	1.74

Molecular weight = 1586.4 g/mole.

Sample weight = 0.1788 g.

χ_D(calc) = -1024×10^{-6} emu/mole.

Intercept = -372×10^{-6} emu/mole.

$\chi_{TIP} = +652 \times 10^{-6}$ emu/mole.

Average moment from slope = 1.65 ± 0.02 B.M.

Table 2A. Magnetic susceptibilities of $(Ph_4As)_2Nb_6Cl_{16}(OH)(H_2O)$

Temperature °K	$\chi_g(10^6)$ emu/gram	$\chi_M(10^6)$ emu/mole	μ(eff) B.M.
299	0.190	366	1.78
183	0.474	916	1.66
140	0.719	1390	1.62
113	0.952	1840	1.59
77	1.52	2940	1.55

Molecular weight = 1930 g/mole.

Sample weight = 0.0985 g.

χ_D(calc) = -1123×10^{-6} emu/mole.

Intercept = -529×10^{-6} emu/mole.

$\chi_{TIP} = +594 \times 10^{-6}$ emu/mole.

Average moment from slope = 1.46 ± 0.01 B.M.

Table 3A. Magnetic susceptibilities of $(Et_4N)_2Nb_6Cl_{17}(DMSO)_2$

Temperature ^oK	$\chi_g(10^6)$ emu/gram	$\chi_M(10^6)$ emu/mole	μ(eff) B.M.
298	0.4055	627 ± 17	1.94
182	0.7813	1208 ± 11	1.77
152	0.9704	1501 ± 12	1.73
126	1.212	1874 ± 11	1.69
113	1.388	2147 ± 11	1.67
110	1.435	2220 ± 14	1.67
77	2.152	3328 ± 20	1.62

Molecular weight = 1546.8 g/mole.

Sample weight = 0.1833 g.

χ_D(calc) = -944×10^{-6} emu/mole.

Intercept = -330×10^{-6} emu/mole.

$\chi_{TIP} = +664 \times 10^{-6}$ emu/mole.

Average moment from slope = 1.50 ± 0.02 B.M.

Table 4A. Magnetic susceptibilities of Nb_6F_{15}

Temperature °K	$\chi_g(10^6)$ emu/gram	$\chi_M(10^6)$ emu/mole	μ(eff) B.M.
298	1.494	1258 ± 6	1.93
294	1.509	1271 ± 4	1.93
217	1.998	1683 ± 7	1.90
176	2.420	2038 ± 8	1.85
142	2.971	2503 ± 12	1.81
122	3.455	2911 ± 12	1.80
113	3.746	3156 ± 16	1.79
103	4.083	3440 ± 15	1.78
97	4.321	3640 ± 26	1.77
93	4.489	3781 ± 22	1.76
89	4.702	3961 ± 21	1.76
87	4.822	4062 ± 25	1.76
83	4.980	4195 ± 34	1.74
79	5.158	4345 ± 15	1.73
77	5.236	4410 ± 35	1.72

Molecular weight = 842.4 g/mole.

Sample weight = 0.3210 g.

χ_D(calc) = -385×10^{-6} emu/mole.

Intercept ($T>90^oK$) = $+85 \times 10^{-6}$ emu/mole.

$\chi_{TIP} = +470 \times 10^{-6}$ emu/mole.

Average moment from slope ($T>90^oK$) = 1.67 B.M.

Table 5A. Magnetic susceptibilities of $(Et_4N)_3Ta_6Cl_{18}$

Temperature	$\chi_g(10^6)$ emu/gram	$\chi_M(10^6)$ emu/mole	μ(eff) B.M.
299	0.244	515 ± 13	1.87
149	0.7628	1613 ± 9	1.75
131	0.9262	1958 ± 12	1.74
113	1.122	2370 ± 19	1.73
77	1.728	3653 ± 15	1.68

Molecular weight = 2114.6 g/mole.

Sample weight = 0.2517 g.

χ_D(calc) = -1054×10^{-6} emu/mole.

Intercept = -557×10^{-6} emu/mole.

$\chi_{TIP} = +497 \times 10^{-6}$ emu/mole.

Average moment from slope = 1.615 ± 0.015 B.M.

Table 6A. Magnetic susceptibilities of $Ta_3Cl_{15} \cdot 6H_2O$

Temperature °K	$\chi_g(10^6)$ emu/gram	$\chi_M(10^6)$ emu/mole	μ(eff) B.M.
302	0.348	601	1.71
267	0.402	694	1.68
215	0.514	886	1.62
186	0.592	1021	1.57
157	0.686	1185	1.51
155	0.694	1198	1.50
113	0.879	1517	1.40
77	1.10	1893	1.25

Molecular weight = 1725.6 g/mole.

Sample weight = 0.3155 g.

χ_D(calc) = -630×10^{-6} emu/mole.

Intercept $(1/T-\theta) = -520 \times 10^{-6}$ emu/mole.

$\theta = -110^{\circ}K$.

$\chi_{TIP} = +170 \times 10^{-6}$ emu/mole.

Table 7A. Magnetic susceptibilities of Ta_6Cl_{15}

Temperature °K	$\chi_g(10^6)$ emu/gram	$\chi_M(10^6)$ emu/mole	μ(eff) B.M.
298	0.438	709 ± 9	1.73
210	0.635	1028 ± 6	1.63
160	0.832	1246 ± 8	1.56
137	0.945	1774 ± 15	1.45
77	1.458	2358 ± 12	1.34

Molecular weight = 1617.5 g/mole.

Sample weight = 0.4001 g.

χ_D(calc) = -552×10^{-6} emu/mole.

Intercept $(1/T-\theta)$ = -220×10^{-6} emu/mole.

$\theta = -50^{\circ}K$.

$\chi_{TIP} = +332 \times 10^{-6}$ emu/mole.

Table 8A. Magnetic susceptibilities of Ta_6Br_{15}

Temperature °K	$\chi_g(10^6)$ emu/gram	$\chi_M(10^6)$ emu/mole	μ(eff) B.M.
298	0.2056	470 ± 10	1.73
219	0.2847	650 ± 7	1.59
139	0.4255	972 ± 7	1.40
113	0.4777	1091 ± 6	1.30
77	0.5873	1342 ± 7	1.15

Molecular weight = 2284.4 g/mole.

Sample weight = 0.4725 g.

χ_D(calc) = -782×10^{-6} emu/mole.

Intercept $(1/T-\theta)$ = -320×10^{-6} emu/mole.

$\theta = -125^{\circ}K$.

$\chi_{TIP} = +462 \times 10^{-6}$ emu/mole.

Table 9A. Magnetic susceptibilities of $(Et_4N)_2Nb_6Cl_{18}$

Temperature °K	$\chi_g(10^6)$ emu/gram	$\chi_M(10^6)$ emu/mole
300	-0.177	-257 ± 14
123	-0.149	-216 ± 14
77	-0.120	-175 ± 15

Molecular weight = 1455.0 g/mole.

Sample weight = 0.1971 g.

Intercept = -286×10^{-6} emu/mole.

Table 10A. Magnetic susceptibilities of $Nb_6Cl_{14} \cdot 8H_2O$

Temperature °K	$\chi_g(10^6)$ emu/gram	$\chi_M(10^6)$ emu/mole
296	-0.026	-32 ± 7
139	+0.026	+32 ± 13
113	+0.057	+69 ± 5
77	+0.119	+142 ± 7

Molecular weight = 1197.8 g/mole.

Sample weight = 0.3662 g.

Intercept = -82×10^{-6} emu/mole.

Table 11A. Magnetic susceptibilities of $Nb_6Br_{14}\cdot 8H_2O$

Temperature °K	$\chi_g(10^6)$ emu/gram	$\chi_M(10^6)$ emu/mole
300	-0.089	-164 ± 4
77	-0.049	-90 ± 3

Molecular weight = 1820 g/mole.

Sample weight = 0.6276 g.

Intercept = -190×10^{-6} emu/mole.

Table 12A. Magnetic susceptibilities of $(Ph_4As)_2Ta_6Cl_{18}$

Temperature °K	$\chi_g(10^6)$ emu/gram	$\chi_M(10^6)$ emu/mole
299	-0.282	-702 ± 38
261	-0.277	-689 ± 26
236	-0.278	-692 ± 25
168	-0.275	-684 ± 24
77	-0.274	-684 ± 31

Molecular weight = 2490.4 g/mole.

Sample weight = 0.2458 g.

χ_M(average) = $-(696 \pm 44)\times 10^{-6}$ emu/mole.

Table 13A. Magnetic susceptibilities of $(Et_4N)_2Ta_6Cl_{18}$

Temperature °K	$\chi_g(10^6)$ emu/gram	$\chi_M(10^6)$ emu/mole
298	-0.223	-442 ± 14
77	-0.213	-424 ± 13

Molecular weight = 1984.3 g/mole.

Sample weight = 0.3934 g.

χ_M(average) = -(433 ± 23)x10^{-6} emu/mole.

Table 14A. Magnetic susceptibilities of $(Et_4N)_2Ta_6Cl_{12}Br_6$

Temperature °K	$\chi_g(10^6)$ emu/gram	$\chi_M(10^6)$ emu/mole
295	-0.2083	-468 ± 9
77	-0.2081	-468 ± 12

Molecular weight = 2251.1 g/mole.

Sample weight = 0.4478 g.

Table 15A. Magnetic susceptibilities of $(Et_4N)_2Ta_6Br_{18}$

Temperature °K	$\chi_g(10^6)$ emu/gram	$\chi_M(10^6)$ emu/mole
298	-0.196	-548 ± 16
186	-0.190	-530 ± 11
113	-0.188	-525 ± 16
77	-0.175	-487 ± 16

Molecular weight = 2784.6 g/mole.

Sample weight = 0.3880 g.

Intercept = $-(570 \pm 26)\times10^{-6}$ emu/mole.

Table 16A. Magnetic susceptibilities of $Ta_6Cl_{12}Cl_2(OH)_2$

Temperature °K	$\chi_g(10^6)$ emu/gram	$\chi_M(10^6)$ emu/mole
297	-0.122	-198
212	-0.122	-198
152	-0.122	-198

Molecular weight = 1616 g/mole.

Sample weight = 0.1832 g.

Table 17A. Magnetic susceptibilities of $(Et_4N)_4Ta_6Cl_{18}$

Temperature °K	$\chi_g(10^6)$ emu/gram	$\chi_M(10^6)$ emu/mole
297	-0.105	-235 ± 30
77	+0.406	+911 ± 20

Molecular weight = 2244.8 g/mole.

Sample weight = 0.2284 g.

Intercept = -634×10^{-6} emu/mole.

Table 18A. Magnetic susceptibilities of $(Et_4N)_2W_6Cl_{14}$

Temperature °K	$\chi_g(10^6)$ emu/gram	$\chi_M(10^6)$ emu/mole
296	-0.293	-550 ± 20
77	-0.290	-540 ± 13

Molecular weight = 1860.0 g/mole.

Sample weight = 0.3180 g.

χ_M(average) = $-(545 \pm 25)\times10^{-6}$ emu/mole.

Table 19A. Magnetic susceptibilities of $(Et_4N)_2W_6Cl_8Br_6$

Temperature °K	$\chi_g(10^6)$ emu/gram	$\chi_M(10^6)$ emu/mole
295	-0.294	-625 ± 20
77	-0.290	-617 ± 18

Molecular weight = 2126.7 g/mole.

Sample weight = 0.3521 g.

χ_M(average) = $-(621 \pm 24)\times10^{-6}$ emu/mole.

Table 20A. X-ray diffraction data for $TaCl_{2.80}$, $TaBr_{2.80}$, and $(Ta_6Br_{12}^{3+})_2(PtBr_6^{2-})_3$

$TaCl_{2.80}$		$TaBr_{2.80}$		$(Ta_6Br_{12}^{3+})_2(PtBr_6^{2-})_3$	
d(A)	I^a	d(A)	I^a	d(A)	I^a
				14.04	(3)
				12.34	(2)
9.15	(10)	9.33	(10)	10.94	(10)
		6.68	(8)	7.36	(10)
6.37	(10)	6.49	(6)	7.04	(9)
4.48	(6)	4.65	(4)		
4.04	(3)	4.21	(4)		
3.95	(3)	4.11	(4)		
3.44	(8)	3.56	(6)	3.56	(2)
2.85	(3)	2.96	(5)	2.94	(2)
2.49	(8)	2.60	(8)		
2.44	(6)	2.54	(5)	2.54	(5)
2.33	(8)	2.43	(5)		
2.30	(8)	2.40	(5)	2.39	(4)
2.22	(8)	2.32	(5)		
2.17	(8)	2.26	(5)		
2.14	(4)	2.24	(3)	2.24	(2)
2.01	(4)	2.10	(4)	2.19	(3)
1.95	(4)	2.04	(4)	2.10	(3)

[a]Relative intensities from visual observation.

Table 21A. Magnetic susceptibilities of $TaCl_{2.80}$

Temperature	$\chi_g(10^6)$ emu/gram	$\chi_M(10^6)$[a] emu/mole	μ(eff.) B.M.
296	0.291	1220 ± 31	2.62
274	0.328	1380 ± 29	2.59
242	0.388	1630 ± 31	2.54
222	0.443	1860 ± 28	2.51
195	0.518	2180 ± 23	2.45
166	0.637	2680 ± 27	2.41
133	0.845	3550 ± 32	2.37
113	1.00	4220 ± 34	2.32
77	1.47	6170 ± 38	2.20

Sample weight = 0.2147 g.

χ_D(calc) = -1660×10^{-6} emu/mole.

Intercept $(1/T-\theta)$ = -900×10^{-6} emu/mole.

$\theta = -16^{\circ}K$.

$\chi_{TIP} = +760 \times 10^{-6}$ emu/mole.

Average moment from slope = 2.29 B.M.

[a]Molecular weight of 4202.4 g/mole for $2Ta_6Cl_{15} \cdot 3TaCl_4$ was used to calculate χ_M.

Table 22A. Magnetic susceptibilities of $TaBr_{2.80}$

Temperature ^{o}K	$\chi_g(10^6)$ emu/gram	$\chi_M(10^6)$[a] emu/mole	(eff.) B.M.
295	0.2246	1364 ± 14	2.85
241	0.3030	1839 ± 11	2.75
203	0.3767	2287 ± 10	2.67
183	0.4279	2597 ± 13	2.62
142	0.5820	3533 ± 14	2.53
126	0.6704	4069 ± 18	2.50
116	0.7309	4437 ± 13	2.46
113	0.7430	4510 ± 22	2.44
77	1.080	6558 ± 32	2.31

Sample weight = 0.7405 g.

χ_D(calc) = -2090×10^{-6} emu/mole.

Intercept (1/T-θ) = -1150×10^{-6} emu/mole.

θ = $-23^{o}K$.

χ_{TIP} = $+940 \times 10^{-6}$ emu/mole.

Average moment from slope = 2.56 B.M.

[a]Molecular weight of 6069.7 g/mole for $2Ta_6Br_{15} \cdot 3TaBr_4$ was used to calculate χ_M.

Table 23A. X-ray diffraction data for $TaBr_{3.01}$, $TaBr_{3.43}$, and $TaCl_{3.03}$

$TaBr_{3.01}$		$TaBr_{3.43}$		$TaCl_{3.03}$	
d(A)	I^a	d(A)	I^a	d(A)	I^a
9.22	(9)	9.14	(8)		
8.45	(9)	8.40	(9)		
6.18	(8)	6.19	(8)	6.10	(10)
3.20	(2)	3.20	(1)	4.46	(3)
3.05	(2)			3.41	(1)
3.02	(5)	3.01	(5)	2.95	(3)
2.88	(3)	2.87	(1)	2.88	(8)
2.62	(10)	2.62	(10)	2.70	(6)
2.40	(2)	2.39	(1)	2.61	(5)
		2.35	(2)	2.47	(5)
2.21	(5)	2.21	(5)	2.27	(1)
2.16	(4)	2.15	(3)	2.23	(1)
2.09	(4)			2.15	(1)
1.86	(7)	1.86	(8)	2.04	(6)
1.85	(7)	1.84	(8)	1.74	(3)
1.79	(2)	1.79	(2)	1.68	(8)
1.64	(2)	1.64	(2)	1.62	(5)
1.58	(3)	1.58	(3)	1.53	(6)

[a]Relative intensities from visual observation.

Table 24A. Magnetic susceptibilities of $WCl_4(C_5H_5N)_2$

Temperature °K	$\chi_g(10^6)$[a] emu/gram	$\chi_M(10^6)$[b] emu/mole	μ(eff.)[c] B.M.
300	2.252	1090 ± 12	1.77
270	2.405	1163 ± 6	1.73
256	2.487	1203 ± 5	1.71
246	2.548	1233 ± 6	1.69
233	2.640	1277 ± 6	1.67
202	2.835	1371 ± 6	1.61
183	2.952	1428 ± 7	1.56
173	3.019	1460 ± 9	1.53
148	3.151	1524 ± 7	1.44
140	3.193	1545 ± 7	1.41
136	3.227	1561 ± 9	1.39
125	3.256	1575 ± 8	1.34
120	3.281	1588 ± 9	1.32
113	3.283	1588 ± 9	1.23
93	3.30	1600 ± 12	1.17
81	3.362	1630 ± 10	1.10
78	3.360	1630 ± 10	1.08
77	3.356	1624 ± 9	1.07
64	3.410	1620 ± 12	0.97
56	3.410	1650 ± 13	0.92
52	3.462	1680 ± 11	0.89
51	3.466	1680 ± 14	0.88

[a]Determined from sample weight of 0.1610 g.

[b]Determined from molecular weight of 483.8 g/mole.

[c]Determined using χ_D(calc) = -228×10^{-6} emu/mole.

Table 25A. Magnetic susceptibilities of $WBr_4(C_5H_5N)_2$

Temperature ^oK	$\chi_g(10^6)$[a] emu/gram	$\chi_M(10^6)$[b] emu/mole	μ(eff.)[c] B.M.
300	1.344	889 ± 5	1.67
273	1.453	961 ± 5	1.64
255	1.518	1005 ± 4	1.61
232	1.659	1098 ± 6	1.59
211	1.749	1158 ± 4	1.55
205	1.771	1172 ± 8	1.54
190	1.864	1234 ± 4	1.51
174	1.956	1295 ± 4	1.47
164	2.019	1336 ± 6	1.45
155	2.107	1394 ± 4	1.44
136	2.209	1462 ± 6	1.37
125	2.264	1498 ± 4	1.33
113	2.298	1520 ± 8	1.27
85	2.443	1617 ± 7	1.13
81	2.469	1634 ± 8	1.11
77	2.488	1646 ± 7	1.09
52	2.565	1698 ± 9	0.90

[a] Determined from sample weight of 0.2321 g.

[b] Determined from molecular weight of 661.7 g/mole.

[c] Determined from χ_D(calc) = -266×10^{-6} emu/mole.

Table 26A. Magnetic susceptibilities of $WCl_4 \cdot 2P(C_6H_5)_3$

Temperature ^oK	$\chi_g(10^6)$[a] emu/gram	$\chi_M(10^6)$[b] emu/mole	μ(eff.)[c] B.M.
299	1.414	1201 ± 12	2.00
253	1.652	1404 ± 6	1.95
227	1.789	1521 ± 8	1.90
186	2.035	1731 ± 7	1.81
145	2.268	1928 ± 9	1.67
120	2.414	2053 ± 8	1.55
113	2.452	2084 ± 8	1.52
77	2.626	2233 ± 15	1.29

[a]Determined from sample weight of 0.2152 g.

[b]Determined from molecular weight of 850.2 g/mole.

[c]Determined from χ_D(calc) = -463×10^{-6} emu/mole.